A TRANSFORMATIVE INVESTIGATION OF ACOUSTICAL TESTING PROTOCOLS FOR RESIDENTIAL VENTILATION DEVICES

A Dissertation

by

WONGYU CHOI

Submitted to the Office of Graduate and Professional Studies of
Texas A&M University
in partial fulfillment of the requirements for the degree of

DOCTOR OF PHILOSOPHY

Chair of Committee,	Michael B. Pate
Committee Members,	Alan B. Palazzolo
	Hamn-Ching Chen
	Partha P. Mukherjee
Head of Department,	Andreas A. Polycarpou

December 2016

Major Subject: Mechanical Engineering

ABSTRACT

Mechanical ventilation plays a crucial role for indoor environment quality as built environments pursue tighter and energy efficient constructions. Therefore, stringent guidelines for proper ventilation are imposed on residential buildings in the U.S, which includes International Energy Conservation Code, ASHRAE 62.2, and state regulations. Likewise, certification and verification programs for residential ventilation devices, such as Energy Star and Home Ventilating Institute (HVI), are continuously mandated by governmental agencies along with usage of associated testing standards such as ANSI, ISO, AMCA, and HVI. Because of the wide interest surrounding standard testing, certification, and verification programs, precision and accuracy by improved testing methodologies are necessary.

In this work, three primary objectives are formulated to address the necessity for improving testing protocols for residential ventilation devices, namely (1) performance evaluations of residential ventilations devices as functions of timelines and energy codes, and (2) identifications of challenges and issues arising from using existing testing methodologies, and (3) introduction of revised and improved testing methodologies to overcome challenges identified. In an effort to address these three objectives, this study presents (1) performance evaluations of large quantity of residential bathroom fan testing data over a decade, (2) improved testing methodologies for precise background steadiness evaluation, (3) uncertainty analytics along with improve metrics and criteria

for better fan-acoustic testing quality, and (4) implementation of revised psychoacoustic loudness models as an update to an existing loudness calculation procedures.

Major overall conclusions from this study are that (1) fan acoustic and energy performances have improved over the last decade, specifically by 50% reductions in loudness and 25% efficacy increase which is a ratio of fan volume flow rate and power consumption, (2) usage of external background noise signal can benefit the background steadiness evaluations by the aid of acoustic transmission signature analysis, (3) a combined use of conventional background-noise uncertainty and SNR analytics in terms of theoretical zero loudness can better tell the background impact to loudness rating, and (4) an update to the conventional loudness calculation can be made by the revised psychoacoustic model, which also address limitations on the conventional loudness, which includes a lack of tonal-component implementation to loudness and outdated equal loudness contour.

ACKNOWLEDGEMENTS

I would like to thank my advisor, Dr. Pate. His guidance led me to the wonderful research of the HVAC engineering and the renewable energy systems for the built environments. His patience, motivation, and knowledge were equivalently invigorating to me as well as his authentic sense of humor and wonderful baking skills.

Also, I would like to express my thanks to Dr. Palazollo, Dr. Chen, and Dr. Mukherjee, for their guidance and support throughout the course of this study. It was a great honor for me to be in their legendary courses and to develop insightful mindset for my ongoing and future researches as an avid learner and a researcher.

My four years at the Riverside Energy Efficiency Laboratory were unique and pleasant. I have developed my HVAC engineering skills and project management skills as a building energy system researcher and as an assistant laboratory manager. One of the foremost I earned was true comradery from hard-working with Dr. Sweeney, Katherine, and others colleagues. They all demonstrated what makes a good researcher: cooperation, high energy, courage, a strong stomach, tacos, etc.

My family has been an infinite source of my commitment to building energy system studies—I am indebted by their patience and love. I would like to express thanks to my wife from the bottom of my heart, who has supported me with love and patience, and my baby girl, who came to me and taught me the true meaning of the life (it was not 42). My graduate study was not available without the support of my father and mother. Lastly, thanks to my parent in-laws for their encouragements.

NOMENCLATURE

A	Amplitude
AC	Alternating current
ANSI	American National Standards Institute
AMCA	Air Moving and Control Association
ASHRAE	American Society of Heating, Refrigeration, and Air-Conditioning Engineers
BGD	Background noise
c	Speed of the sound
d	Difference or distance
DC	Direct current
E	Excitation (Pa)
EPA	Environmental Protection Agency
ERB	Equivalent rectangular bandwidth
ESMER	Energy Star Most Efficient Recognition
F	Loudness weighting factor
f	Frequency (Hz)
G	Low level gain of cochlear amplifier
g	Normalized frequency
H	Statistical hypothesis
h	Thickness of material
HVI	Home Ventilating Institute

I	Sound intensity (W/m^2)
IQR	Interquartile Range
ICC	International Code Council
IECC	International Energy Code Council
IL	Insertion Loss
ISO	International Organization for Standardization
K	Background correction factor
k	Coverage factor for expanded uncertainty
N	Loudness (sone)
n	Integer (n= 1, 2, 3, …) or number of samples
p	Sound pressure (Pa) or exponential factor (in loudness)
Q	Directivity factor
R	A statistical software package (The R Project)
R^2	Coefficient of determination
r	Radius or radial distance
RCR	Room characteristic ratio
RSS	Reference Sound Source or a measurement phase of the same
S	Surface area (m^2)
s	Sensitivity coefficient
SE	Standard error
SNR	Signal-to-Noise Ratio
SPL	Sound Pressure Level (dB)

SWL	Sound Power Level (dB)
T	Test Statistic
U	Expanded uncertainty
u	Standard uncertainty
UUT, UT	Unit under test
W	Weighting function
w	Square of sound pressure (Pa^2)
X	Signal of test specimen
Y	Noisy signal

Greek Symbols

α	Acoustic absorption coefficient
Δ	Differences between variables
θ	Wave incident angle (rad)
χ^2	Chi-Square distribution
μ	Mean of squared sound pressure (Pa^2)
ξ	Random variable
ρ	Pearson product-moment correlation coefficients
σ	Standard deviation
φ	Phase of sinusoid (rad)
ω	Angular velocity (rad/s)

Subscripts

e	Outside an acoustical testing chamber
i	Inside an acoustical testing chamber
m	Frequency component
n	Phased sinusoidal contribution
nb	Non-acoustic-barrier
pf	Sound pressure level (dB) of fan excluding background noise
t	Total (in loudness)
THRQ	Human hearing threshold
w	Acoustic paths, such as wall, roof, door, floor, etc.
wf	Sound power level (dB) of fan excluding background noise
wr	Sound power level (dB) of RSS excluding background noise

Superscripts

B	Measurement phase of background noise *B1, B2* Measurement phase of background noise with number designations
RSS	Measurement phase of reference sound source (RSS)
U	SPLs indicating an exclusion of measured background noise
UT	Measurement phase of a unit-under-test

Superscripts (continued)

zl	Zero loudness
*	Estimator based on assumptions
^	Sample variable

TABLE OF CONTENTS

Page

LIST OF FIGURES

Page

LIST OF TABLES

Page

CHAPTER I

GENERAL INTRODUCTION

Dissertation Organization

This dissertation is organized into chapters with individual topics. Chapters II through VI present journal papers that are either published or in preparation. Chapter I presents a general introduction of the topics presented in this thesis along with an overview of the completed work. Chapter II presents multi-year statistical analysis of residential bathroom fan performances. The statistical analysis is conducted along with over 1,500 fan testing data for the test period 2005-2013 with focuses on energy and acoustical performances. Chapters III and IV presents an improved methodology to evaluated background-noise steadiness for fan acoustical testing. Specifically, Chapter III introduces acoustic transmission characterization methodologies as a pre-requisite for background steadiness assessment methodology introduced in Chapter IV. Because the methodology relies on the external acoustic signature, which is measured outside of an acoustic testing chamber, acoustic transmission characterization is necessary. Chapter IV introduces the background steadiness assessment methodology by monitoring acoustic signatures measured by an external microphone where the background noise sources are located. Chapter V discusses uncertainty metrics for background noise and signal-to-noise ratio (SNR) between the signal of interest (i.e., fan sound or noise) and the background noise. Based on finding that modern ventilation fans generate low levels of fan noise, more comprehensive analysis was conducted in order to address low SNR

issues. Lastly, Chapter VI presents an implementation of a revised psychoacoustic loudness model for the conventional fan loudness calculation procedure and its impact to the fan certification or rating programs.

Objectives

The objectives of this work are provided as follows.

1. Performance evaluations of modern residential ventilation devices over an extended time-period for the most recent decade along with international energy codes and guidelines.
2. Identifications of challenges and issues in standard testing for residential ventilation devices for certification or rating purposes.
3. Development of strategies and/or technique to overcome identified challenges and issues.

To meet these objectives, the study herein presents following research topics.

1. Study of Bathroom Ventilation Fan Performance Trends for Years 2005 to 2013—Data Analysis of Loudness and Efficacy
2. Methodology for Evaluating Sound Transmission to the External Background
3. Methodology for Evaluating Background Steadiness by Monitoring External Background Signatures
4. Uncertainty and Signal-to-Noise Ratio for Unsteady Background Noise
5. An Impact of an Improved Psychoacoustic Model on Fan Loudness and Acoustic Ratings

Background and Problem Statements

The thesis will be organized into chapters that encompass specific focus areas. The following text describes the chapter topics and their associated problem statements. As noted earlier, each chapter is structured as a research paper that has either been submitted or will be submitted to a research journal. In this light, the below chapter titles also form the basis for paper titles.

1. Study of Bathroom Ventilation Fan Performance Trends for Years 2005 to 2013—Data Analysis of Loudness and Efficacy

Only a limited number of studies dealing with real world applications has been conducted over the years that show improvements in energy and acoustic performances for residential ventilation fans have been reported [1-3]. This is in contrast to the large number of studies focusing on individual components of the residential ventilation devices, such as fan/impeller fluid dynamic and heat transfer modelling, acoustic characterizations of fan blades, ventilation capacity simulations and experiments on different ventilation inputs and loads [3-7]. It should be noted that these past studies on various components have targeted performance improvements of residential ventilation fans. To document improvements and changes, a multi-year study is needed for residential bathroom ventilation fan energy and acoustic performances with a focus on analyzing statistical data. The focuses of this study will be to identify and document how energy and acoustic performances changed (either performance improvements or decreases). As noted, these changes could be the result of component studies, but they

could also correlate with the timelines of international/national codes and guidelines relevant to residential ventilation being implemented.

2. Methodology for Evaluating Sound Transmission to the External Background

The intrusion of acoustic background noises has an effect on characterizations of acoustic performance evaluations and measurements of sound sources (or unit under test) as mandated by various international standards [8-11]. The effects of background noise on sound evaluation, as studied by past researchers and organizations, has mainly focused on eliminating its effect on the signal emitted from the unit under test, such as signal-to-noise ratios, background corrections, spectral subtractions, etc. [8, 9, 12-16]. However, the assessments of steady background, which is defined as the background noise free from change, variation, or interruption, have been less studied primarily because major focuses have been on reducing the impact of the background itself. Furthermore, the criteria defining the steady background for the background steadiness have not been widely discussed, and the methodologies are limited to measurement uncertainty [17] or comparison of the two average background sound pressure levels measured individually [9]. As such, more research for the improved methodologies is necessary.

The research in this chapter (along with the chapter to follow) is a background steadiness assessment based on monitoring the external background noise outside the semi-reverberant chamber, while the signal of the unit under test is being measured. In order to analyze the external background noise for the steadiness assessment, the background noise should not be influenced by the sound of the unit under test or the

reference sound source (RSS) that may be transmitted through the chamber envelop. This in turn demands a sound transmission characterization of the acoustic chamber when the unit is under test or the RSS generated sound is evaluated. Therefore, the development of the transmission characterization methods is necessary, which can be widely applicable to different acoustic testing setups, environments (including background noise levels), acoustic field characteristics (free-field, anechoic, reverberant, semi-reverberant, etc.).

3. Methodology for Evaluating Background Steadiness by Monitoring External Background Signatures

As discussed in the previous problem statements for Part 1, the steadiness of the background noise, which was defined earlier as the degree of the background noise being free from change, variation, or interruption, has not been adequately studied compared to background correction techniques, which address an effect of the background noise intrusion to the sound of the unit under test, such as uncertainties, signal-to-noise ratios (SNRs), etc. The weakness in these techniques as studied is that they inherently assume either (1) the background noise is the same throughout an acoustic test, so one time-average of the background measurement suffices for the remainder of the test [8, 10, 11], or (2) the background noise is steady throughout a sound test if two different averages (e.g., 30 sec each) of the background noise sound pressure levels are close within a certain limit [9]. These assumptions may not hold true when poor signal-to-noise ratios (SNRs) cause large variations of sound levels when a testing environment is subject to unsteady background noise. For example, many of

modern residential HVAC devices generate less noise than in the past, and, as a result, multiple SNR violations routinely occur because of the introductions of the SNR criteria in our standards test. In order to resolve this issue, more robust background steadiness assessment is necessary. Therefore, a background steadiness assessment is proposed in this research based on monitoring the external background noise outside the semi-reverberant chamber while the acoustic testing for the test subject is performed inside the chamber. Specifically, based on the transmission characteristics determined by the methodologies presented in the Part 1, the external background signals are compared and then assessed for background steadiness.

4. Uncertainty and Signal-to-Noise Ratio for Unsteady Background Noise

The background noise is a random combination of noise sources, such as sound emitting from human speech and other activities, electrical devices, automobiles, heavy machineries, aircrafts, microclimate effects, structural vibrations, etc. [13]. As a result, the background noise is broad-band such as white or pink noise with uncorrelated tonal components. Most of these random noise sources are uncorrelated to the point that one cannot easily develop relationships for noise sources [18]. Furthermore, the background noise is constantly changing because uncorrelated noise sources are pronounced at random instances with varying durations of random noises. Therefore, the averaged background noise may not be representative, especially when a testing environment is subject to unsteady background noise. For example, the sampling of the background noise over an extended period of time (e.g., monthly, quarterly, seasonal, yearly, etc.) may not explain fluctuations of the background for the given short time periods, e.g. 30

sec., because sources of the background noise, such as meteorological condition, traffic, construction, human occupants, etc., are randomly combined.

In this light, the ever-changing nature of the background noise is the reason that we need to measure background noise per each sound testing. Furthermore, the background steadiness assessment should not simply be limited to the uncertainty analysis, which states confidence levels of the test data with respect to the entire population mean of the background noise. Instead, the assessment needs to reflect the background variation during a test period by using a stochastic analysis of a single set (for an individual test) of measurement data.

5. An Impact of an Improved Psychoacoustic Model on Fan Loudness and Acoustic Ratings

Conventional loudness rating procedures for the residential ventilation devices, as shown in AMCA 301, HVI 915, Energy Star Program, etc., are based on ANSI S3.4-1980 [19] and a psychoacoustics study conducted by Stevens [20]. The procedure proposed by ANSI S3.4-1980 is proven to be effective to predict broadband homogeneous spectra especially in the mid-frequency region [21]. However, limitations on the standard procedure have been found in the recent three decades since the ANSI procedure was implemented [22]. First, the ANSI S3.4-1980 fails to give accurate calculations of tonal components, which are relatively prevalent in rotating machineries and air moving devices. Second, the loudness calculation procedure in the ANSI S3.4-1980 is not based on the state-of-the-art human equal-loudness contour in ISO 226:2003. The use of outdated equal-loudness contours in ANSI S3.4-1980 has a broad impact on

accurate and precise loudness determinations, especially because the equal-loudness contour is the backbone of the loudness calculation procedure. Third, ANSI S3.4-1980 does not provide relationships between loudness levels in “phon”, which is sound levels especially designed to describe sounds that are equally loud to the human-hearing perception, and loudness in “sone”, which is used for a linear scale of loudness perception, for the loudness levels less than 20 phon. Of special importance, the 20 phon is far louder than the human hearing threshold (approximately 2 phon ≈ 0.003 sone). Considering that the noise emissions of the modern residential ventilation devices has been reduced in the recent decades, the lack of relationships near the hearing threshold is a critical issue. In order to address the lack of the lower-loudness-range relationships between “phon” and “sone”, AMCA 301 and HVI 915 have extrapolated the equal-loudness contour down to -0.02 sone. However, along with the revised equal-loudness contour such as ISO 226:2003, the extrapolated equal-loudness contours in AMCA 301 and HVI 915 need revisions.

CHAPTER II

STUDY OF BATHROOM VENTILATION FAN PERFORMANCE TRENDS FOR YEARS 2005 TO 2013—DATA ANALYSIS OF LOUDNESS AND EFFICACY[1*]

Overview

Whole-house ventilation, which is defined as systems that supply and exhaust or relieve ventilation air for a residence, has been a mandatory provision since the announcement of IECC 2012. As a result, an increasing number of publications and standards are now addressing residential ventilation in terms of performance and efficiency. In addition, loudness is increasingly addressed in standards and guidelines, especially in the last decade as it is now considered to be a significant factor for certified performance ratings of ventilation fans. Because of the above interest in fan performance, this paper provides statistics of bathroom ventilation fan tests and their results for an almost decade-long period from 2005 to 2013. Also, the paper interprets these statistics with regards to the recent development of residential ventilation standards and guidelines.

In order to investigate year-to-year changes, this paper first evaluates changes in loudness ratings for the test period 2005-2013, and its relevance to applicable standards, including ASHRAE 62.2. Then, noticeable transitions in loudness and efficacy in

[*] Reprinted from Energy and Buildings, Vol. 116, Wongyu Choi, Michael B. Pate, and James F. Sweeney, Study of bathroom ventilation fan performance trends for years 2005 to 2013—Data analysis of loudness and efficacy, pg. 468-477, Copyright (2016), with permission from Elsevier.

specific time frames are investigated. The test results of DC-motor high-efficiency bathroom fans are also compared to AC-motor fans. Relationships between performance variables and loudness are investigated, and formulated by developing regression models.

Introduction

Whole-house ventilation that supplies and exhausts or relieves ventilation air for a residence appeared as a new mandatory provision in the 2012 International Energy Conservation Code (henceforth, IECC) in section R403.5 [23]. Although the concept of whole-house ventilation has been discussed [24, 25] for the last two decades as a result of ASHRAE 62.2, the application of international mandatory regulations meant that ventilation fans must meet more robust requirements for performance and energy consumption throughout the qualification process. The Department of Energy (DOE) also announced a new residential fan efficiency code in 2012 [26] as an assisting description of IECC 2012 R403.5. As well as defining the concept of whole-house ventilation, the DOE 2012 code also provided quantitative measures for fan efficiency in terms of efficacy, which is defined as the ratio of volumetric flow rate (VFR) and power in units of $ft^3/W \cdot min$ or $L/W \cdot s$. For instance, bathroom fans whose volumetric flow rates are below 90 ft^3/min (42.5 L/s) are required in the code to meet a minimum efficacy of 1.4 $ft^3/W \cdot min$ (0.66 $L/W \cdot s$).

The introduction of a ventilation code to IECC 2012 escalated the necessity of studying performances and efficiencies of various ventilation fans. In addition, several governmental agencies have published U.S. household energy-consumption statistics

and trends, which has accelerated energy demand and consumption discussion. For instance, the Annual Energy Review (AER) and the Annual Energy Outlook (AEO) provide annual summaries and predictions for residential energy intensity in the U.S., which is measured by annual energy use per household unit [27, 28]. The AEO 2013 Reference case expects declines in the energy intensity of residential demand of about 22 percent from 97.2 million Btu (28.5 MW) in 2011 to 75.5 million Btu (22.1 MW) in 2040. With regards to electricity demand, a decrease from 12.3 MW to 11.5 MW from 2011 to 2040, which is about 6 percent, is anticipated. However, electricity consumption in heating, cooling, and ventilation continues to increase by 70 kWh per household in the same period with several facts in the recent AER and AEO explaining this increase. First, space cooling consumption is expected to increase by 42 percent, which overshadows space and water heating decreases of 20 percent. Second, although the AEO Reference case assumes improved efficiency as a result of standards, average household square footage is expected to expand from 1662 to 1858 ft^2 (154.40 to 172.61 m^2), which accordingly demands an increase in HVAC overhead. Based on these observations and forecasts, the IECC 2012 ventilation code is an important element in encouraging better indoor comfort while achieving higher energy efficiencies.

It is important to note that the ventilation performance rating requirements in IECC 2012 R403.5 are limited in scope to volumetric flow rate and efficacy. Missing from the requirements are noise limits even though loudness is a major factor affecting the performance of ventilation devices in the general context because 1) sound power

represents a thermodynamic loss due to turbulent and structural vibration [29], and 2) noise from the fan can have an influence on physical and psychological stress [30].

Several leading standards or publications, such as HVI 915[31], AMCA 301 [8], and ANSI/AHRI 260 [32], have established acoustic rating procedures for ventilation fans, with these rating procedures being widely accepted by industry and trade organizations. In addition, these procedures are routinely used by testing laboratories as they measure and evaluate fan noise performances. Furthermore, ASHRAE 62.2 specifies the maximum loudness level in units of sone for different types of ventilation fans [33]. For example, ASHRAE 62.2 specifies that demand-controlled mechanical exhaust fans with rated volumetric flow rates less than 400 ft^3/min or 200L/s be rated for loudness to a maximum of 3 sone. However, the same standard does not consider a minimum efficiency of mechanical ventilation fans in contrast to other standards such as IECC 2012. In addition to the lack of efficiency requirements, ASHRAE 62.2 does not categorize different types of 'demand-controlled' ventilation fans for the sound rating. It is widely accepted fact that kitchen range hoods operate at higher volume flow rates and thus generate more noise than bathroom ventilation fans, with both of them being demand-controlled. Furthermore, most bathroom fans run at volumetric flow rates under 130 ft^3/min (61.4 L/s) [34]; therefore, using 3 sone for fans less than 400 ft^3/min is not a practical limit for bathroom fans. It should also be noted that IECC 2012 R403.5 classifies volumetric flow rates for bathroom fans into two range categories, namely below and equal to or greater than 90 ft^3/min (42.5 L/s).

Manufacturers are interested in sound ratings of residential fans, and as such, they view a residential ventilation fan performance as not being merely limited to air flow performance but also to acoustic and noise characteristics. In response to industry demands, the Home Ventilating Institute (HVI) and the Air Movement and Control Association (AMCA) as well as the aforementioned rating standards and publications now provide requirements for certified sound tests for ventilation fans.

Various studies by academic and governmental sectors have been conducted for evaluations and predictions of the residential ventilation performances for different types of fans. As a milestone to the Energy Star 2.0 Program, the U.S. Environmental Protection Agency (EPA) conducted analysis on 51 different fans having different volumetric flow rates from 50 ft^3/min (24 L/s) to 1,200 ft^3/min (566 L/s) [2]. The agency found large efficacy distributions, ranging from 0.2 ft^3/W·min (0.1 L/W·s) to 8.5 ft^3/W·min (4 L/W·s), and they concluded that there was no clear trends for different types of ventilation fans in their efficacies versus volumetric flow rates. This observation of no clear trends is also supported by other studies that categorized types of ventilation fans, and conducted performance evaluations for individual fans. For instance, studies performed by Delp and Singer [1, 3] revealed that many residential range hoods or cooking exhaust devices are operating more than 200 ft^3/min or 90 L/s at 0.1 in water gauge or 25 Pa, while generating noises more than 4 sone of loudness. However, the study was limited to testing only 7 to 15 range hoods depending on installation type and price, with only limited details of energy efficiencies and noise being presented. Studies for other residential ventilation devices such as bathroom fans have had the same

constraints of limited sample volumes, i.e. the number of ventilation devices tested. For bathroom ventilation fans, most studies have been conducted for ventilation schemes and air exchange rates along with different ventilation configurations [4, 7], operation schemes [35], and electrical power sources and motors [5, 6]. However, those studies were limited in size and did not provide extensive performance measurements and evaluations. Of special importance, an energy performance study by McWhinney *et al.* pointed out that ventilation fans can be expected to have potentials of energy savings up to 65 %, which is significant considering such a large market (nearly 6 million units) being open [36]. Therefore, a need exists for not only more studies of residential ventilation devices in terms of multi-year performance analysis, but also a study of an extensive number of ventilation devices.

As an HVI certified testing laboratory for residential ventilation devices, the laboratory facilities used in this study have conducted both airflow and sound tests of ventilation devices for several decades. Therefore, this paper summarizes the sound and airflow performance of bathroom ventilation fans over a 9-year period from 2005 to 2013 with the purpose being to evaluate and analyze fan performance from both statistical and established energy code standpoints. Specifically, this paper presents loudness as a sound performance, and fan efficacy as an energy performance for a large number of multi-year bathroom ventilation fan tests. In addition to an evaluation and analysis of almost a decade of laboratory data, this paper also develops relationships and correlations among efficacies, sound ratings, and other variables

Testing Procedure

The data taken, evaluated, and analyzed in this study utilized a semi-reverberant sound test chamber and test set-up shown in Figure 2-1 which conforms to ANSI standard S12.51 and HVI 915 [31, 37].

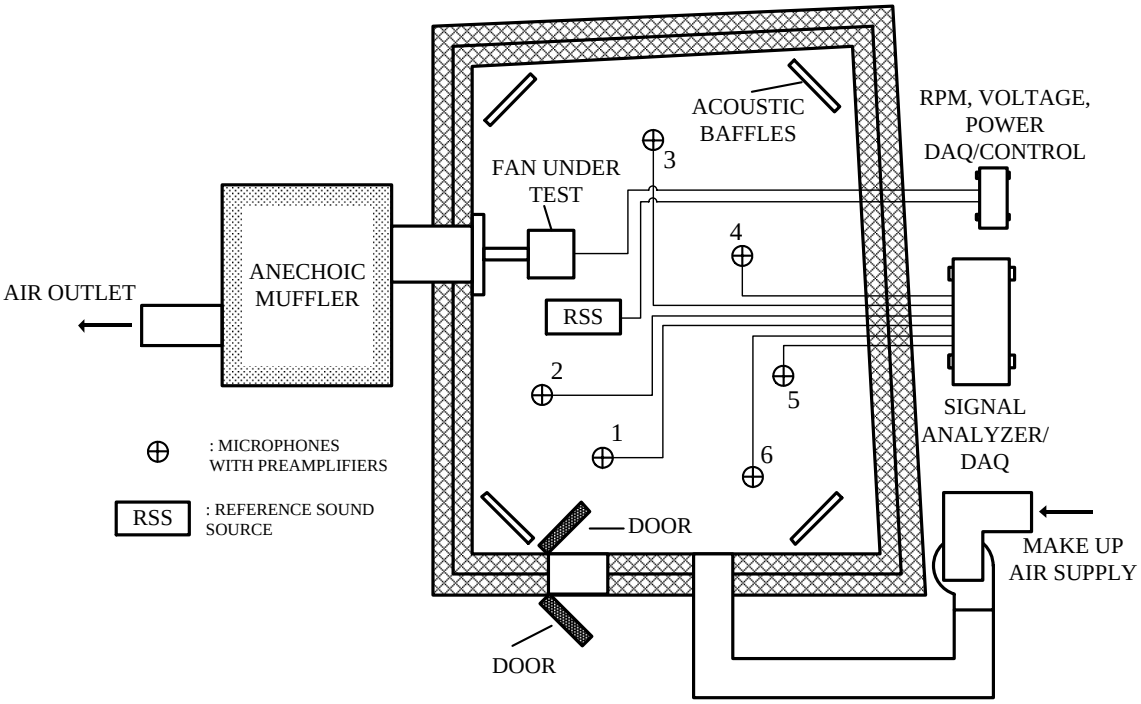

Figure 2-1 Schematic of semi-reverberant sound test chamber and instruments

The test chamber is constructed with heavy duty, multi-layer insulating walls in order to eliminate any undesired infiltration of airflow as well as noise transmissions through the structure. Also, as per standard requirements, the test chamber has non-parallel walls for the purpose of obtaining the uniform reverberation characteristics over all surfaces. At each of the four chamber corners, acoustic baffles are located and

equipped in order to minimize three-dimensional standing waves. The chamber inlet is connected to an insulated labyrinthine duct with a throttling device for adjusting the static pressure and volumetric flow of a fan under test. Also, the chamber outlet is connected to an anechoic muffler that prevents the entry of environmental sounds. Six random incident microphones and preamplifiers are used for all tests, and their placement has been determined by the multiple-microphone qualification process as described in ANSI S12.51. Test conditions including temperature, humidity, atmospheric pressure, and the fan static pressure are monitored and controlled by data acquisition devices and control software. Relevant instruments and data acquisition equipment along with corresponding uncertainties are listed in Table 2-1. Of special importance for every instrument, certified calibrations are maintained so that the uncertainty of the resulting sound data can be analyzed.

Table 2-1 Sound test equipment list with uncertainty

Equipment Name	**Description**	**Uncertainty**
Microphones with preamplifiers	Sound pressure measurement in dB (15 – 148 dB(A), 3.15 – 20000 Hz)	0.35dB
Reference Sound Source (RSS)	Generating reference sound (sound pressure level at 83.38 dB(A))	0.54 dB
Data analyzer and data acquisition device	Performing frequency domain analysis (0 – 25.6 kHz, 5mV – 5 V RMS)	0.10 dB
Voltage meter	Measuring and monitoring voltage (0-1000 V)	0.068 V (up to $300V_{AC}$)
Tachometer	Measuring Fan RPM (5 – 999990 RPM)	0.50 RPM

The procedure used for measuring the sound pressure levels of a fan in the semi-reverberant chamber conforms to HVI 915. Each set of sound tests for a fan consists of 4 major steps, namely the unit, the first background, the RSS, and the second background measurement. Pre-test setup and post processing also take place. In the pre-test setup, a fan under test is warmed up by operating it for at least 30 min, or until the power and voltage reading are stable at any given operating value (e.g., 35 W at 120 V), whichever is longer. After the fan is mounted inside the chamber, the volumetric flow rate, fan RPM, and static pressure are adjusted by using the throttling device connected to the make-up air supply duct. The sound test then follows the following four major steps.

1. The sound pressure level, L_p^{UT}, is measured for the fan unit under the specified operating static pressure and rpm, which were previously measured in an airflow test (FAN+BKG).
2. The background sound pressure level, L_p^{B1}, is measured after the unit is turned off (BKG1).
3. The sound pressure level, L_p^{RSS}, of the reference sound source is measured (RSS+BKG).
4. A second background sound pressure level, L_p^{B2}, is taken (BKG2).

During each sound test, the signal analyzer performs real-time signal processing in order to transform the time-domain sound-pressure measurements into the 1/3 octave band frequency domains from 50 to 10,000 Hz. After completing a fan sound test, the background steadiness is determined by comparing two sets of background measurement

data, BKG1 and BKG2, in one third octave frequency bands. The HVI 915 document puts an arithmetic difference limit on the background sound pressure of each one-third octave band. For example, if the limit of the 630 Hz band is 1 dB and the arithmetic difference between BKG1 and BKG2 is less than the limit, then background steadiness is achieved at this 630 Hz band.

The measured data is converted to a loudness index through a series of conversions and calculations during post processing. The semi-reverberant fan sound pressure levels are obtained by eliminating the background noise (BKG1), and then the semi-reverberant sound pressure levels are converted to the sound pressure levels in a spherical-free field at a distance of 5 ft (1.52m) from the fan under test. The loudness rating in sone is then obtained by using the ANSI S3.4 and HVI 915's equal-loudness indices that are weighted contours for human-dominant tone sensitivity as a function of sound pressure levels and one-third octave band frequencies [31, 38]. Loudness at each band can be obtained by looking up the loudness at the corresponding band frequency for the converted sound pressure. The single-value loudness rating in sone is then obtained by adding 85 percent of the maximum loudness (in sone) at the most dominant band and 15 percent of the sum of the other 23 loudness values as directed by ANSI S3.4.

Statistical Makeup of Sound Test Data

The flow and noise performance data to be evaluated and analyzed for fans in this paper consists of 1532 individual fan tests performed over the period from 2005 to 2013. The number of bathroom fan models tested was 947, which represents 48 different

manufacturers. Because of the numerous physical difference among the fans, each fan required a different setup (e.g., discharge direction, discharge size, grille and fixture type, etc.). Table 2-2 is a statistical makeup summary of the fan test data analyzed and evaluated for sound in this paper.

Table 2-2 Statistical makeup of sound test data

Classification	Number
Sound tests performed	1532
Fan models tested	947
Fan manufacturers represented	46

Loudness Rating Statistics by Year

The laboratory used in this study has performed loudness rating tests along with airflow performance tests since the adoption of HVI 915 in the early 2000s. As the loudness rating standards and procedures evolved to provide more in-depth information to fan manufacturers, test data have been recorded in different types and forms. All acoustic data recorded in our laboratory has undergone post-processing and data-mining by using homebrew programs based on visual basic and C++. It should be noted that the loudness data in this paper were obtained by operating all fans at external static pressures of 0.10 in water gauge (24.9 Pa). Furthermore, prior to performing sound tests on any fans, airflow measurements were performed to measure the static pressure and airflow rates following procedures described in the AMCA 260 standard [39].

Figures 2-2 and 2-3 are box plots of the loudness distributions of bathroom fans for the test period 2005-2013 in two volumetric flow rate groups, namely less than 90

ft^3/min(42.5 L/s) and more than or equal to 90 ft^3/min(42.5 L/s). Of special note, 90 ft^3/min (42.5 L/s) was chosen as the border of the two volumetric flow rate groups throughout this study in accordance with VFR groups delineated by IECC 2012 R403.5 [23], and Energy Star Programs [40, 41], which are discussed in an earlier section. The statistical data of importance for each of 9 years such as average, interquartile range (IQR), and range are presented in Figures 2-4, 2-5, and 2-6, respectively.

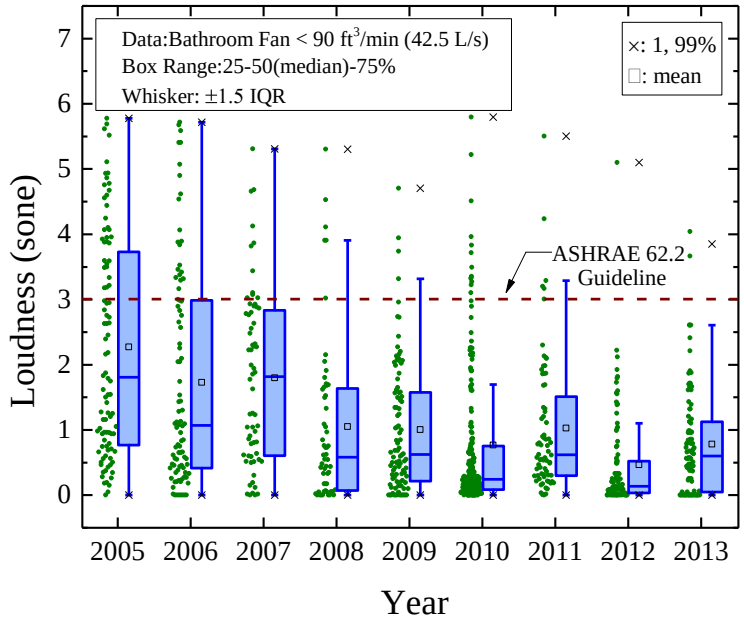

Figure 2-2 Annual loudness of bathroom fans less than 90 ft^3/min (42.5 L/s)

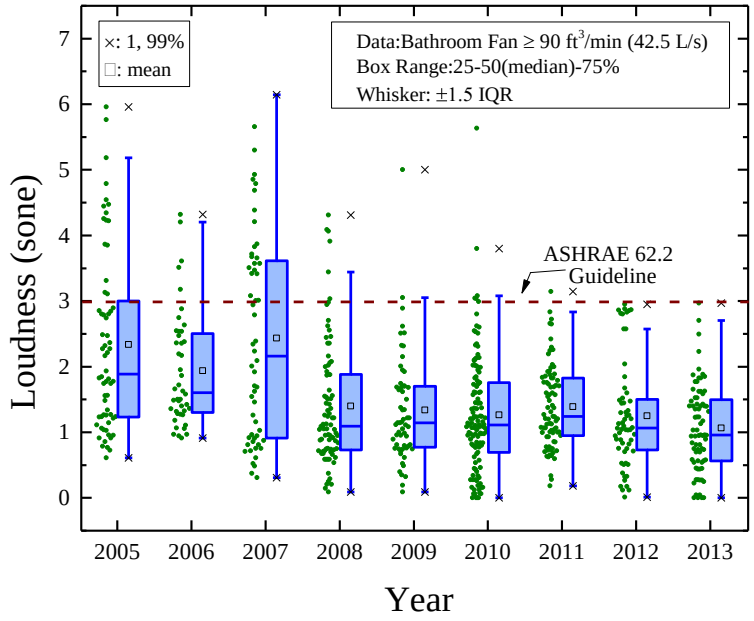

Figure 2-3 Annual loudness of bathroom fans greater than 90ft^3/min (42.5 L/s)

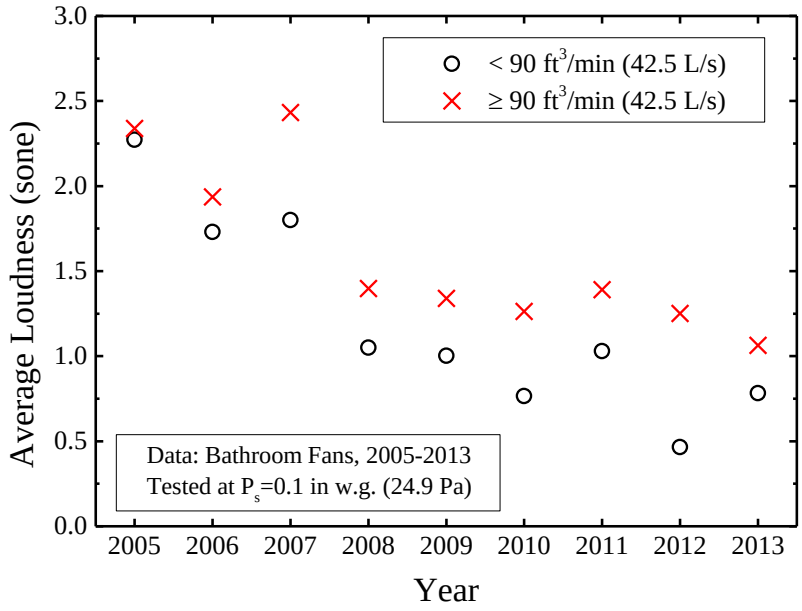

Figure 2-4 Annual average loudness of bathroom fans

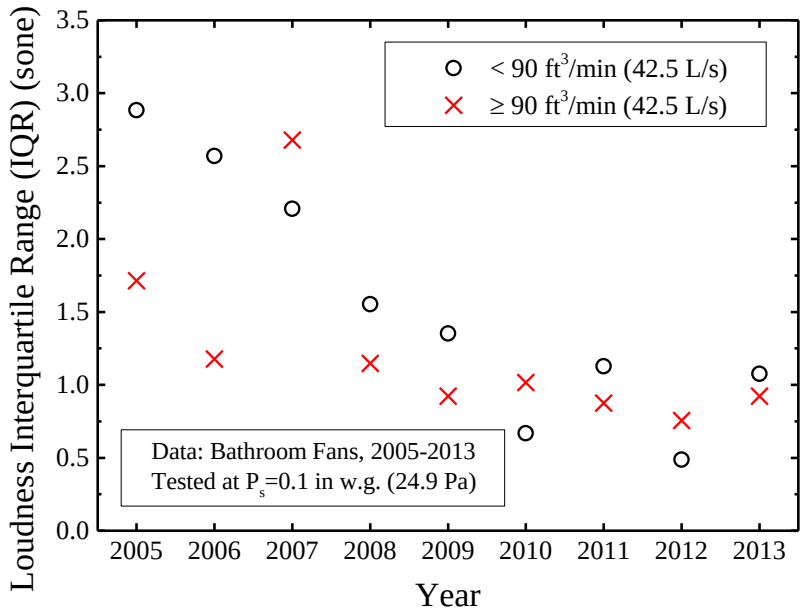

Figure 2-5 Interquartile range (IQR, Q3-Q1) of bathroom fan annual loudness

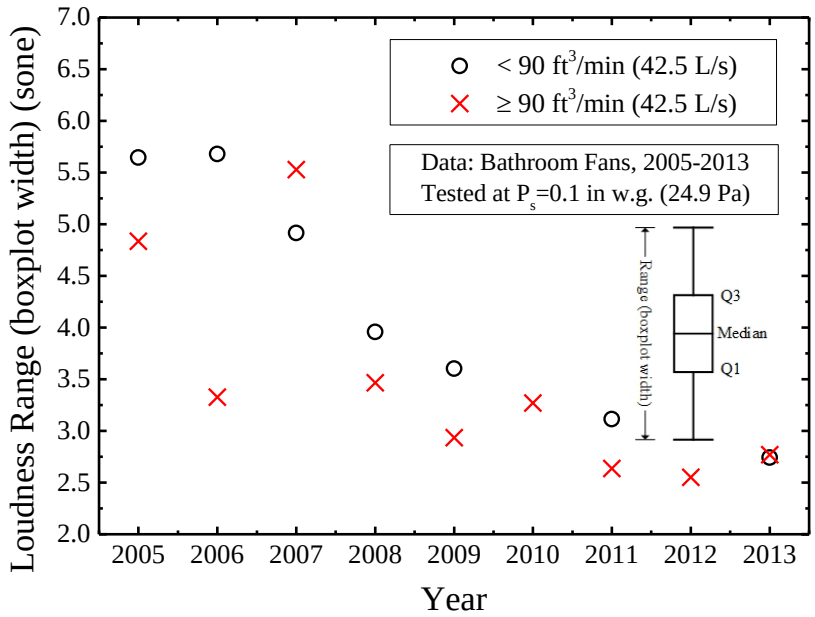

Figure 2-6 Annual loudness range (boxplot width) of bathroom fans

The reason for dividing the fans into two groups of low and high volumetric flow rates, with 90ft^3/min (42.5 L/s) as the dividing line, was to analyze acoustic performances by following the IECC 2012 ventilation fan criteria, which divides fans into two volumetric flow rates, namely above and below 90 ft^3/min (42.5 L/s). For the fan data plotted in Figures 2-2 and 2-3, 65.5 percent of the fans have rated flow rates under 90 ft^3/min (42.5 L/s), which are shown in Figure 2-2, and 34.5 percent of the fans are above or equal to 90 ft^3/min (42.5 L/s) , which are shown in Figure 2-3. It can be also observed in Figures 2-2 and -23 along with averages plotted in Figure 2-4 that fan loudness has decreased over the years from 2005 to 2013, with the decreasing loudness trends indicating better designs for fan noise reductions.

Along with the average loudness reductions, which can be observed in Figure 2-4, it is also important to look how fan loudness ratings are distributed and scattered in each testing year. Figures 2-5 and 2-6 provide representations of loudness distributions in terms of the interquartile range (IQR) and the box-plot width from 2005 to 2013. For example, for fans under 90 ft^3/min (42.5 L/s) in 2005, half of the fan loudness was distributed within 2.8 sone near the median loudness of 1.9 sone; however, in 2013, half of loudness ratings was located within 1.0 sone near the median loudness of 0.6 sone. The shrinkage of boxplot width and IQR from 2005 to 2013 denotes that the loudness of samples are increasingly amassed near median loudness ratings over the years. Of even greater importance is the fact that the fans have become quieter over the years as evidenced by the median loudness decreasing from 1.9 sone to 1.0 sone in 2013.

Comparing the results in Figure 2-2 through 2-6 with a timeline of publications provides insight into how governing fan standards and guidelines for fan noise and vibration control have influenced fan design and performance in actual practice. For example, HVI 915 and fan certification tests started in the third quarter of 2007, and in the following year there were noticeable reductions in fan noise from 1.82 to 0.57 sone for fans under 90 ft^3/min (42.5 L/s) and from 2.17 to 1.10 sone for fans above or equal to 90 ft^3/min (42.5 L/s). Also, it should be noted that ASHRAE 62.2 first included in 2007 a fan sound rating procedure in accordance with HVI 915, which followed the test setup standard ANSI/AMCA 300 [31, 33, 42]. One can assume that all of these standards and guidelines affected the design of ventilation fans in the direction of making fans more quiet over time from 2005 to 2013, as evidenced by 66 and 53 percent median loudness decreases for fans under 90 ft^3/min (42.5 L/s) and above or equal to 90 ft^3/min (42.5 L/s), respectively.

Efficacy Statistics for AC and DC-Motor Fans by Year

Fan efficacy, which is defined as the ratio of volumetric flow rate and power in units of ft^3/min·W, is widely used as an efficiency measure in codes and regulations such as IECC 2012. This approach is in contrast to non-dimensional expressions of efficiency, which can be also used for small air-moving devices such as residential ventilation fans. Following HVI recommendations, measured and recorded efficacies were determined as a part of airflow performance tests for all of the fans presented in this paper. In addition, all data in this section has undergone the same data-processing procedures that were described in the previous section.

Earlier in this paper when fan loudness was analyzed year-to-year, it was not necessary to distinguish between motor types, either AC or DC, because fan loudness is not only influenced by motor type. Rather, the fan loudness is a complex function of the duct and component design including enclosures, fan outlets, grilles, etc. [43, 44], the acoustic properties of materials [45] including transmittance, acoustic impedance, longitudinal/shear/surface velocities, etc., and, finally, fan/impeller dynamics in terms of fan/impeller type, rotational speeds, blade passing frequencies, cut-off distance, etc. [46, 47]. In addition, the human response to the noise, which is the basis of the psychoacoustic term loudness, is another major contribution to the fan loudness assessment [48, 49]. However, because efficacy is more directly influenced by the fan motor type, it is now necessary to consider motor type in the efficacy analysis.

As a start to the year-to-year analysis of efficacy, it is important to note that over the years there is an increased usage of DC-motor fans resulting in an increased number of performance tests, which is the result of the introduction of the ENERGY STAR Most Efficient Program [40, 41], whose ventilation fan criteria has been developing since 2011. As per program requirements developed in 2011 and started in 2013, the minimum efficacy for bathroom fans to obtain a "Most Efficient" recognition was 7.5 ft^3/W·min (3.5 L/W·s) for fans less than 90 ft^3/min (42.5 L/s) and 6.8 ft^3/W·min (3.2 L/W·s) for fans greater than 90 ft^3/min (42.5 L/s). Meeting these more stringent efficacy requirements has resulted in an increased usage of DC motors, which are more efficient that AC-motor fans. When considering a realistic time frame from fan design to

certified testing and then to market availability, which can take a year or more, the growing number of DC-motor fans tested as shown in

Table 2-3 seems reasonable, especially as manufacturers anticipated mandated energy efficiency requirements even before 2013 or 2011 for that matter. Evidence of this trend can be seen in

Table 2-3 year-to-year data as a percent of all tests from 2005 to 2013, which shows that DC-motor fan tests went from 27.6% in 2009 to 41.4% in 2010. Further evidence of this trend is that in the last year of 2013, which is the last year that fan data is available in this paper, DC motors make up 40.5% of the total tests, which is in contrast to the first year of 2005 when DC-motor fans represented only 5% of the total tests.

Table 2-3 DC-motor fan testing statistics

Year	Number of DC-motor Fans Tests (percent of total)	Number of DC-motor Fan Models
2005	8 (5.0 %)	2
2006	26 (19.4 %)	3
2007	0 (0 %)	0
2008	12 (8.5 %)	1
2009	43 (27.6%)	5
2010	139 (41.4 %)	28
2011	27 (17.6 %)	17
2012	70 (45.5 %)	11
2013	72 (40.9 %)	20

Figures 2-7 and 2-8 are year-to-year distributions and box plots of AC motor fan efficacies for the period 2005-2013. In contrast to DC fan technology, as will be shown later, AC-motor fans have not experienced significant breakthroughs in efficacy

improvements during the testing period of 2005 through 2013. The lower efficacies of AC-motor fans compared to the higher efficacies of DC-motor fans can also explain the reason why the efficacy of AC-motor fans in Figure 2-7 and 2-8 show rather narrow distribution in the efficacy of less than 6 $ft^3/W \cdot min$ (2.83 $L/W \cdot s$). The IQR of each box in Figures 2-7 and 2-8 has not deviated significantly since the year 2007, which strongly suggests that a majority of AC-motor fans, namely about 87.5 percent, already meet the IECC 2013 efficacy requirements.

Similar to the AC motor fan plots in Figures 2-7 and 2-8, the year-to-year efficacy data for DC-motor fans is plotted in Figures 2-9 and 2-10. An obvious difference between AC and DC motor fans tested is that the number of DC-motor fans tested, which can be observed by comparing the plots, is considerably less than the number of AC types except in recent years. Besides the fact that all samples satisfy IECC 2013 efficacy requirements, most of the DC-motor fan samples since 2009 (about 89.9 percent) meet ENERGY STAR Most Efficient Recognition 2013 (henceforth, ESMER 2013) requirements. However, Figures 2-9 and 2-10 reveal that the efficacy among the tested fan samples varies more appreciably in DC-motor fans compared to AC-motor fans. These differences can possibly be a statistical anomaly because of either a lesser number of DC-motor fans having been tested compared to AC-motor fans or because of the relatively early stages of DC-motor fan development and introduction to the residential ventilation sector.

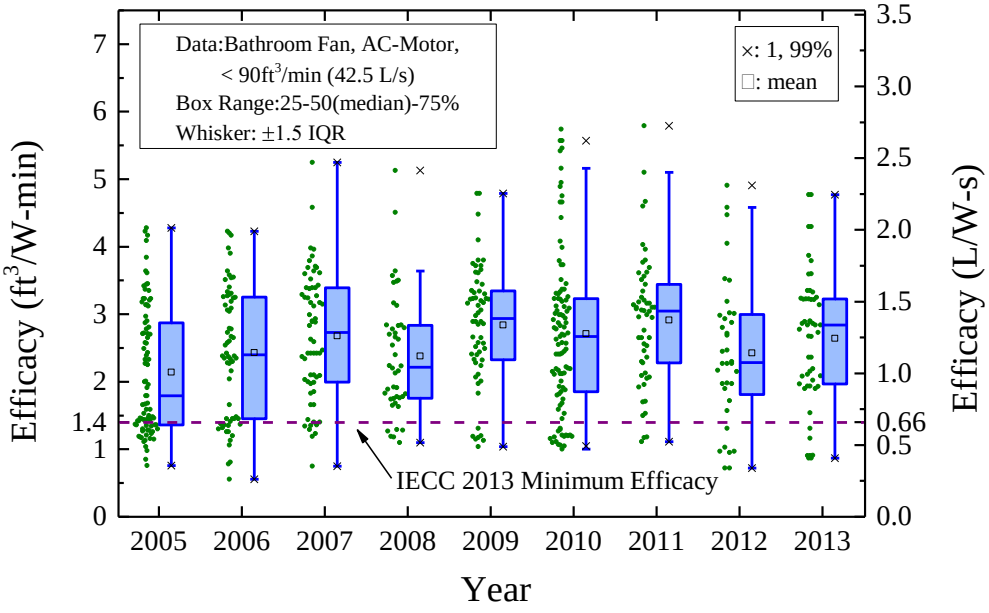

Figure 2-7 Annual efficacy of AC-motor bathroom fans less than 90 ft^3/min (42.5 L/s)

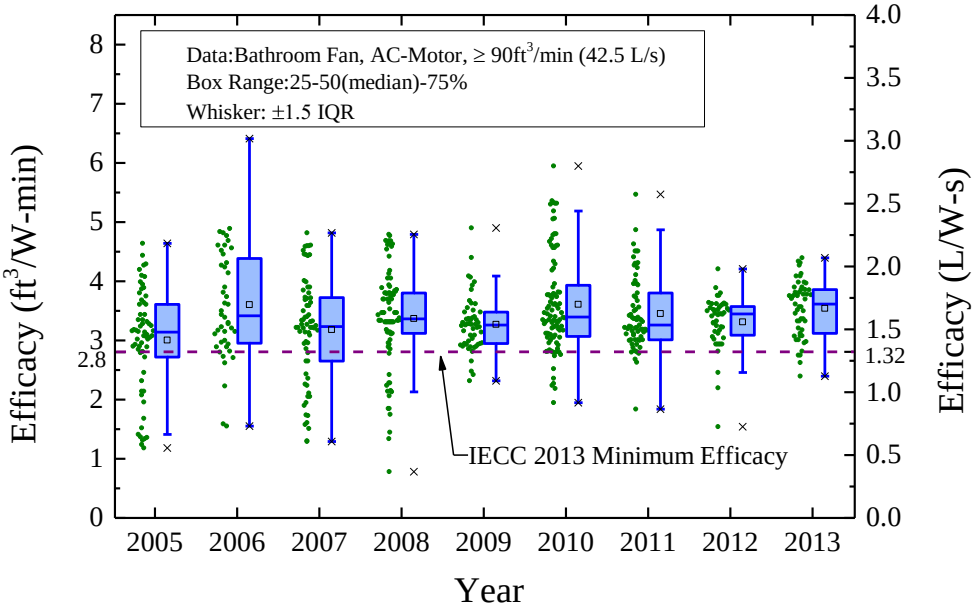

Figure 2-8 Annual efficacy of AC-motor bathroom fans greater than 90 ft^3/min (42.5 L/s)

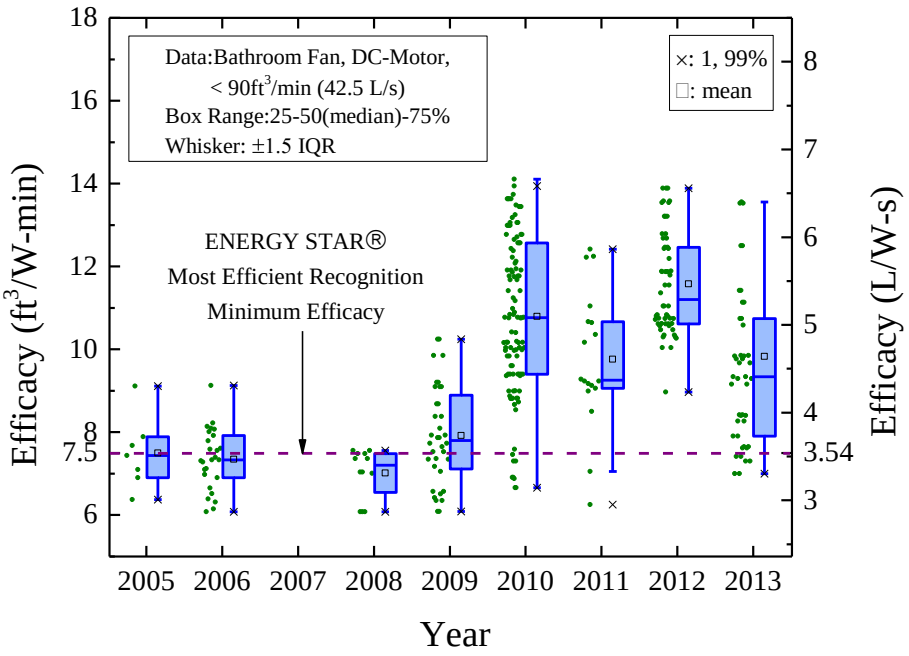

Figure 2-9 Annual efficacy of DC-motor bathroom fans less than 90 ft^3/min (42.5 L/s)

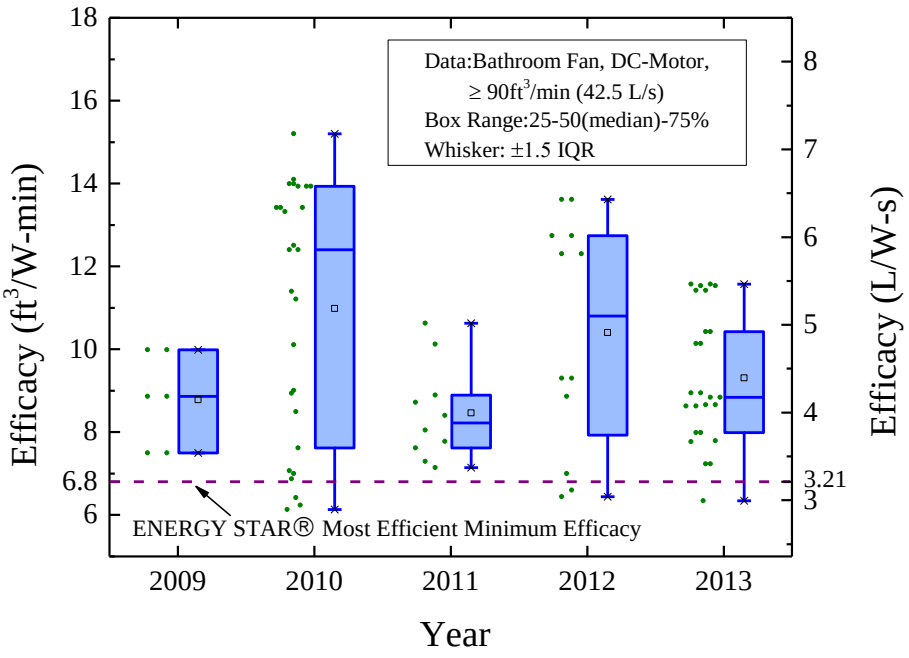

Figure 2-10 Annual efficacy of DC-motor bathroom fans greater than 90 ft^3/min (42.5 L/s)

As noted previously, ESMER 2013 has set different efficacy baselines for the two different groups of volumetric flow rates, namely one group less than 90 ft^3/min and the other equal to or higher than 90ft^3/min. Efficacies for the lower and higher flow rate groups are shown in Figures 2-9 and 2-10, respectively. It is noticeable that for both volumetric flow rate categories most of the samples have satisfied ESMER 2013 baselines since 2010, which is also the time of an abrupt increase in the number of tests, especially DC motor fan tests. One can assume that the energy performance of DC-motor fans significantly increased as they became the subject of more interest to manufacturers, which was then followed by more stringent energy codes such as ESMER 2013. In addition, it can be observed in Figure 2-9 and 2-10 that most of the DC-motor fan efficacies for the period 2010 through 2013 fall between 8 and 14 ft^3/W·min (3.78 and 6.61 L/W·s) for both volumetric flow rate groups.

Another observation on DC-motor fans for the same period, namely 2010 through 2013, is a weak relationship between fan variables, such as volumetric flow rate and efficacy. This relationship can be seen in Figure 2-11, which is a scatter plot of volumetric flow rate versus efficacy for DC-motor fans tested for the period from 2010 to 2013. Also shown in Figure 2-11 is a regression curve with the regression equation and coefficient of determination (R^2) being given as follows

$$\begin{cases} y = 6.3113 + 0.1298x - 0.0087x^2 \\ R^2 = 0.1384 \end{cases} \tag{2-1}$$

, where R^2 is defined as:

$$R^2 \equiv 1 - \frac{\sum (y_i - f_i)^2}{\sum (y_i - \bar{y})^2} \tag{2-2}$$

with y_i, $\bar{y}$, and f_i mean actual efficacy, mean efficacy, and estimated efficacy by the regression, respectively.

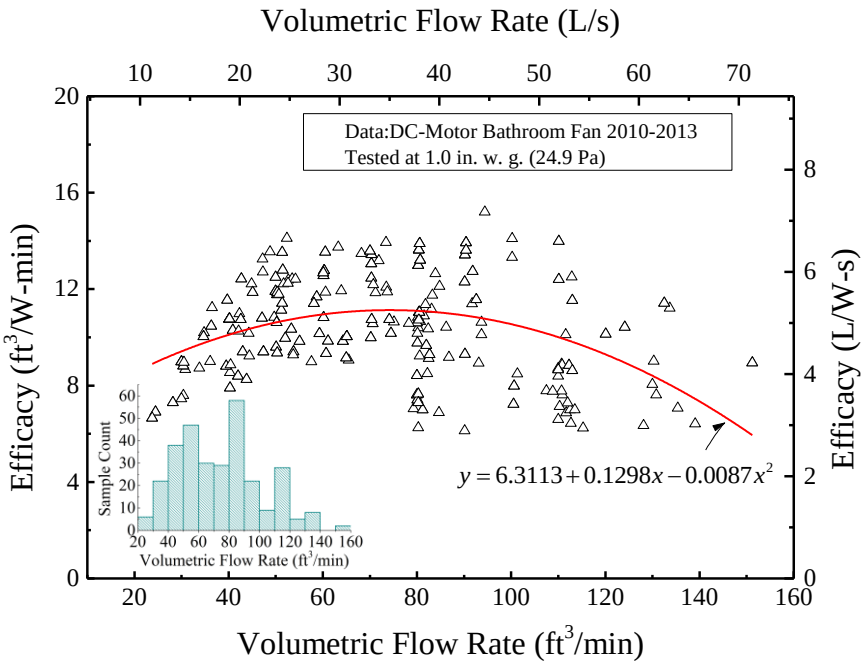

Figure 2-11 Scatter plot and regression curve of DC-motor fans since 2010 in terms of efficacy and volumetric flow with the inset showing the histogram of volumetric flow rates

Because of the low R^2 values, physical insight based on this correlation might not be achievable; instead, Figure 2-11 with examples of efficacy distributions over any given volumetric flow rate range might be used to provide understanding. For example, fans exhibiting volumetric flow rates within 80-90 ft^3/min (37.76-42.48 L/s) occupy a

significant portion of samples in Figure 2-11, and their efficacies vary considerably. However, as indicated by the regression curve results, for this volumetric flow range a better efficacy above 10 ft^3/W·min (4.72 L/W·s) results compared to other volumetric flow ranges.

The above trends are comparable to previous EPA findings where the agency reviewed data and designs from 51 AC-motor fans and asserted that no clear relationship exists between efficacy and volumetric air flow rate [2]. The EPA findings may in fact be valid if one attempts to find a single relationship for different types of ventilating fans with different designs. However, it is quite possible to assume that relationships among fan parameters exist for fans of the same, specific type of design, such as the bathroom fans shown in Figure 2-11.

Another discernible trend shown in Figure 2-12 is a change in fan efficacy between two years of 2007 and 2008. Specifically, about 8.5 percent of samples exhibited enhanced efficacies greater than 6 ft^3/W-min (12.7 L/W-s) in 2008 while there were none in 2007. These trends are also evident in Figure 2-12 as one compares the mean fan efficacies for 2007 and 2008.

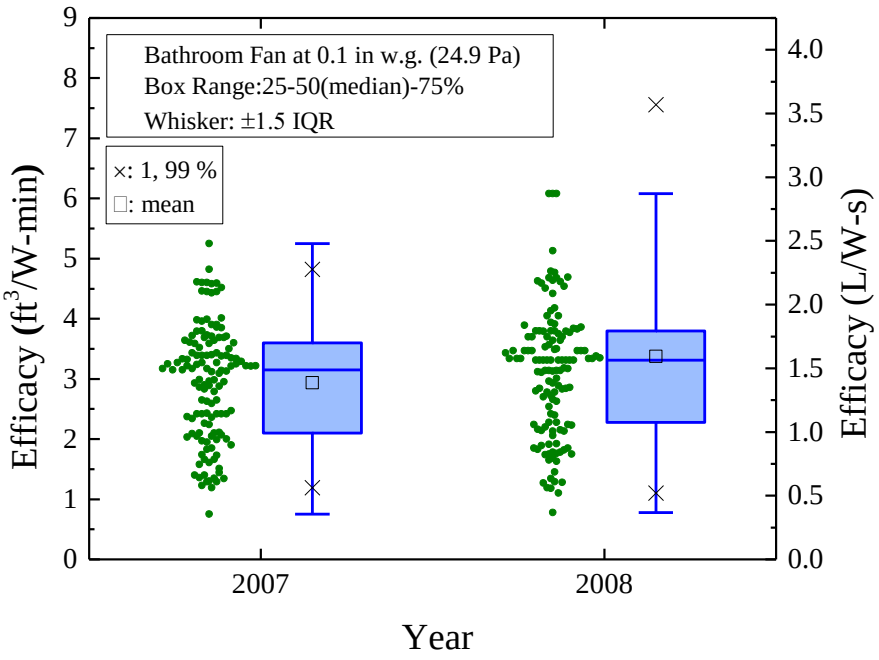

Figure 2-12 Bathroom fan efficacy in 2007 and 2008

An efficacy exceeding 6 ft^3/W-min (12.7 L/W-s) is considered to be a 'higher' efficacy, and it has not been observed in any AC-motor bathroom fan. As shown in the efficacy distribution and box plots in Figure 2-12, none of the samples in 2007 exceed 6 ft^3/W-min (12.7 L/W-s). However, fans that features efficacies that exceed 6 ft^3/W-min (12.7 L/W-s) in 2008 in Figure 2-12 were operated by a DC motor. Even though DC-motor bathroom fans were produced earlier than 2008, most of the DC-motor fan testing has been performed since 2008.

Table 2-3 summarizes the number and models of the DC-motor fans tested, and it can be noted that the DC-motor fan testing in each year throughout the test period 2009-2013 occupies an increasing proportion of units tested.

Relationships in Efficacy and Loudness

Additional analysis was performed by studying the relationship between fan efficacy and loudness by interpreting AC and DC fan data for at the two flow rate ranges. Specifically, Figures 2-13 through 2-16 are scatter plots showing fan efficacy versus loudness (sone), along with regression lines for AC and DC bathroom fans operating in the two volumetric flow rate ranges.

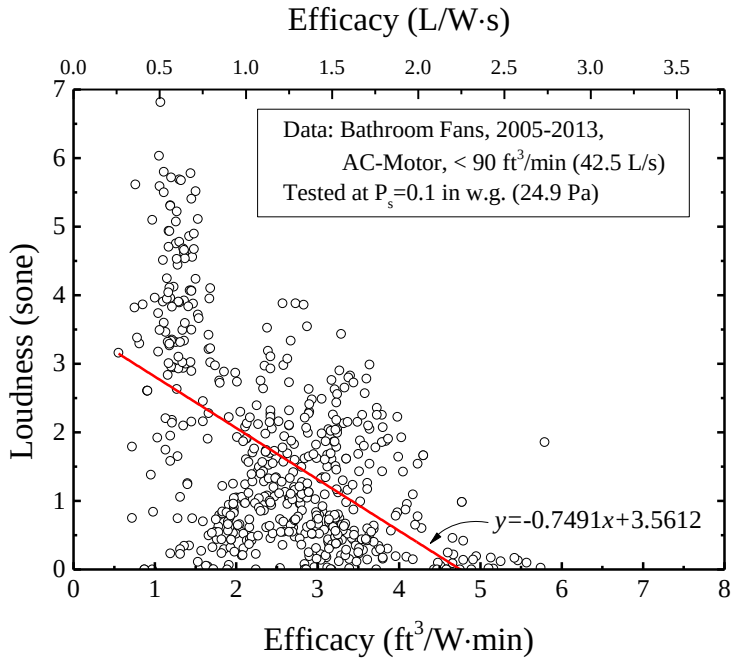

Figure 2-13 Efficacy and loudness of AC-motor fans less than 90 ft^3/min (42.5 L/s)

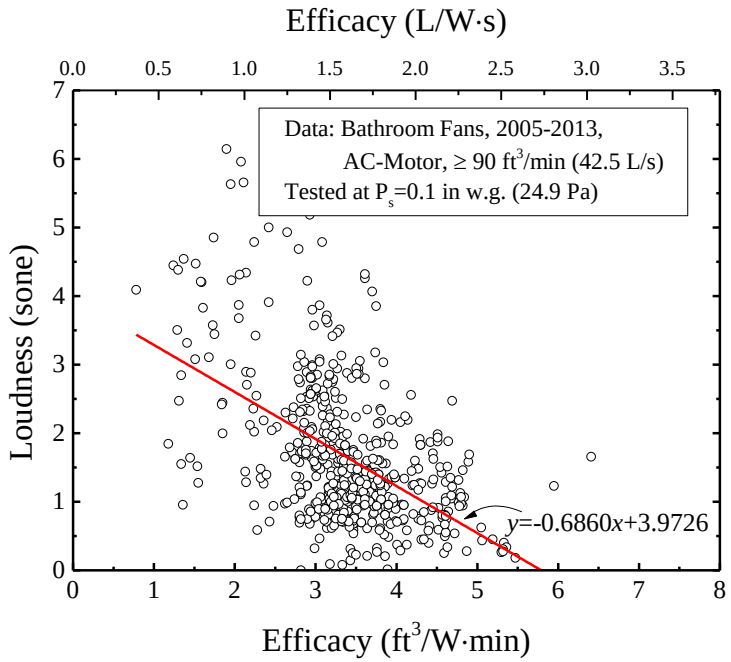

Figure 2-14 Efficacy and loudness of AC-motor fans equal to or greater than 90 ft^3/min (42.5 L/s)

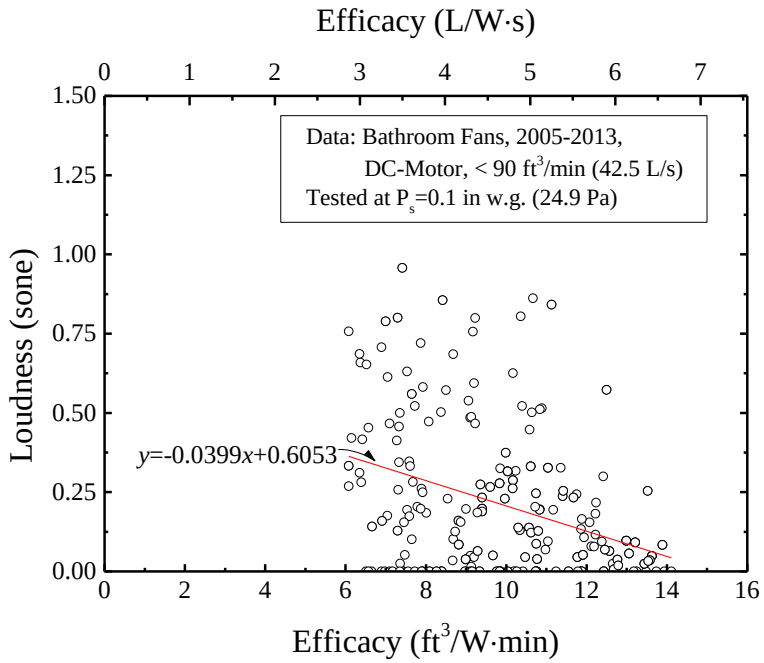

Figure 2-15 Efficacy and loudness of DC-motor fans less than 90 ft^3/min (42.5 L/s)

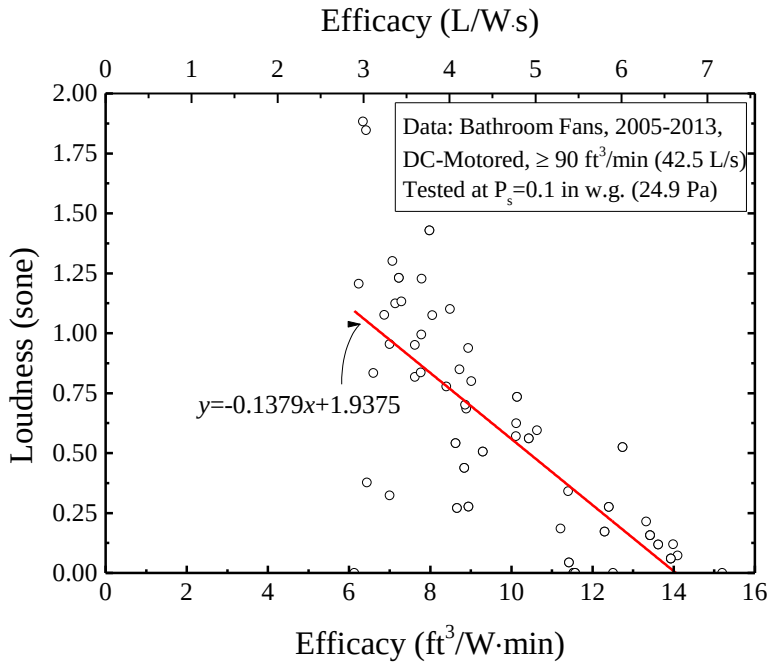

Figure 2-16 Efficacy and loudness of DC-motor fans equal to or greater than 90 ft^3/min (42.5 L/s)

Linear regression expressions showing the relationships of efficacy and loudness along with their R^2 values for each case are shown in Figure 2-13 through 2-16 and formulated in the following equations as follows:

For AC-motors, < 90 ft^3/min (42.5 L/s) – Figure 2-13:

$$y = -0.7491x + 3.5612$$
$$R^2 = 0.2862 \quad (2\text{-}3)$$

For AC-motors, ≥ 90 ft^3/min (42.5 L/s) – Figure 2-14:

$$y = -0.6860x + 3.9726$$
$$R^2 = 0.2503 \quad (2\text{-}4)$$

For DC-motors, < 90 ft^3/min (42.5 L/s) – Figure 2-15

$$y = -0.03986x + 0.6053$$
$$R^2 = 0.1154 \quad (2\text{-}5)$$

For DC-motors, ≥ 90 ft^3/min (42.5 L/s) – Figure 2-16

$$y = -0.1379x + 1.9375$$
$$R^2 = 0.5442 \qquad (2\text{-}6)$$

The low R^2 values and large loudness scatters for any given flow rate is not surprising considering that the database represents 47 different manufacturers, with each having their own individual fan designs. Also, it is important to note that because the R^2 values are quite low these relationships cannot be used to predict one parameter from the other; however, they can be used to show the overall trends of decreasing efficacy with increased loudness. Also of importance, the above 4 relationships can be used to provide an overall comparison of the behavior of AC and DC motors in the low and high volumetric flow ranges. For ease of comparison these four curves are presented on the same plot in Figure 2-17 and in the same table in Table 2-4.

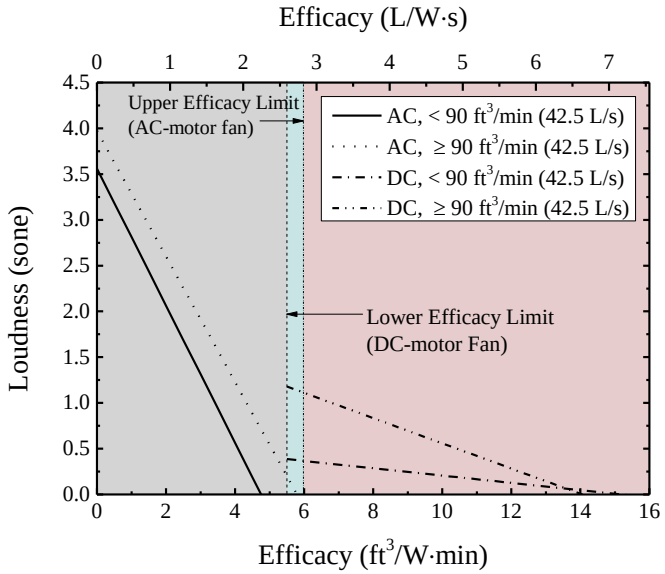

Figure 2-17 Summary of regression lines for AC and DC motor fans

Table 2-4 Loudness from efficacy-loudness regression models Eqs. 3 through 6

Efficacy (ft^3/W·min, L/W·s)	Loudness (sone) for low VFR fans (< 90 ft^3/min or < 42.5 L/s)		Loudness (sone) for high VFR fans (≥ 90 ft^3/min or ≥42.5 L/s)	
	AC-motor, Eq. (3)	DC-motor, Eq. (5)	AC-motor, Eq. (4)	DC-motor, Eq. (6)
0.5 (0.24)	3.19	-	3.63	-
1 (0.47)	2.81	-	3.29	-
2 (0.94)	2.06	-	2.60	-
3 (1.42)	1.31	-	1.91	-
4 (1.89)	0.56	-	1.23	-
5 (2.36)	-	0.41	0.54	1.25
6 (2.83)	-	0.37	-	1.11
7 (3.30)	-	0.33	-	0.97
8 (3.78)	-	0.29	-	0.83
9 (4.25)	-	0.25	-	0.70
10 (4.72)	-	0.21	-	0.56
11 (5.19)	-	0.17	-	0.42
12 (5.66)	-	0.13	-	0.28
13 (6.14)	-	0.09	-	0.14

The fan test data and the efficacy-loudness relationships in Figures 2-13 through 2-17 can be analyzed to provide the following insights.

1. One common observation from the Figures 2-13 to 2-17 is that the efficacy of both AC and DC-motor fans increases as the loudness decreases. A possible reason is that the flow phenomenon that increases vibrations and turbulences also lead to a loss of efficiency and an increase in loudness through vibrational, acoustic irreversible losses. Another reason from a system design and manufacturing perspective is that better designs have simultaneously targeted both a better efficiency and less noise.

2. As previously noted in Figures 2-8 and 2-12, AC-motor efficacies showed denser distributions than DC-motor fan efficacies as evidenced by smaller IQRs and shorter whisker lengths. Likewise, Figure 2-14, which is for AC-motor fans above or equal to 90

ft^3/min (42.5 L/s) now shows condensed efficacy distributions with most of samples being focused on fan efficacies from 3 and 5 $ft^3/W \cdot min$, rather than being scattered over the full range of possible efficiencies.

3. Although all four regression models in Figure 2-17 share the same trend in negative slopes, meaning loudness decreases as efficacy increases, the AC and DC-motor fans show different regression representations. For example, AC-motor fan curves are significantly steeper (more than five times) than the curves for DC-motor fans. Several analysis developed in previous sections can provide insight into this behavior. For the period 2005-2008 there was a significant reduction in loudness as shown in Figure 4. Therefore, the steeper decrease in the loudness of AC-motor fans compared to DC-motor fans as the fan efficacy increased in Figure 2-13 and 2-14 is partly driven by the earlier loudness reductions in the period 2005-2008. Likewise, one can explain the less steep slope of the regression models for DC-motor fans in Figures 2-15 and 2-16 as being consistent with the number of tested DC-motor fans being increased since 2009 and the possibility that many fan noise had mostly been addressed by this late data and later years.

4. In Figures 2-15 and 2-16, the R^2 values for the DC-motor fan regression lines vary from 0.1154 for the low VFR to 0.5442 for the high VFR. Part of the reason for the low R^2 values at the low VFR could be the smaller number of DC-motor fans compared to AC-motor fans. It should be noted that R^2 is affected by both the number of samples [50] as well as sample values. Therefore, the direct comparison of R^2 values between

Figures 2-15 and 2-16 is unlikely to reveal enough information to identify possible trends.

Further analyzes of efficacy and loudness and their relationships can be gained by comparing fan efficacies versus loudness plots for 2007 and 2008 in Figure 2-18.

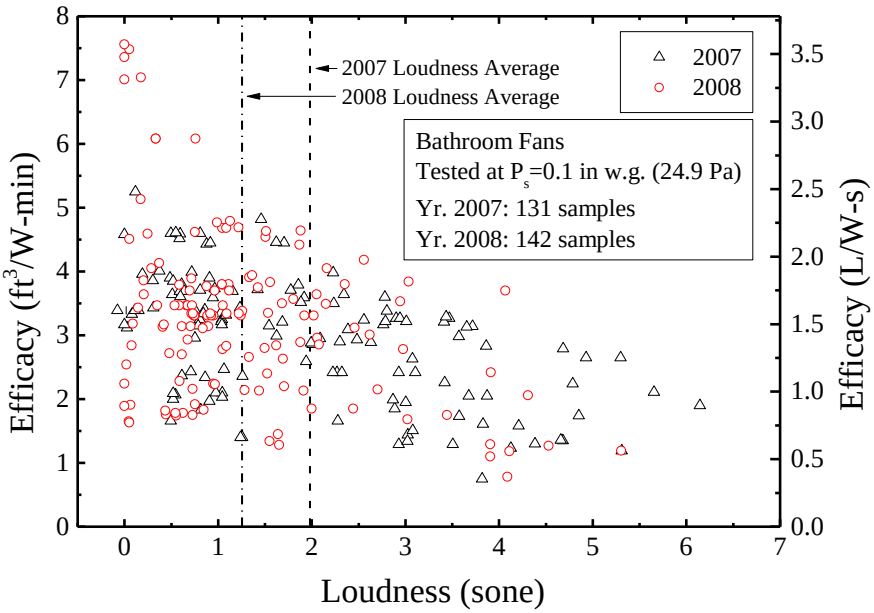

Figure 2-18 Efficacy and loudness scatter plot for the years 2007 and 2008

As noted, the average fan efficacies increased from 2.94 ft^3/W·min (1.39 L/W·s) in 2007 to 3.38 ft^3/W·min (1.60 L/W·s) in 2008, and the average loudness ratings decreased from 2.0 to 1.3 sone in 2007 and 2008, respectively. As shown in Figure 2-18, distributions of fan performance data in 2007 and 2008 overlap over a wide loudness range of 0.5 to 3.0 sone and a wide efficacy range of 0.5 through 5 ft^3/W·min (0.24 through 2.36 L/W·s). However, one can observe two major differences in 2007 and 2008

fan performance distributions that reflect improvements in fan performance in statistical terms. First, it can be observed that the number of the high-loudness and low-efficacy fans decreased from 2007 to 2008. Second, it can also be observed in Figure 2-18 that the high-performance fans characterized by low-loudness (less than 1 sone) and high-efficacy fans (over 6 ft^3/W·min or 2.832 L/W·s) appear only in 2008 and not in 2007.

Conclusions

This paper presented a statistical analysis of AC and DC motor-driven bathroom fan performance data that was measured for numerous fans throughout the period 2005-2013 in a flow and noise performance testing laboratory, following established guidelines and standards. An evaluation and analysis of this fan data, consisting of measured external static pressures, flow rates, power consumptions, and noise, resulted in the following conclusions.

1. The average loudness of fans with volumetric flow rates under 90 ft^3/min (42.5 L/s) decreased from 2.27 sone in 2005 to 0.78 sone in 2013 and for fans with flow values being equal to or above 90 ft^3/min (42.5 L/s) the decrease was from 2.34 sone in 2005 to 1.06 sone in 2013. In addition, over time the loudness distributions have narrowed around loudness medians for the same years. For example, the interquartile range (IQR) for fans under 90 ft^3/min (42.5 L/s) has decreased from 2.89 to 1.07 sone in 2005 and 2013, respectively, and for fans equal to or above 90 ft^3/min (42.5 L/s) the decrease was from 1.71 sone to 0.92 sone in 2005 and 2013, respectively. All of the decreases in average loudness and distributions for the test period can be attributed to performance improvements in fan design.

2. Fan efficacy statistics in each year for AC and DC motor fans reveal that most of the fans satisfy IECC 2012 efficiency requirements, which are 1.4 ft^3/W·min (0.66 L/W·s) for fans under 90 ft^3/min (42.5 L/s) and 2.8 ft^3/W·min (1.52 L/W·s) for fans equal to or above 90 ft^3/min (42.5 L/s). Reflecting improvements in designs, with improvements being AC-motor fans showed gradual increases in efficacies over the 2005 to 2013 test period from 2.15 to 2.66 ft^3/W·min (from 1.01 to 1.26 L/W·s) and from 3.02 to 3.51 ft^3/W·min (from 1.43 to 1.66 L/W·s) for fans under 90 ft^3/min (42.5 L/s) and above (or equal to) 90 ft^3/min (42.5 L/s), respectively. However, DC-motor fans did not show clear trends of efficacy increases or decreases over the years although their fan efficacies exceeded AC-motor fan efficacies in all cases.

3. In addition to the ENERGY STAR Most Efficient criteria being implemented, the increased usage of DC-motor fans has led to better efficacy ratings over the year. DC-motor fan efficacy statistics reveal that a majority of DC-motor fans exceed the ENERGY STAR Most Efficient criteria of DC efficacies being 7.5 and 6.8 ft^3/W·min (3.54 and 3.21 L/W·s) for fans under and over 90 ft^3/min (42.5 L/s), respectively.

4. A weak relationship between efficacy and volumetric flow rate was found for in DC-motor bathroom fans. Although the low R^2 statistics at value of 0.14 did not provide a satisfactory correlation between fan flow rates and efficacies, it was found that higher fan efficacy values over 10 ft^3/W·min (4.72 L/W·s) are achievable at the volumetric flow rate ranges of 80-90 ft^3/min (37.76-42.48 L/s). This observation can be compared with the AC-motor fan studies conducted by EPA, where the agency concluded that

there was no distinct and identifiable relationship between AC fan volumetric flow rates and fan efficacies.

5. Relationships was analyzed including linear regression lines with negative coefficients between fan efficacies and loudness ratings for AC and DC motor fans. The relationships show varying degrees of variance characterized by R^2 values of 0.29 under 90 ft^3/min (42.5 L/s) and 0.25 over 90 ft^3/min (42.5 L/s) for AC-motor fans, and values of 0.11 under 90 ft^3/min (42.5 L/s) and 0.54 over 90 ft^3/min (42.5 L/s) for DC-motor fans. Also, AC and DC motor fans showed different linearly decaying trends with DC-motor fans having less slope of -0.04 W·sone·min/ft^3 (-0.08 W·sone·s/L) and -0.14 W·sone·min/ft^3 (-0.29 W·sone·s/L) for under and over 90 ft^3/min (42.5 L/s) respectively compared to AC-motor fan regression slopes of -0.75 W·sone·min/ft^3 (-1.59 W·sone·s/L) and -0.69 W·sone·min/ft^3 (1.45 W·sone·s/L) for under and over 90 ft^3/min (42.5 L/s), respectively. The reason to these negatively sloped correlations between efficacy and loudness is that vibrations and turbulences lead to both a loss of efficiency and an increase in loudness.

6. A noticeable difference in loudness was observed for tested fans between the year 2007 and 2008, as measured loudness went from 1.82 to 0.57 sone for fans under 90 ft^3/min (42.5 L/s) and from 2.17 to 1.10 sone for fans above or equal to 90 ft^3/min (42.5 L/s). Also, the number of the high-loudness and low-efficacy fans, which is considered to be fans with low acoustic and energy performances, decreased from 2007 to 2008. Furthermore, the high-performance fans characterized by low-loudness (less than 1 sone)

and high-efficacy fans (over 6 ft3/W•min or 2.832 L/W·s) appear only in 2008 and not in 2007, which refers to the emergence of DC-motor fans.

The study results presented herein can be utilized as a measure of residential ventilation fan performances. Of special importance, the linear trends discovered between the fan efficacy and the loudness can be useful for comparing the energy and sound performance of fans with AC- or DC-motor types being specified. Based on observations presented herein, further study is underway to determine relationships of other fan parameters in terms of the energy and sound performances.

CHAPTER III

METHODOLOGY FOR EVALUATING SOUND TRANSMISSION TO THE EXTERNAL BACKGROUND

Overview

Background noise is an unavoidable element of the acoustic measurement process, and, of special importance, it must be identified in order to process any signal of interest. Although a number of techniques have been developed for the treatment of background noise for acoustic rating purposes, an assessment of background steadiness requirements and needs has not been adequately studied for the practical purpose of testing codes and standards. Therefore, this study proposes a method of monitoring an external background noise while conducting an acoustical test. In order to analyze the external background noise itself, acoustic transmissions of sound sources or test specimens through the construction material making up the measurement chamber space needs to be clarified. This paper investigates two methods for evaluating the acoustic transmission characterization of walls, namely the spatial background difference method and the insertion loss method. These two methods are based on the spatial and temporal comparison process of the sound transmission. Despite the simplicity of the methods, the spatial background difference has the potential to overestimate the wall sound transmission, depending on the background noise level. The insertion loss can be utilized in order to compensate for the overestimation although the method requires an assumption or a statistical inference for determining a reference sound source

transmission. For this study, 200 different tests are performed and analyzed for 200 specimens by using the two aforementioned methods. The results of this study shows that both methods need to be utilized simultaneously in order to avoid the overestimation of the sound transmission. Also, an analysis of the signal-to-noise ratio of the external background signal and the transmitted sound reveals that the background unsteadiness, meaning background noises are varying while testing is being performed, can also influence the SNRs, along with sound levels of the sound source itself.

Introduction

Background noise, which is defined as extraneous sounds that exist in addition to the signal of interest, is an unavoidable element of the acoustic measurement process, and, of special importance, it must be identified in order to process any signal of interest. However, because the background noise is unsteady in most cases, an identification of background noise must encompass a process to evaluate background steadiness. As such, an overview of background noise and its impact on acoustic testing according to standards are presented in this section. In addition, methodologies or strategies for eliminating of background-noise effects used in leading acoustic standards are presented as they pertain to this study. Then, conventional methodologies for addressing background steadiness such as signal-to-noise ratio are presented. Lastly, limitations of the conventional methodologies are discussed for practical and real-world applications for low-noise source acoustic testing, such as residential ventilating devices or blowers, which is a primary motivation of the present study.

Background Noise and Its Correction in Acoustical Testing

The intrusion of background noises is inevitable part of the measurement process. In order to increase yields of the signal of interest for measurement purposes, characterizations and treatments of background noises have long been investigated as an important part of signal processing in many different research areas, such as the audio engineering [51], video-signal processing [52], speech recognition [18, 53], and, in a broader sense, digital signal processing [54]. One major reason for pursuing the different characterization approaches is that different governing natures and durations of background noises exist. For example, meteorological background noise is frequently analyzed for several years with decades of data [55], because most climate phenomenon usually recur with specific periods of years, decades, etc. Another example is background noise characterizations of fluid flows and/or motions of mechanical components, which are usually analyzed for shorter durations of background noise by using microphone arrays or beam forming techniques [56].

However, most signal-processing practices that consider acoustic background noises require some degree of modeling of noise patterns or schemes to account for background noise, such as an identification of background-noise colors, grey, pink, white, etc. [57]. For precision methods of measurements, standards, such as ANSI, ISO, etc., use robust but simple methods for treating background [10, 11]. For example, in ANSI S12.51/ISO 3741 and ISO 3744 standards, a background correction factor is calculated for background noises for free field or reverberant field measurements by using transducers such as accelerometers and microphones as follows.

$$K = -10\log\left(1-10^{-0.1\left(\Delta L_p\right)}\right) \quad (3\text{-}1)$$

, where K is a background correction factor, and ΔL_p is defined as follows.

$$\Delta L_p \equiv L_p^{UT} - L_p^B \quad (3\text{-}2)$$

, where L_p^{UT} is a sound pressure level of a unit under test (UT), and L_p^B is a sound pressure level of background or ambient noise with the absence of the acoustic emission of the unit under test. These ISO and ANSI standards limit usage of Eq. (3-1) for the following conditions.

- One-third-octave-band SPL measurements at 200 Hz and below, and 6,300 Hz and above should satisfy 6 dB $\leq \Delta L_p \leq$ 15 dB, and
- Other frequencies, namely 250-5,000 Hz, should be at least 10 dB $\leq \Delta L_p \leq$ 15 dB.

Because ΔL_p explicitly means a ratio of sound pressures of two signals (i.e., logarithm) then the background SPL L_p^B can be negligible for the background correction when L_p^B is far less than a sound-source SPL, L_p^{UT}, such as by 15 dB or over.

Signal-to-Noise Ratio (SNR) Issues for Low Noise Sources

Separating a device signal of interest from a background noise is subject to the magnitude of the signal-to-noise ratio (SNR). Specifically, a ΔL_p less than the lower limit, namely 6 dB at 200 Hz and below and at 6,300 Hz and above, while 10 dB at other band frequencies, results in an inaccurate separation of the signal of interest from the background noises, primarily because acoustic measurement are more susceptible to the negative effects of unsteady background noises.

Sound tests for heavy machineries or musical instruments are able to avoid background separation issues and SNR issues [58], because of signals being large enough to provide background separations, which are usually from heavy machineries, or because of extremely low background noises, which are frequently pursued in instrumental acoustics. However, background separation and SNR issues are unavoidable when testing small mechanical devices, such as fans, automobile electronics, house appliances, ventilators, etc., because these devices generate low levels of noise, which incur low SNRs. In addition, semi-reverberant acoustics that are relevant to the study herein, as will be explained later, with their moderate levels of external sound isolation from the background noise are likely to suffer considerably from background isolation quality in terms of the separation and SNR at least compared to anechoic acoustics [58].

If acoustic measurements are subject to low SNRs, it is important to maintain steadiness of background noise for determining precise sound pressure levels or sound power levels of sound sources, especially when using procedure that require multiple measurement stage occurring over a period of time. Of special importance, fluctuating background noises result in varying background correction factors, K_i, where the subscript i refers to an i-th measurement at a low SNR, for example, less than a 15 dB measured-SPL. To evaluate background steadiness, leading standards such as ANSI, IEC, ISO, etc. have implemented an uncertainty analysis of measurement variables approach (henceforth, the uncertainty method) that addresses background steadiness as a part of expanded measurement uncertainty. Furthermore, the uncertainties associated

with the background noise are obtained by repeated measurements of the background noise at given locations. As a result, determining background standard uncertainties result in collections of multiple background SPL measurements $L_{p,i}^{B}$ at different test instances over extended durations. Therefore, background uncertainties focus on long-term background instabilities or variations.

An alternative to the above uncertainty method for assessing the background-steadiness is a comparison of two or more different backgrounds at given time intervals, usually within several minutes. For example, HVI 915 demands that the background steadiness be assessed by measuring the different background noise SPLs for 30 sec each in 1/3 octave bands before (BGD1) and after (BGD2) a reference sound source (RSS) measurement [9]. Table 3-1 shows the tolerance of the background SPL differences, ΔL_{p}^{B}, in 1/3 octave band center frequencies in Hz. In Table 3-1. ΔL_{p}^{B} is defined as the absolute value of the arithmetic difference of two 30-sec-averaged background noise SPLs for the same band frequency. As can be seen in Table 3-1, low frequencies have larger ΔL_{p}^{B} tolerances compared to values at higher frequencies because more acoustic energy transmissions occur at low frequencies for semi-reverberant chambers.

Table 3-1 HVI 915 background steadiness tolerance [9]

1/3 Octave Band Frequency (Hz)	Limit of BGD Difference ΔL_p^B (dB)	1/3 Octave Band Frequency (Hz)	Limit of BGD Difference ΔL_p^B (dB)
50	2.0	800	2.0
63	4.0	1,000	0.5
80	2.0	1,250	0.5
100	2.0	1,600	0.5
125	2.0	2,000	0.5
160	1.0	2,500	0.5
200	1.0	3,150	0.5
250	1.0	4,000	0.5
315	1.0	5,000	0.5
400	1.0	6,300	0.5
500	1.0	8,000	0.5
630	1.0	10,000	0.5

Limitations on the Conventional Criteria

Among testing laboratories that utilize testing protocols promulgated by certification bodies for acoustic ratings, many follow specified acoustic performance guidelines or criteria, such as Energy Star, LEED, etc. [59-64]. However, each of the methods described may not completely address the temporal and random fluctuations of the background noise. As noted previously, the background comparison method in Table 3-1 only provides ‘pass or fail’ criteria, rather than assessing the impact of the background variation, which in contrast was partly available by the uncertainty method. Specifically, focusing merely on background noise differences fails to give quantitative evidences of background steadiness. For example, a background SPL difference of 0.8 dB at 800 Hz center frequency is considered as an ‘acceptable’ background steadiness by the

conventional background steadiness criteria shown in Table 3-1; however, such a difference might not guarantee the precision of a unit under test where a quiet noise-source having a small sound separation from background noise exists.

Likewise, the Uncertainty Method prescribed by ISO/ANSI does not clearly incorporate varying background noise patterns at different times and locations. For example, ANSI S12.51/ISO 3741 and ISO 3744 standards specify without supporting evidences probability distributions of a background noise correction as a normal distribution. This normal distribution may hold true for the distribution of each sample mean of the background noise corrections [65]; however, it does not provide insight necessarily into the nature of the background noise, especially the uncorrelated nature of background noise sources.

It is well known that the background noise is a random combination of noise sources, such as noises emitted from human speech, electrical devices, automobiles, heavy machineries, aircrafts, microclimate effects, structural vibrations, etc. [66], and thus the noise is often considered to be broad-band, such as white or pink noise with several tonal components. Most random noise sources are uncorrelated in that one cannot easily find relationships of noise sources, making delving into relationships cost-prohibitive [66, 67]. Also it should be noted that because of their uncorrelated nature, background noise is constantly changing.

Importance of the Present Study

In order to address the steadiness of random uncorrelated fluctuations in background noise, a characterization method based on using the external background noise

monitoring technique is formulated and reported in this paper along with real-world applications herein. As the first step toward assessing background noise, the study herein investigated of the influence of sound transmission through the acoustic chamber wall construction in the presence of a sound source, such as the unit under test or the reference sound source for the case of the background noise producing low SNRs. In order to investigate this sound transmission, two different methods were formulated, namely a spatial background difference method approach and the insertion loss method approach. In addition to formulating and presenting the mathematical process, examples of real-world applications are presented with these methods being applied to data from 200 fan samples tested, with the results being discussed.

Relevance of Transmission Characterization to External Monitoring

As noted in the Introduction, this part of the study presents two transmission characterization methodologies that are applicable to standard acoustic testing conducted inside a chamber. These the methodologies are presented and compared herein because transmission characteristics must be identified as a prerequisite step to external background noise monitoring, which is the topic of this study.

This section introduces an overview of the external background monitoring process, and then explains in detail where the transmission characteristics are used for the monitoring process.

The monitoring process is basically a comparison of sound pressure levels measured outside the chamber (henceforth, external background), $L_{p(e)}$, by using the external microphone depicted in Figure 3-1, and SPLs measured inside the chamber, $L_{p(i)}$. It

should be noted that the subscription *e* and *i* inside the parenthesis denote outside the chamber (or external) and inside the chamber (or internal), respectively. The following lists SPL designations associated with the monitoring process.

- $L_{p(i)}^{UT}$ and $L_{p(e)}^{UT}$: SPLS inside and outside, respectively, the acoustic chamber at a unit measurement phase (or UNIT phase)
- $L_{p(i)}^{B}$ and $L_{p(e)}^{B}$: SPLS inside and outside, respectively, the acoustic chamber at a background noise measurement phase (or BGD phase)
- $L_{p(i)}^{RSS}$ and $L_{p(e)}^{RSS}$: SPLS inside and outside, respectively, the acoustic chamber at a reference sound source (RSS) measurement phase (or RSS phase)

As the subscripts *e* and *i* denote, two locations of the background noise measurements are used for the process, namely the internal signal and the external signal. Figure 3-1 shows a schematic of the three major steps of the monitoring process along with noise sources and their transmission paths.

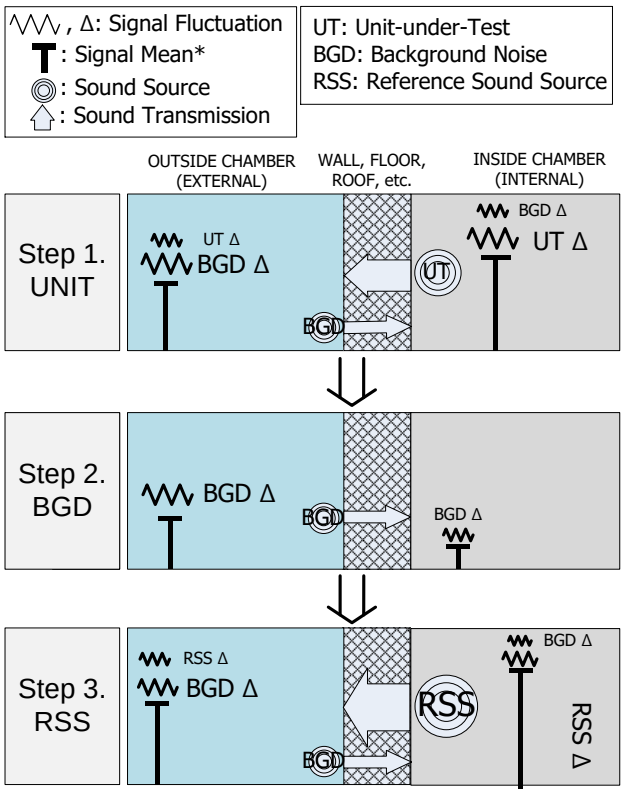

Figure 3-1 Three steps of the internal and external background (BGD) noise measurements
(* length of the signal mean symbol is a measure of its magnitude)

In Figure 3-1, each signal with its own source locations (i.e., inside or outside the chamber) is decomposed into a signal mean and a signal fluctuation. At each measurement phase, there are several different sets of noises emitted from different noise source locations. In Figure 3-1, each row represents a measurement phase, which consists of

1. UNIT phase: SPL measurements inside and outside the chamber while a unit-under-test is operating,

2. BGD phase: SPL measurements inside and outside the chamber while neither the unit-under-test nor the RSS is operating, which means ‘background noise’ only, and

3. RSS phase: SPL measurements inside and outside the chamber while the RSS is operating.

In addition, arrows across of the crosshatched columns in Figure 3-1 represent where the sound sources are originated and then transmitted to. For example, the sound of both the unit under test and the RSS is generated from inside the chamber, and then the sound travels through the chamber construction to the outside, which means the signal strength measured by the external microphone will be less than the signal strength measured internally. In contrast, the reverse occurs with the background noises originating outside the chamber, which is the result of background noise generation inside the chamber being strictly avoided by adopting low-noise microphone traverse or rotating booms, or, more preferably, microphone arrays at specific locations. Therefore, the background-noise signal measured inside the chamber is the result of the acoustic transmission through the chamber construction, which is expressed in the cross-hatched rectangle in Figure 3-1.

The above signal originations and final destinations, often being transmitted through the wall constructions, can be readily followed and understood in Figure 3-1 by focusing on component symbols and regional strength represented by the sign of the wavy/fluctuating line symbols.

Because of these noise sources depicted in Figure 3-1, it is necessary to evaluate the transmission of the sound emitted by the unit-under-test or the RSS signal through the

chamber construction. Otherwise, the comparison of the external SPLs $L_{p(e)}$ at each measurement phase, namely UT, BGD, and RSS phases, can differ significantly because of the intrusion of the transmitted sound toward outside the chamber. The following section describes the evaluation process of two different methodologies, namely the spatial background difference method and the insertion loss method, along with the validation process in terms of SNRs.

Transmission Characterization Methods

As described in the previous section and shown in the Figure 3-1 schematic, the acoustic signals developed inside the chamber (e.g., noises from unit-under-test or RSS) and transmitted through the chamber construction should be quantified and compared against the external background noise. If the sound transmission does not significantly affect the external background noise, then background steadiness can be evaluated by monitoring external backgrounds. The following procedures explain two transmission characterization methodologies, namely Spatial Background Difference Method and Insertion Loss Method. Next, a process to evaluate impacts of the transmitted sound for the proposed methodologies is introduced, meaning that signal-to-noise ratio (SNR) analysis is presented for the process.

Of special importance, there are a number of SPL designations used throughout the study. Therefore, moving forward to presenting methodologies, a list of the SPL designations is provided below in Table 3-2 for reference purposes.

Table 3-2 List of the sound pressure levels (SPLs) either measured or calculated for the transmission characterization

Measurement Location	**Inside the chamber (internal, i)**		**Outside the Chamber (external, e)**	
Designation	**SPL,** $L_{p(i)}$	**Description**	**SPL,** $L_{p(e)}$	**Description**
UNIT phase	$L_{p(i)}^{UT}$	Measured SPL (having both unit-under-test and background sound)	$L_{p(e)}^{UT}$	Measured SPL (having both background and transmitted sound of unit-under-test)
	$L_{p(i)}^{U}$	Calculated SPL after excluding background noise	$L_{p(e)}^{U*}$	Calculated SPL of transmitted unit-under-test sound (excluding external background)
BGD phase	$L_{p(i)}^{B}$	Measured background noise inside the chamber	$L_{p(e)}^{B}$	Measured background noise outside the chamber
RSS phase	$L_{p(i)}^{RSS}$	Measured SPL (having both RSS and background sound)	$L_{p(e)}^{RSS}$	measured SPL (having both background and transmitted RSS sound)
			$L_{p(nb)}^{RSS}$	Calculated SPL assuming no chamber (or non-acoustic-barrier)
			$L_{p(e)}^{RSS*}$	Calculated SPL of transmitted RSS sound (excluding external background)

Spatial Background Difference Method

The first method for characterizing acoustic transmission is the Spatial Background Difference Method, where two SPLs are measured simultaneously inside and outside the chamber, $L_{p(i)}^{B}$ and $L_{p(e)}^{B}$, and then the BGD phase is used to identify the amount of the acoustic transmission. After the amount of spatial background difference SPL is identified, the difference is applied to the measured SPLs of the unit-under-test. Next, the SNR of the estimated transmitted sound and measured external background noise is determined to validate the use of the background monitoring technique. This method is based on the sound transmission loss (STL) formulation, and is relatively simple compared to the second method to be presented in a later section, namely the Insertion

Loss Method. Key parameters for the spatial background differences include following sound levels.

- Measured SPLs at the BGD phase inside an acoustic chamber, or internal BGD SPLs
- Measured SPLs at the BGD phase outside an acoustic chamber, or external BGD SPLs

Theoretical Background of Spatial Background Difference

The spatial background difference is based on the mathematical expression of the sound transmission loss (STL), which are commonly found in many acoustical texts [13, 58, 68]. The following equation is the expression of the STL [68].

$$STL \equiv 10\log\frac{I_e}{I_i} = 10\log\frac{\bar{p}_e^2 S_w}{\bar{p}_i^2 S_i \alpha} = L_{p(e)}^B - L_{p(i)}^B + 10\log\frac{S_w}{S_i\alpha} \quad (3\text{-}3)$$

, where

I: sound intensity (W/m^2)

$\bar{p}$: averaged sound pressure (Pa)

S: surface area (m^2)

α: acoustic absorption coefficient of the chamber construction

The subscripts in Eq. (3-3) denotes:

e: external or outside the acoustic chamber,

i: internal or inside the acoustic chamber, and

w: acoustic paths, such as wall, roof, door, floor, etc.

The expression encompasses the measured quantities (the sound pressure levels, L_p, or sound power, p) and the transmission characteristics (the absorption coefficient, α) as

well as the dimensions (surface area, S). The last term in Eq. (3-3) can be treated as being constant because of material and dimensions of the acoustic chamber are invariant (i.e. the same dimensions and the chamber construction).

Evaluation of the Spatial Background Difference

The arithmetic difference of $L^B_{p(e)}$ and $L^B_{p(i)}$ quantifies the background-noise transmission through the chamber construction because these two SPLs are measured at the same time thus eliminating the possibility of an inconsistent background. For convenience, the spatial background SPL difference is defined as $\Delta^B_{e,i}$.

$$\Delta^B_{e,i} \equiv L^B_{p(e)} - L^B_{p(i)} \tag{3-4}$$

As an aside, the spatial background difference is also commonly known as the "noise reduction (NR)" in acoustic literatures [54, 58, 68]; however, the study herein uses the term 'the spatial background difference' in order to avoid possible confusions arising from the terms 'noise' and 'reduction'.

By using this spatial background difference, $\Delta^B_{e,i}$, transmited SPLs from the sound source inside the chamber, such as sound from the unit-under-test and the RSS, are calculated in the next step.

Estimation of the Transmitted Sound by Using Spatial Background Difference

In order to perform the calculation, the signal of the unit under test or the RSS needs to exclude the background noise that coexists with the unit or RSS sound. The measurement taken at the BGD phase can be used to remove the background noise from the measured SPL at the UNIT phase, which are combined SPLs of the unit-under-test

and the background noise. The SPLs at the UNIT phase $L_{p(i)}^{UT}$ is logarithmically subtracted by the background noise SPLs at the BGD phase $L_{p(i)}^{B}$.

$$L_{p(i)}^{U} = 10\log\left(10^{L_{p(i)}^{UT}/10} - 10^{L_{p(i)}^{B}/10}\right) \quad (3\text{-}5)$$

, where superscript *U* denotes the unit under test signal subtracted by the background noise. The arithmetic difference $\Delta_{e,i}^{B}$ is then applied to the $L_{p(i)}^{U}$ to obtain the unit signal transmitted, expressed in superscript *U**, through the chamber construction.

$$L_{p(e)}^{U*} = L_{p(i)}^{U} - \Delta_{e,i}^{B} \quad (3\text{-}6)$$

It is interesting to note that an underlying assumption of the conversion to the transmitted signal in Eq. (3-6) is an acoustic symmetric transmission. In fact, an asymmetric transmission is not dominant phenomenon in the condensed, bulk structure such as the chamber construction used herein the study because the asymmetric transmission [69, 70] or acoustic scattering usually happens in the systems or the arrays of structures whose distances between material or structure are comparable to the wavelength of a wave as shown in Bragg's law.

$$2d\sin\theta = n\lambda \quad (3\text{-}7)$$

, where *d*, θ, *n*, and λ denote the distance of the spacing, the wave incident angle, a wave integer for constructive interference, and the wavelength, respectively. As can be seen in Eq. (3-7), the spacing is of the same wavelength order, for example, about 0.17-meter spacing for a sound wave at 1,000 Hz traveling through air at 293 K, which is not the case for the materials that make up for chamber construction.

Insertion Loss Method

An alternative method to that presented in the previous section for evaluating acoustic transmission is the Insertion Loss (*IL*) method, which is defined as the sound pressure level difference with and without the acoustic barrier (i.e., the chamber construction herein the study) [13]. The insertion loss is determined by identifying or utilizing the following key parameters.

- the sound power levels of the RSS, which is determined by a calibration process such as ISO 6926 [71],
- the calculated SPLs with absence of the sound barrier, namely the chamber construction, and
- the measured sound pressure levels of the RSS outside the chamber, which is transmitted through the chamber construction.

Evaluation of Insertion Loss

As outlined above, the calibrated sound power levels of the RSS is used as the first parameter to determine *IL*. The following describes the procedure to determine the insertion loss and its usage for the sound transmission. First, the sound pressure level without the presence of the acoustic barrier is determined along with the hemispherical free field assumption.

$$L_{p(nb)}^{RSS} = L_{w}^{RSS} - 10\left|\log\frac{Q}{4\pi r^2}\right| \tag{3-8}$$

, where $L_{p(nb)}^{RSS}$ is hemispherical free field SPL without acoustic barrier (i.e. the chamber construction), *Q* is the directivity factor, which equals to 2 for the hemispherical free

field, *r* is the distance between the RSS and the external microphone. In Eq. (3-8), the hemispherical free-field assumption can be valid irrespective of the field characteristics of the test site although the outside of the chamber used for this study has the free field characteristics. The reason for this validity is that the conversion from free field back to the physical acoustic field under test will be performed when the transmitted unit SPL is calculated. Next, the measured sound pressure level of the RSS outside of the chamber is obtained by the logarithmic subtraction of the background SPL measured at the BGD phase from the background SPL measured at RSS phase outside the chamber.

$$L_{p(e)}^{RSS*} = 10\log\left(10^{L_{p(e)}^{RSS}/10} - 10^{L_{p(e)}^{B}/10}\right) \tag{3-9}$$

It should be noted that, in Eqs. (3-8) and (3-9), the external SPL measured at RSS phase is combination of the background noise itself and the transmitted RSS sound though the wall. It should be noted that RSS-s are purposely designed to generate large, broadband response as being denoted by international standards [11, 72] with having the larger sound power distinguishable from the background noise in terms of the exceedingly larger SNRs. Next, the insertion loss is determined by subtracting the SPL outside the chamber at RSS measurement phase $L_{p(e)}^{RSS}$ from $L_{p(nb)}^{RSS*}$ in Eq. (3-10).

$$IL = L_{p(nb)}^{RSS} - L_{p(e)}^{RSS*} \tag{3-10}$$

Estimation of the Transmitted Sound by Using Insertion Loss

Then, the spatial background SPL difference $\Delta_{e,i}^{B}$ is replaced with the insertion loss by using the following equation.

$$L_{p(e)}^{U*} = L_{p(i)}^{U} + \left(L_{w}^{RSS} - L_{p(i)}^{RSS}\right) - 10\left|\log\frac{Q}{4\pi r^2}\right| - IL \tag{3-11}$$

Of special importance, the second term on the right hand side in Eq. (3-11), ($L_w^{RSS} - L_{p(i)}^{RSS}$), is called the room characteristic ratio (*RCR*), which is used to obtain the sound power levels of sound, source under test in the comparison method of the reverberant acoustics [10, 11]. Because the insertion loss is determined by setting the hemi-spherical field assumption of the sound pressure level without the acoustic barrier (i.e. the chamber construction), the same field assumption should be applied when the transmitted sound of the unit under test is determined in Eq. (3-11). As such, the first three terms in Eq. (3-11) reflect the field assumption.

Signal-to-Noise Ratio for Validating External Background Monitoring

Once transmitted sound pressure levels are evaluated by using either the spatial background difference method or the insertion loss method, their impact to the external background noise needs to be identified. If the transmitted sounds are sufficiently less than the external background noise, the proposed external background monitoring methodology can be used without difficulties. In contrast, if the difference between the transmitted sounds and the external background noises are not significant, the proposed methodology may not reveal enough information. In this sub-section, A signal-to-noise ratio (SNR) analysis is introduced as a methodology for comparing the transmitted sounds and the external background noises.

The transmitted sound levels, $L_{p(e)}^{U*}$, which is determined by either Eq. (3-6) for the spatial background difference method or Eq. (3-11) for the insertion loss method, is compared with the external background noise, $L_{p(e)}^{UT}$, by the following SNR expression.

$$SNR_e^{UT} = L_{p(e)}^{UT} - L_{p(e)}^{U*} \tag{3-12}$$

In Eq. (3-12), the sound generated inside the chamber, and then transmitted through the chamber construction is conceptually considered to be a 'noise', because as the transmitted sound energy gets smaller than the comparison of the $L_{p(e)}^{i}$ yields meaningful results.

One can establish criteria for the minimum SNR_e^{UT} determined in Eq. (3-8) order to guarantee the negligible contribution of the acoustic transmission of the sound emitted from the unit-under test, $L_{p(i)}^{UT}$, to the external background noise $L_{p(e)}^{UT}$. The study herein sets the required SNR as 20 dB in order to use $L_{p(e)}^{UT}$ without corrections being made, particularly because combining two SPLs having a 20 dB difference results in a 0.043 dB increase in the SPL, which can be less than the typical significant digit (0.1) for reporting the sound levels discussed in the study herein. In addition, the study herein considers $L_{p(e)}^{UT}$ that needs to be corrected for the background steadiness assessment purpose when SNR_e^{UT} lies between 6 and 20 dB by using the background noise correction *K* in Eq. (3-1), where ΔL_p is taken as SNR_e^{UT} in Eq. (3-8). The corrected SPL of the external background noise is then determined.

$$L_{p(e)}^{UT*} = L_{p(e)}^{UT} - K \tag{3-13}$$

In order to avoid confusions arising from the use of the correction *K*, the term transmission correction is used henceforth if Eq. (3-9) is used for the external background signal. Of special interest, the procedure reflected in Eqs. (3-6) through (3-8) follow a framework that is similar to that of the spectral subtraction methods [16, 18,

53] in that the noisy signal is decomposed to the useful signal and the various noise sources, and then the useful signal is utilized for the acoustic evaluations. However, the method discussed herein the study does not involve a fundamental assumption of the spectral subtraction method, namely identical noise measured at different measurement In other words, the simultaneous measurement of $L_{p(i)}$ *and* $L_{p(e)}$ avoids the excessive guesswork of the noise. Furthermore, the SPL difference $\Delta_{e,i}^{B}$, in Eq. (3-4), a spatial differences are the only variables in the sound transmission loss (STL) in Eq. (3-3) while other terms are material properties and dimensions. Therefore, the procedures in Eq. (3-6) through (3-8) can be interpreted as a legitimate noise separation technique.

Experimental Setup for Reverberant Chamber

Before the sound transmission characteristics are presented and analyzed in detail, it is necessary to describe the configuration of the reverberant chamber used in this study because the measured background noise is dependent on acoustic properties of the reverberant chamber structure, such as reflection, absorption, transmission, etc. Figure 3-2 is the schematic of the semi-reverberant chamber (henceforth, the chamber) used in this study.

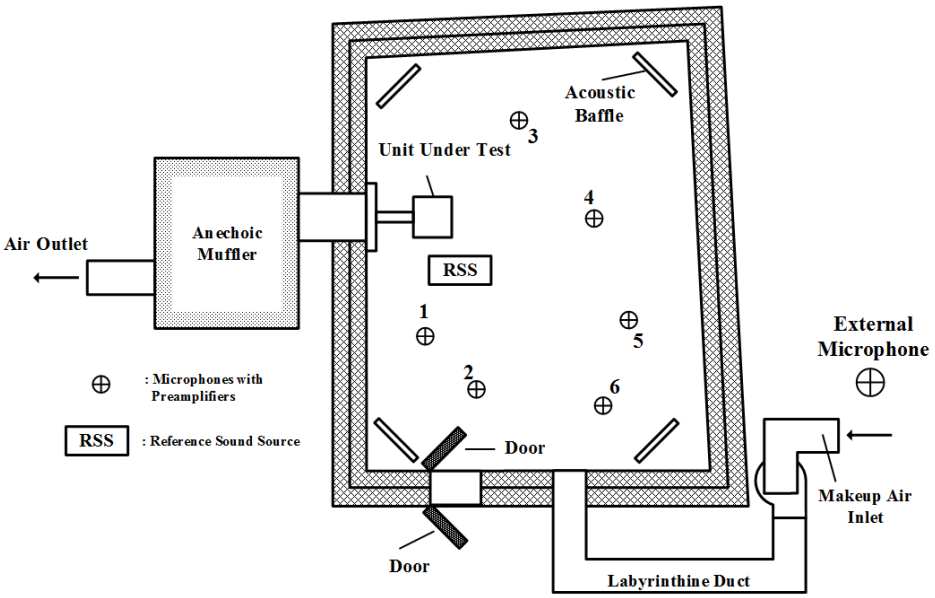

Figure 3-2 Schematics of the semi-reverberant chamber for this study

The chamber has been constructed with heavy-duty and multi-layer insulating walls for the air-tightness in order to provide an operation-control capability for the air-moving devices such as blowers, and fans that undergo acoustical testing, etc. As noted in Figure 3-2, the walls are non-parallel so as to minimize the effects of the three-dimensional standing waves, which are further minimized with the aid of acoustic baffles. The inlet duct is constructed with a tortuous pass through labyrinthine in order to avoid excessive background noise that might otherwise enter through the make-up air supply. The outlet duct is directly adjacent to an anechoic chamber, which provides an anechoic termination. The operating conditions including temperature, humidity, atmospheric pressure, and the external static pressure for the air-moving devices being tested, are controlled and recorded as are the electrical power sources.

As shown in Figure 3-2, positions of the six internal microphones with preamplifiers were determined in accordance with ISO 3741/ANSI S12.51 [11, 73]. The external microphone is located adjacent to the make-up air inlet in order to capture background noise sources traveling through both the labyrinthine inlet duct and the chamber walls. The required test-setup and procedures are described in detail in ISO 3741/ANSI S12.51 [11, 73] with equipment, specifications, and uncertainties listed in Table 3-3. Of special importance for every instrument, up-to-date certified calibrations are maintained so that the uncertainty of the resulting sound data can be analyzed.

Table 3-3 Sound test equipment list with uncertainty

Equipment Name	**Description**	**Uncertainty**
Microphones with preamplifiers	Sound pressure measurement in dB (15 – 148 dB(A), 3.15 – 20000 Hz)	±0.35dB
Reference Sound Source (RSS)	Generating reference sound (sound pressure level at 83.4 dB(A))	±0.54 dB
Data analyzer and data acquisition device	Performing frequency domain analysis (0 – 25.6 kHz, 5mV – 5 V RMS)	±0.10 dB
Voltage meter	Measuring and monitoring voltage (0-1000 V)	±0.068 V (up to $300V_{AC}$)
Tachometer	Measuring Fan RPM (5 – 999990 RPM)	±0.50 RPM

As an aside, the chamber is located inside of a large building that has more than 40 times the volume of the semi-reverberant chamber. Furthermore, the outside of the semi-

reverberant chamber is located away from significantly reflecting fields so that the outside of the chamber is closer to a free field with only the small reverberations. In addition, the encompassing building is located in an underpopulated rural area (latitude: 30.65, longitude: -96.47) surrounded by farms, pastures, and roads. Therefore, environmental noises along with intermittent traffic, airplane, and rare machinery noises may be encountered. The average sound pressure levels of background noises outside the chamber was found to be 47.1 dB, which is considered to be less than the average residential noise level by more than 10-20 dB [74].

Results and Discussion

In this section, transmission characterization results for the spatial background difference method and the insertion loss method are presented as examples of real-world applications for the acoustic chamber setup introduced and described earlier in this study.

The results of the first method, namely the spatial background difference method, are discussed in three different subsections that are briefly explained below.

1. Variations in Spatial Background Difference: Variations in the spatial background difference are presented and discussed, which includes both a short-term and long-term analysis, along with possible explanations and other details about the variations.

2. Overestimation of Sound Transmission: It was found that there exists a possibility for overestimations of the sound transmission when the spatial background difference method is utilized. This section discusses reasons for overestimated sound

transmission, which includes either low background noises or larger sound transmission losses because of the chamber construction (i.e., chamber envelopes).

3. Diagnosis of Overestimated Sound Transmission: For standard testing purpose, it is useful to develop a diagnosis procedure for validating the overestimation of the sound transmission when the spatial background difference method is utilized. This section discusses several strategies for diagnosing the overestimation issue.

The results of the second method, namely the insertion loss method, are discussed in four different subsections that are briefly explained below.

1. Using RSS Transmission for Insertion Loss: This section discusses a prerequisite condition for utilizing the insertion loss method, which is a transmission of the RSS sound through the chamber. This section discusses the RSS sound transmission along with statistical distributions that show evidence of the transmission.

2. Hypothetical Test for RSS Transmission: Based on the finding of the RSS transmission, this section further investigates the statistical significance of the RSS transmission, which will directly by used as an input to determine the insertion loss.

3. Using Sample Mean for Insertion Loss: Based on the statistical inference in the previous section, two options to calculate the insertion loss are suggested for implementation of the insertion loss method. This section discusses the first option, which use the average of the measured RSS SPLs.

4. Using Absolute SPL Difference for Insertion Loss: This section discusses the second option to calculate the insertion loss, which is based on the absolute SPL difference between RSS and BGD phases.

Lastly, results of the two methods are compared and reviewed for real-world applications, which qualifies the use of the external background monitoring (discussed in the next part (Part 2) of this study) by assuring that the transmitted sounds generated inside the chamber do not influence the external background.

Fan Testing Data Used in This Study

The input data for the study reported herein are a test database obtained for 200 fans, which comprise residential bathroom ventilation fans, utility-room ventilators, and kitchen range hoods. All tests were conducted in the semi-reverberant chamber that was described in an earlier section with the experimental setup for the reverberant chamber by conforming to HVI 915, ANSI S12.51, AMCA 301, ANSI S3.4 [8, 9, 11, 19].

As mentioned in the Introduction section, the HVI 915 criteria does not guarantee whether the background noise present at the UNIT phase is similar to the background noise measured at the BGD phase. Therefore, as the initial step for the background steadiness assessment, the transmission characterization is necessary by using either one of the methods, namely the spatial background difference method and the insertion loss method presented earlier in the Description of Methods section.

Transmission Estimation by Using Spatial Background Difference

As noted in the beginning of the Result and Discussion, the results of the spatial background difference method are presented in the following sections. Next, transmission overestimation issue, which may occur when the spatial background difference method is used, are presented and discussed. Specifically, the discussion

includes (1) reasons of the overestimation issue and (2) diagnosis of the overestimation issue.

Variations in Spatial Background Difference

As the first step to characterize the transmission characteristics of the chamber construction, the graphical contour mapping of the spatial background SPL difference expressed in Eq. (3-4) is presented in Figure 3-3. It is noticeable that the contour illustrated in Figure 3-3 shows a trend of having maximum transmission losses near 125 through 315 Hz bands in general and more transmission occurring at both ends of the 1/3 octave bands. However, the different spectra of the spatial background SPL difference, $\Delta_{e,i}^{B}$, can be frequently observed, which deviates from the general trends of the contour. It should be noted that the variation is not caused by the variations in the background noise, because the external and internal SPLs, $L_{p(e)}^{B}$ and $L_{p(i)}^{B}$, are measured simultaneously. Specifically, the temporal background difference due to the background fluctuations between the inside and outside the chamber does not affect the varying spectra of the spatial background SPL difference $\Delta_{e,i}^{B}$ observed in several samples in Figure 3-3.

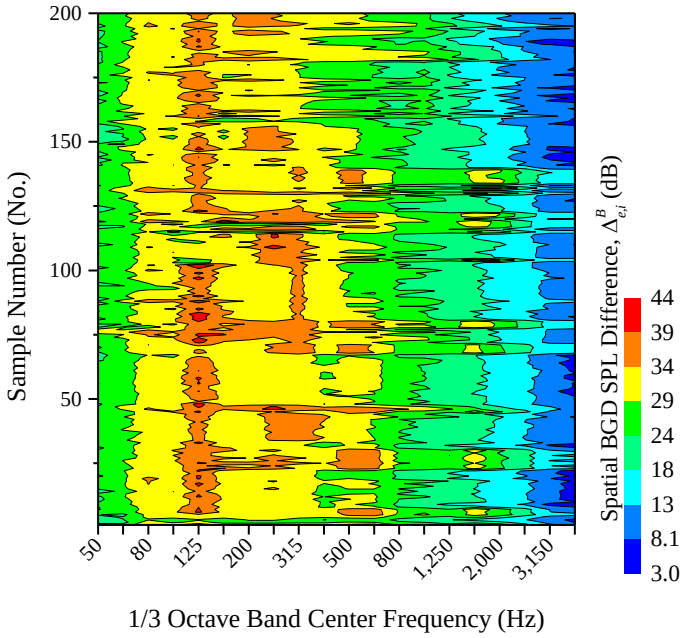

Figure 3-3 Contour mapping of the spatial background sound pressure level difference $\Delta^B_{e,i}$ in Eq. (3-4)

These different spectra are rather the outcome of the different background conditions that are predominant at different locations surrounding the chamber construction. In addition, the semi-reverberant chamber wall, the roof, and the floor were built by using different layers of material, which means the transmission characteristics of the chamber construction is inhomogeneous. Therefore, the background noise will be measured differently if the background noise source is located at different locations. For example, the background noise transmission was found to be dominant at specific locations of the chamber construction when the noise is influenced by prevailing wind directions, different sound intensities of the gust, noise emitted from trains, airplanes, highway traffics, etc. [75]. As such, Figure 3-3 shows that each different background noise

source affected a specific side of the chamber although the base background noise, which is omnidirectional such as white noise, constitutes the baseline of the spectra.

Another observation found in Figure 3-3 is that similar trends in spectra are continued for several consecutive sample numbers. For example, the spatial background SPL differences of sample numbers 34 through 44 show similar trends. It should be noted that the sample data are sorted in chronological order, being grouped with samples tested at a given time frame. Therefore, the spatial background SPL difference, $\Delta_{e,i}^{B}$, tends to remain constant for a limited time frame.

However, when the spatial background SPL difference are plotted against time of measurements irrespective of the testing dates and years, noticeable trends were not found. For instance, three bands represented by the center frequencies of 125, 500, 1,600 Hz are chosen because of the relatively larger variations of the spatial background SPL difference, which is also noticeable in Figure 3-3. In order to take a closer look at variations, Figure 3-4 shows variations of the spatial background SPL difference at the 125, 500, and 1,600 Hz bands. It should be noted that the time between 4:00 and 21:00 were not plotted because of insufficient samples (less than 3 samples per hour). The following are observations made from Figure 3-4.

1. Adjacent bands, e.g., 125 Hz and 500 Hz bands or 500 Hz and 1,600 Hz bands, have relatively similar SPL trends.

2. Distant bands, e.g. 125 Hz and 1,600 Hz bands, shows less correlation.

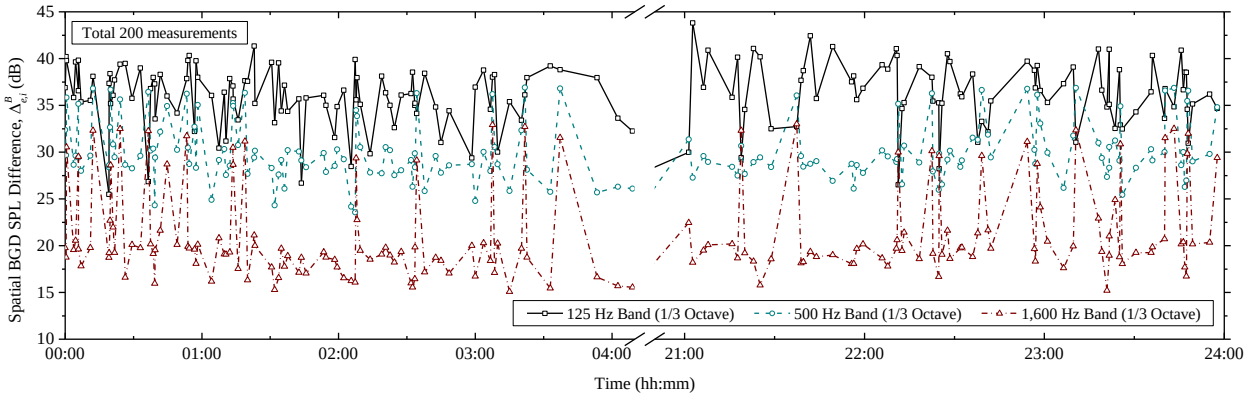

Figure 3-4 Spatial background SPL variations of three 1/3 octave bands, 125, 500, and 1,600 Hz center band frequencies, plotted against time

Overestimation of Sound Transmission

Another Figure 3-3 and Figure 3-4 observation is the spatial background SPL difference $\Delta_{e,i}^{B}$ at higher bands are relatively lower than $\Delta_{e,i}^{B}$ at lower bands. Specifically, the first derivative of the spatial background SPL difference with respect to 1/3 octave band center frequency f, $d\Delta_{e,i}^{B}/df$, reveals decreasing values over 125 Hz.

The negative values of the first derivatives can be interpreted as the chamber material being devoid of mass controlled regions or damping controlled regions, where the sound transmission loss is increase by 6 dB/octave and 10 dB/octave, respectively, over the 125 Hz band. However, the argument that the chamber construction does not have these mass controlled and damping controlled regions as sound transmission characteristics is physically invalid [68]. Therefore, the overestimation of the sound transmission through the chamber construction is suspected at higher bands.

The spatial background difference method is able to overestimate the sound transmission of the unit under test by having lower spatial background SPL difference $\Delta_{e,i}^{B}$, when the background noise is quiet. Specifically, the overestimation of the sound transmission happens when the quiet background noise is not distinguished from the inherent noise of microphones, which is primarily caused by thermal Brownian motion of the air and the electrical noise [76-78].

The overestimation of the sound transmission can cause the significantly low SNR of the The overestimation of the sound transmission can cause significantly low SNR of the $L_{p(e)}^{UT}$ and $L_{p(e)}^{U*}$ expressed in Eq. (3-8), which does not reflect the true sound transmission of the unit under test through the chamber construction. As such, there is a need for a

criterion in order to determine whether the sound measurement suffers from the overestimation of the sound transmission due to the quiet background. A simple criterion can be made by setting the lower limit of the sound pressure levels, which indicates a quiet background along with the inherent microphone noise on the same level. However, the inherent microphone noise for the criteria depends on individual microphone specifications and meteorological conditions, which can be arbitrary for each system and circumstances. Furthermore, many of the laboratory-grade microphones provide limited detail of the inherent noise data without the spectral characteristics of the inherent noises on extended range of frequencies and meteorological contributions. In addition, modeling of the individual microphone along with the environment is intricate because of the complicated influences of environmental variables [77].

Diagnosis of Overestimated Sound Transmission

Assuming overestimated transmission exists based on physical interpretations, then there is a need for identifying those frequency bands that are affected by the overestimated transmission. The study herein utilizes a two-fold diagnosis process for the spatial background difference, namely (1) applying a free field relationship, and then (2) the insertion loss method is used to overcome the overestimation of the sound transmission. As an aside It should be noted that both qualifications are applicable irrespective of the type of microphone, because arbitrary numerical limits are not used for the verification process.

As the first step, the free-field relationship can be used in order to guarantee that the spatial background difference may not reflect the real transmission characteristics. The free field propagation factor (henceforth, the propagation factor) Δ_f is set by the calculation of the free field SPL reduction for the distance of microphones inside and outside the chamber with respect to the sound source (i.e. unit under test) as follows.

$$\Delta_f = 10\left|\log\frac{Q}{4\pi r^2}\right| - RCR \tag{3-14}$$

The physical interpretation of Eq. (3-14) is that SPL reduction (or difference) due to the acoustic transmission through the chamber construction should exceed the amount of the SPL reduction due to the free-field sound propagation by a great margin. In other words, if the spatial background SPL difference $\Delta_{e,i}^{B}$ is found to be less than the propagation factor Δ_f in Eq. (3-14), the overestimation of the sound transmission must have occurred, and then the alternative method to assess the sound transmission and its contribution to the external background measurement is necessary. In this study, the propagation factor expressed in Eq. (3-14) is found to differ for each test, primarily because of the varying RCRs, introduced in Eq. (3-13). Having different RCRs is attributed to different meteorological conditions, and thus different air acoustic properties and different field characteristics that is caused by the different chamber configuration.

The semi-reverberant chamber depicted in Figure 3-2 has shown possibilities for different field characteristics because of the varying installation of the unit, which can work as an acoustic baffle when the RSS operates, and different inlet and outlet setups

based on configuring the throttling device and the inlet make-up air. As evidence of the varying RCR, Figure 3-5 presents the propagation factor Δ_f with respect to varying tests. The test sample number follows the same chronological order in Figure 3-3. It is distinctively noticeable in Figure 3-5 that the patterns do not significantly differ for each sample because the RSS in principle operates with consistent performance with lesser contribution of the environments. However, several bands, such as between 100 and 250 Hz, and between 3,150 and 10,000 Hz, show relatively inconsistent propagation factors.

Also in Figure 3-5, several groups of similar trends are observed, such as the first 75 samples, which are found to be seasonal effects. Aside from the different trends of the propagation factors which appears by groups of samples, there are minor variations along with the several non-seasonal fluctuations. It was found that different unit and chamber setups resulted in these variations in the RCRs and the propagation factors.

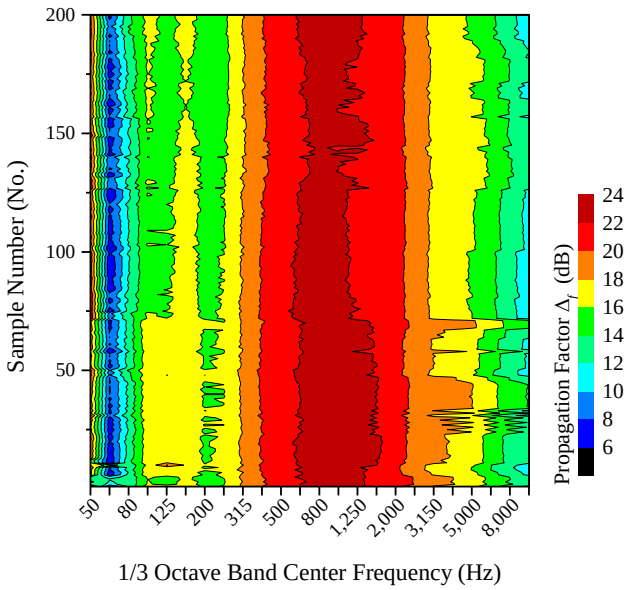

Figure 3-5 Contour mapping of the propagation factor Δ_f of 200 tests

Based on the propagation factor illustrated in Figure 3-5, the large portion of the spatial background SPL difference, about 1/3 of the higher octave bands (approximately above 2,000 Hz), were found to be under the propagation factor, and this indicates the spatial background difference have overestimated the sound transmission. Furthermore, the overestimation is likely to be traced further down lower bands, because the slope or the first derivative of the spatial background SPL difference were found to be monotonically negative above 315 Hz bands without revealing mass controlled regions, which is frequently observed in hard walled sound transmissions [68].

The use of the propagation factor is relatively simple; however, limitations of this validation by using the propagation factor still exist in that the propagation factor is not able to estimate how much overestimation has occurred. Therefore, the propagation factor only serves as a quick estimator of the overestimated transmission of the spatial background SPL difference, and thus further calculations based on the insertion loss is necessary.

Transmission Estimation by Using Insertion Loss

If the overestimated transmissions are found, the insertion loss method can be used as an alternative method. The following sections discuss results of the insertion loss calculations for the 200 fan test database. Of special importance, the insertion loss method utilizes SPL differences of the RSS and BGD, and several different results can be made for evaluating the logarithmic differences. This section presents variations of these differences and its impact to the insertion loss is also presented.

Using RSS Transmission for Insertion Loss

As discussed in the earlier 'Insertion Loss Method' section, the insertion loss is defined as the SPL differences of the RSS between (1) a setup such that the acoustic barrier does not exists, and (2) the other setup with an acoustic barrier (i.e. the chamber construction) that exists and. Therefore, the Insertion Loss intrinsically assumes noticeable or measurable acoustic transmissions through the chamber construction when the RSS is generating a noise for the calculation of the setup. Specifically, the transmitted RSS SPL through the acoustic barrier, i.e., SPLs, might not be readily determined at the specific situations that are listed below.

1. An acoustic transmission is not dominant in the measured SPL because of the weak sound power of the RSS against the impedance of the barrier, and
2. Background noises are in flux so that the transmitted sound can be smudged or insufficiently separated by the background noise fluctuation.

Most commercially available RSS devices are capable of avoiding the issue described in (1) by generating large sound levels (e.g., over 80 dB SPL), while issue (2) cannot be easily addressed when the external background noise sources are highly uncorrelated and/or inadequately controlled, which often results in unsteady backgrounds.

Our preliminary tests revealed that sound transmissions of the RSS signal through the chamber construction were observed at multiple bands provided that the background is quiet and stable. However, among the 200 sample tests used in this study, a large fraction of the tests showed that the background noise has negatively influenced the

separation of the transmitted RSS signal through the chamber construction from the external background signal mixed with the RSS transmission. For example, there were several cases showing larger external background noise at BGD phase than the measurements at RSS phase, $L^{B}_{p(e)} > L^{RSS}_{p(e)}$.

However, it is expected by intuition that more than half of the samples can have external SPLs as $L^{B}_{p(e)} < L^{RSS}_{p(e)}$, even with both the transmitted RSS sound energy and uncorrelated random background present. Figure 3-6 shows the distributions of the external SPLs for the BGD phase, $L^{B}_{p(e)}$, and for the RSS phase, $L^{RSS}_{p(e)}$, at the (a) 50 Hz and (b) 1,250 Hz bands. These two bands were chosen as an example because distinctive features were found at low frequency bands and medium-to-high frequency bands. The histogram of the 50 Hz band in Figure 3-6 shows that the largest separation of the transmitted RSS signal from the background noise with less overlap, which is in contrast to the distribution of the 1,250 band being close, although some separation is observed with different mean SPLs.

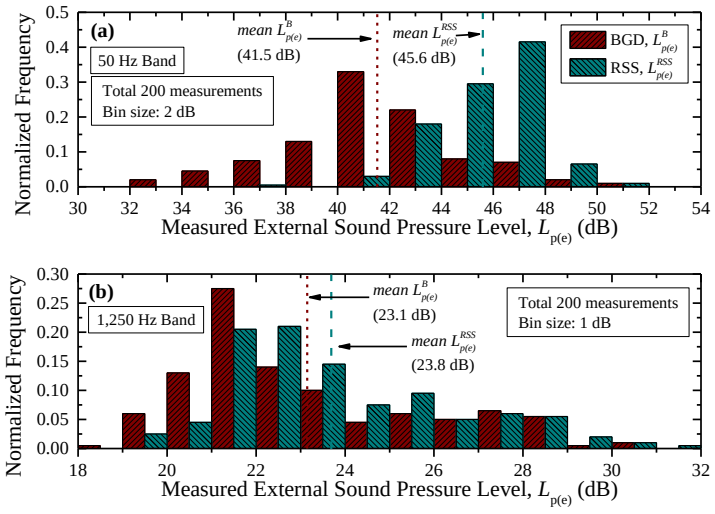

Figure 3-6 Histograms of external sound pressure levels at BGD, $L^{B}_{p(e)}$, and RSS phases $L^{RSS}_{p(e)}$ (a) 50 Hz band, and (b) 1,250 Hz band

Hypothetical Test for RSS Transmission

In order to investigate this overlapped but expected different external SPLs for the BGD and RSS phases, statistical inference can be established, namely the pair sample t-test for $L^{B}_{p(e)}$ and $L^{RSS}_{p(e)}$. The use of the paired sample t-test is adequate for this background SPL differences because (1) two sample groups, $L^{B}_{p(e)}$ and $L^{RSS}_{p(e)}$, are correlated under the background noise, and (2) the treatment of the RSS signal transmitting through the chamber construction affects only the latter measurements, $L^{RSS}_{p(e)}$, which is a type of the investigation of the 'before-and-after' effect [65]. As noted, the only difference is the presence of the transmitted RSS signal. The null hypothesis $H_0(f)$ of each frequency band *f* set to this inference is

$$H_0(f): L^{B}_{p(e)} > L^{RSS}_{p(e)}$$

, and the alternative hypothesis is set to

$$H_1(f)\colon L^B_{p(e)} \leq L^{RSS}_{p(e)}.$$

The significance level is set to α=5%. The t-statistic, *T*, is defined below [65].

$$T = \frac{\bar{d}(f)}{SE\left(\bar{d}(f)\right)} \tag{3-15}$$

, where

- $\bar{d}(f)$ is the mean of the SPL differences of the frequency band *f*, i.e. the mean value of $d(f) = L^B_{p(e)} - L^{RSS}_{p(e)}$, and
- $SE(\bar{d}(f))$ is the standard error of the frequency band *f*, which is obtained by dividing the sample standard deviation of *d* (degree of freedom: $n-1$=199) by the square root of the number of sample $\sqrt{n}$=$\sqrt{200}$, respectively.

The critical value, which is the value to test the hypothesis, for the left-tail t-distribution is found to be $t_{crit} = -1.65$, based on the degree of freedom $n-1$ being 199, and α=0.05. In other words, if the test statistic value, *T*, is larger than the t_{crit}, the hypothesis is significantly valid.

Table 3-4 presents a summary of the statistical inference made for the external comparison. In Table 3-4, boldfaced test statistic *T* with **(R)** denotes the null hypothesis being rejected because the test statistic is found to be at the rejection region by *T* being less than t_{crit}.

As expected, the null hypothesis for most of the frequency bands were found to be rejected because the test statistic *T* is less than the critical t-distribution value t_{crit}, which means external SPL at a RSS phase is likely to be larger than the external SPL at

the BGD phase ($H_1(f)$), or there is strong evidence of the RSS sound energy transmitting through the chamber construction. Of special interest, the mean external RSS difference $\bar{d}$ along with the 95% confidence interval of the difference is plotted in Figure 3-7.

Table 3-4 Summary of the statistical inference for the external SPL comparison, $L^{B}_{p(e)} - L^{RSS}_{p(e)}$

1/3 Octave Band Frequency (Hz)	Test Statistic, T (t_{crit}=-1.65)	p-value (α=0.05)	1/3 Octave Band Frequency (Hz)	T-test Statistic, T (t_{crit}=-1.65)	p-value (α=0.05)
50	**-23.12 (R)**	<0.001	800	**-4.95 (R)**	<0.001
63	**-5.77 (R)**	<0.001	1,000	**-5.19 (R)**	<0.001
80	**-4.05 (R)**	<0.001	1,250	**-6.55 (R)**	<0.001
100	**-4.96 (R)**	<0.001	1,600	**-5.49 (R)**	<0.001
125	2.20	0.986	2,000	**-4.78 (R)**	<0.001
160	**-2.06 (R)**	0.020	2,500	**-3.41 (R)**	<0.001
200	**-2.62 (R)**	0.005	3,150	**-2.30 (R)**	0.011
250	**-2.32 (R)**	0.011	4,000	**-1.79 (R)**	0.038
315	**-3.02 (R)**	0.001	5,000	-1.00	0.160
400	**-6.39 (R)**	<0.001	6,300	-1.22	0.113
500	**-4.05 (R)**	<0.001	8,000	-0.21	0.418
630	**-3.97 (R)**	<0.001	10,000	1.65	0.949

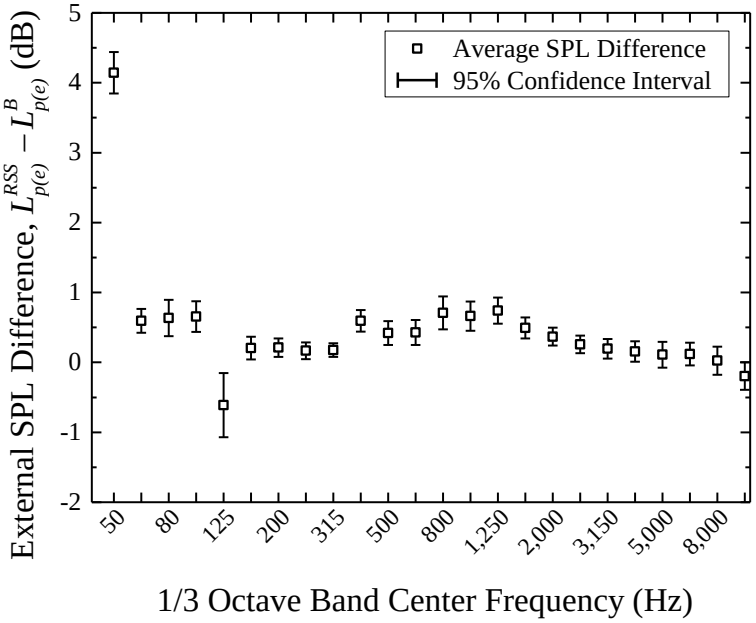

Figure 3-7 Measured average external SPL differences in each 1/3 Octave frequency band along with the 95% confidence interval

When Table 3-4 and Figure 3-7 are interpreted along with Figure 3-6, a higher likelihood of $L_{p(e)}^{B} \leq L_{p(e)}^{RSS}$, or the RSS sound transmission, is expected in each test despite the background randomness, which occasionally covers the transmitted RSS sound to undetectable levels. Furthermore, the span of the confidence interval, most of which spans in the positive region, suggests that the population mean of $L_{p(e)}^{RSS} - L_{p(e)}^{B}$ is expected to be positive in many attempts of the 95% confidence interval in most bands only except 125, and 5,000 through the 10,000 Hz bands.

As an aside, both the mean SPL differences $\bar{d}(f)$ and the 95% confidence intervals of the last four bands, namely f =5,000 through 10,000 Hz bands, are aligned near zero or less than zero. It is expected that the RSS sound transmission is suppressed due to the

larger transmission loss in these bands. However, the SPL difference $\bar{d}(f = 125\text{Hz}) = -0.6$ is distinctively less than that of the other bands with the larger confidence interval, which means the population mean of the SPL difference can range from -1 to 0 at the 95% confidence. Because of the larger confidence interval of $\bar{d}(f = 125\text{Hz})$, which implies a larger uncertainty, and the reverberant field developed inside the chamber, it is not appropriate to ascertain that there was a destructive interference during RSS operations.

Using Sample Mean for Insertion Loss

Although the RSS transmission was expected to exist in a majority of the bands, the practical usage of the sample mean $\bar{d}(f)$ for Eq. (3-12) has several limitations when determining the residual RSS signal transmitted through the chamber construction. First, the determination of $\bar{d}(f)$ involves the collection of a large amount of statistical information, at least enough to guarantee the repeatability of future tests. Next, $\bar{d}(f)$ is not able to address the different testing setup or varying field characteristics along with the different meteorological conditions, which were discussed in Figure 3-3 through Figure 3-5. Lastly, as discussed in the statistical inference process earlier, $\bar{d}(f)$ is expected to be within the specific confidence level prescribed, rather than to be an exact population mean. In this regard, there are at least two options for Eq. (3-11) to treat the RSS sound transmission concealed by background unsteadiness.

The first option is using the sample mean SPL difference after the statistical inference. Despite the aforementioned limitations, the insertion method can get a significant benefit by using the $\bar{d}(f)$ in order to determine the transmitted RSS sound

with an acceptable precision. In order to show the applicability of the sample mean SPL difference $\bar{d}(f)$ for the IL, Figure 3-8 presents the insertion loss along with the expanded uncertainty associated with the precision of the sample mean. As a side note, the expanded uncertainty in Figure 3-8 incorporates all terms subjected to individual uncertainties in Eq. (3-10) and Eq. (3-11), specifically the sound power levels of the RSS L_W^{RSS} as well as the confidence interval of the sample mean SPL differences. Therefore, an expanded interval of the uncertainty is observed in Figure 3-8.

When comparing the uncertainty with respect to the *IL of each frequency band*, it was found that the uncertainties do not exceed more than five percent of the IL above the 125 Hz band. In addition, the frequency bands between 160 and 8,000 Hz had an uncertainty of less than two percent in Figure 3-8. Based on these observations, the usage of the sample mean SPL difference $\bar{d}(f)$ for determining *IL* can be reasonable above certain frequencies, such as above 125 Hz band.

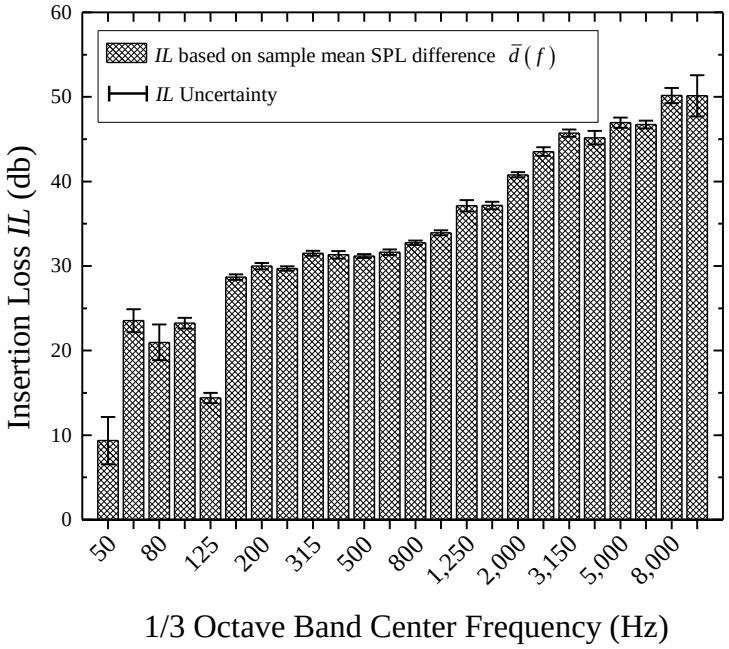

Figure 3-8 Insertion loss when using the sample mean SPL difference $\bar{d}(f)$

Using Absolute SPL Difference for Insertion Loss

Another option to determine the RSS transmission is taking the absolute value of the SPL differences in Eq. (3-11), which is shown below.

$$L_{p(e)}^{RSS*} = 10\log\left|10^{L_{p(e)}^{RSS}/10} - 10^{L_{p(e)}^{B}/10}\right| \tag{3-16}$$

The implication underlying the use of Eq. (3-16) instead of Eq. (3-11) is that the RSS sound transmission is substituted by the amount of the background unsteadiness because the extent of the background unsteadiness can be either equivalent to or larger than the RSS sound transmission. As an illustration, Figure 3-9 shows the variations of the insertion loss associated with the background unsteadiness, when the RSS transmission

in Eq. (3-11) is substituted by the background difference in Eq. (3-16). Figure 3-9 shows distributions of *IL* calculated based on the background differences in Eq. (3-16).

As can be seen in the box plots in Figure 3-9, variations can be observed in each frequency band. *IL* values are concentrated in specific portions of *IL* values along with the largest span of the outliers up to 30 dB. For example, the interquartile ranges (IQR), the values between the first quartile and the third quartile, were found to be between 3.7 and 8.7 dB for the entire *IL*s in Figure 3-9. Specifically, the 50 Hz band has shown minimum variations with 3.7 dB of IQR. The minimum *IL* variations at the 50 Hz band is also consistent to the test statistic in Table 3-4, which turned out to be largest possibility for the observation of the RSS transmission through the chamber construction.

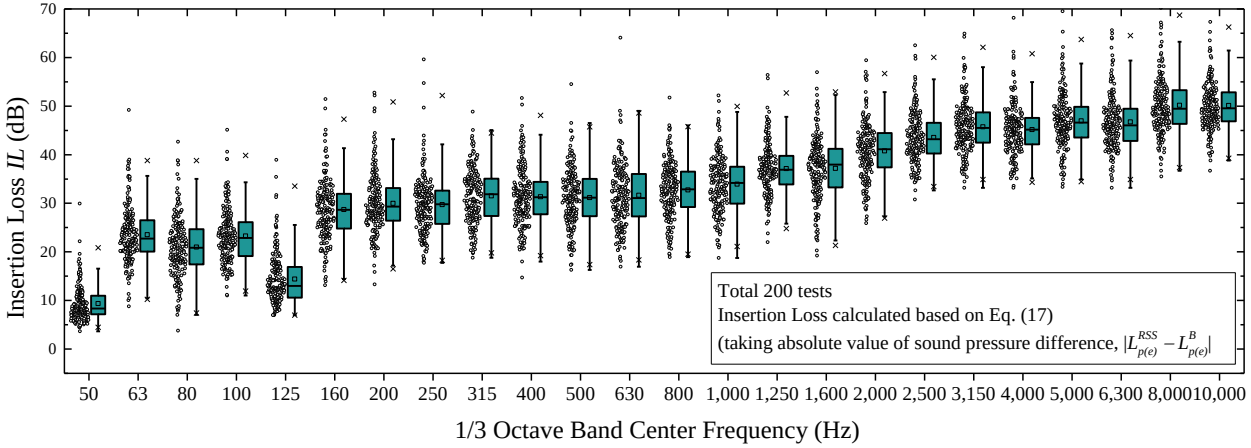

Figure 3-9 Distributions of the insertion loss by taking the absolute sound pressure difference in Eq. (3-16)

Comparisons of Spatial Difference and Insertion Loss

Unlike the spatial background SPL difference shown in Figure 3-3, there is an increasing trend of the insertion loss, which is also observed in the *IL* based on the sample mean SPL difference. Specifically, the increasing trend of the *IL* is distinctively noticeable between 630 and 3,150 Hz bands. Of special importance, the critical frequencies f_c, which are defined as frequencies when the material bending wavelength coincides to the sound wavelength of the air, are found to be 520, 1164, and 3,132 Hz at walls, roof, and the door consisting of the non-concrete portions of the chamber, based on the following expression along with the composite wall calculations [13].

$$f_c = \frac{\sqrt{3}c^2}{\pi c_L h} \tag{3-17}$$

, where c is the speed of the sound in air (340 m/s at 300K), c_L is the longitudinal speed of the acoustic wave of the medium, and h is thickness of the medium, respectively. Because the chamber construction is a complicated system consisting of different layers of materials with varying dimensions, each frequency band is the combination of several transmission characteristics, such as the stiffness-controlled region, the mass-controlled region and the damping-controlled region. However, the frequency bands showing the increasing *IL* trend in Figure 3-8 and Figure 3-9 falls approximately into the mass-controlled region and the damping controlled region. Therefore, contribution of these regions is expected between 630 and 3,150 Hz bands.

Once the spatial background SPL difference and the insertion loss are determined, it is important to compare both methods. Prior to comparing both methods, it is necessary to convert *IL* to a quantify equivalent to the spatial background difference by

accommodating the actual acoustic field conversion. This field conversion can be done by taking the negative sign of the last three terms in Eq. (3-18) as follows.

$$IL_{fc} = IL - RCR + 10\left|\log\frac{Q}{4\pi r^2}\right| \tag{3-18}$$

, where IL_{fc} refers to the insertion loss after the field conversion.

A graphical summary and comparison are presented in Figure 3-10. The solid lines A graphical summary and comparison are presented in Figure 3-10. The solid lines with the square and circle symbols represent the spatial background SPL difference $\Delta_{e,i}^{B}$ and the insertion loss after the field conversion IL_{fc}, respectively, that are accepted as the transmission characteristics for this study. These two transmission characteristics are obtained by averaging the 200 sample tests. The solid line with X symbols represents the propagation factor Δ_f, which were used for validating the overestimated sound transmission of the spatial background SPL difference along with the first derivatives of the spatial difference. The dash-dot lines in Figure 3-10 are the spatial background SPL differences $\Delta_{e,i}^{B}$ that experienced the overestimation of the sound transmission (right triangle symbols) or the insertion loss IL_{fc} after the field conversion, which had larger uncertainties (inverted triangle symbols) as shown in Figure 3-8 and Figure 3-9. These dash-dot lines represent calculated transmission characteristics that are less accurate compared to alternative method or that are expected to be invalid.

There are three regions in Figure 3-10 that are zones based on the scheme used.

1. Region I: It is where the spatial background difference is likely to provide more accurate transmission characteristics because the statistical inference or the background randomness affected the insertion loss.

2. Region II: It is a band center frequency gap between two methods. If the analysis is performed with frequency filters such as 1/n-th octave frequency bands, an interpolation is unnecessary because two end points of the Region II is of importance, and this region is merely the band-filter-overlapped region. However, if the finer resolution is necessary by using the Fast Fourier Transform, etc., this region can be affected by boundary conditions or interpolation schemes. For example, the study herein uses 1/3 octave bands. Therefore, any numerical treatment such as boundary conditions or interpolation is unnecessary.

3. Region III: It is the region where the insertion loss provides more accurate transmission characteristics while the spatial background difference method is invalid due to the overestimation. The propagation factor was found to be larger than the spatial background SPL difference in this region above a certain band frequency, i.e. 1,250 Hz.

As discussed previously in Figure 3-8 and Figure 3-9, there is a noticeable increase of the insertion loss after the field conversion, which is in contrast to the spatial background SPL difference. Of special importance, it should be noted that Figure 3-10 is an example of the usage of the two methods presented and discussed in this study. Various field characteristics inside acoustic chambers, transmission characteristics, and background noises can result in acoustic signatures that differ from one another in Figure 3-10. For example, when the background noise is louder than the background noise in

this study, then the Region I is going to be dominant. On the contrary, if the background noise is quieter than the background noise herein, then there is possibility that Region I is not developed, which means only the insertion loss method is useful. In addition, if the background is highly unstable, such as for acoustic facilities that continuously suffer from random loud impulses, then Region III might not readily be developed because both the sample mean SPL difference $\bar{d}(f)$ and the substation the RSS sound transmission with the external background difference expressed in Eq. (3-16) fail to guarantee the statistical significance.

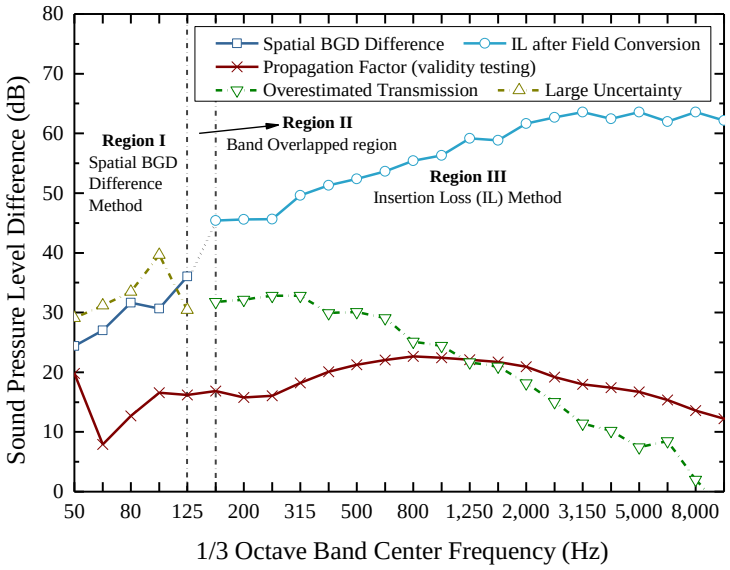

Figure 3-10 Summary of the two methods, namely the spatial background difference method and the insertion loss along with the field correction

Based on observations in Figure 3-10, comparisons between the spatial background difference method and the insertion loss method are made.

1. First, the spatial background difference method can overestimate the sound transmission, which limits applications of the method. It was found that the overestimation occurred when the background noise is similar or less than the propagation factor. It should be noted that measured background noise levels (average 47.1 dB) were quieter than the moderate background noise levels (usually 55-65 dB) [74], and this quiet background caused the limited use of the spatial background difference method. Therefore, the spatial background difference method can still be useful when the method is used along with the presence of the moderate to loud background noise such as in manufacturing facilities, laboratories with noise emitting devices, or testing laboratories in an urban area.

2. Second, the spatial background difference method is not affected by the background unsteadiness because the simultaneous measurement inside and outside the chamber is utilized rather than two signals measured at different time. Therefore, the spatial background difference method does not require the statistical inference used for the insertion loss or the further assumption of the RSS sound transmission in Eq. (3-16). It is in contrast to the insertion loss in that the calculation of the insertion loss requires a treatment of the background randomness when determining the RSS sound transmission.

3. Third, despite the trade-off of the aforementioned disadvantages of the insertion loss, the insertion loss method can provide a reliable estimation of the transmission characteristics without the overestimated sound transmission. The insertion loss method using the sample mean SPL difference $\bar{d}(f)$ was found to be especially reliable at medium to high frequency bands with lower uncertainties. However, if the background

noise is intense, then the insertion loss method can suffer from the lower resolution of the RSS sound transmission through the chamber when calculating the transmitted RSS sound by using Eq. (3-11) and Eq. (3-16).

4. Lastly, both methods take into account the temporal test conditions and the field characteristics for the transmission characterization as shown in Figure 3-3, Figure 3-5, and Eq. (3-13). Thus, when assessing the background steadiness, it is important to utilize the concurrent sound transmission characteristics by using either the spatial background difference method or the insertion loss method eclectically. In conclusion, the eclectic use of the acoustic transmission signature is necessary by utilizing information gathered by measurements.

Signal-to-Noise Ratio Analysis Inside and Outside Chamber

The SNR of the transmitted unit signal versus the measured external background noise, SNR_e^{UT}, in Eq. (3-8) are obtained by using the combined sound transmission characteristics plotted in Figure 3-10 as the solid lines with the circle and the square symbols. Prior to the calculation of SNR_e^{UT}, it can be intuitively understood that tested units that generate sound far quieter than the RSS do not affect the sound transmission significantly based on the observations in Figure 3-10.

As an aside, the SNR, SNR_e^{RSS}, of the external background SPL and the transmitted RSS sound through the chamber construction, namely $L_{p(e)}^{RSS} - L_{p(e)}^{RSS^*}$, was found to be between 2.3 and 11.0 dB, when the 200-sample-average of the external background SPL difference in Eq. (3-16) was used. Therefore, it would be trivial to look into the test units that were quieter than the RSS, for instance by more than 20 dB. As such, most of the

200 sample SNR_e^{UT} were found to exceed 20 dB, which was set as 'correction unnecessary' in the methodology description section, because most of the samples were significantly quieter than the RSS.

Among 200 sample tests, Six tests were found to have SNR_e^{UT} less than 20 dB. Furthermore, four of the six tests by using a centrifugal-squirral-cage fan were the loudest measurements but none of the 1/3 octave band SPLs $L_{p(i)}^{UT}$ were less than the RSS SPL $L_{p(i)}^{RSS}$. Figure 3-11 is the graphical comparison of the SNRs, namely the median SNR_e^{UT} of the 200 test samples, SNR_e^{UT} of the test, which showed the minimum SNR_e^{UT}, and the averaged RSS, SNR_e^{RSS}. The median of SNR_e^{UT} was chosen as the representative of the overall test samples due to the fact that the median is less influenced by the two extremes of the lowest and largest SPLs, especially when considering varying SPLs of the test samples. In contrast, the average of the RSS SNR_e^{RSS} was chosen as the representative because the entire RSS measurement was done for the single unit, which operates at very consistent performances, which is the dictating nature of the RSS.

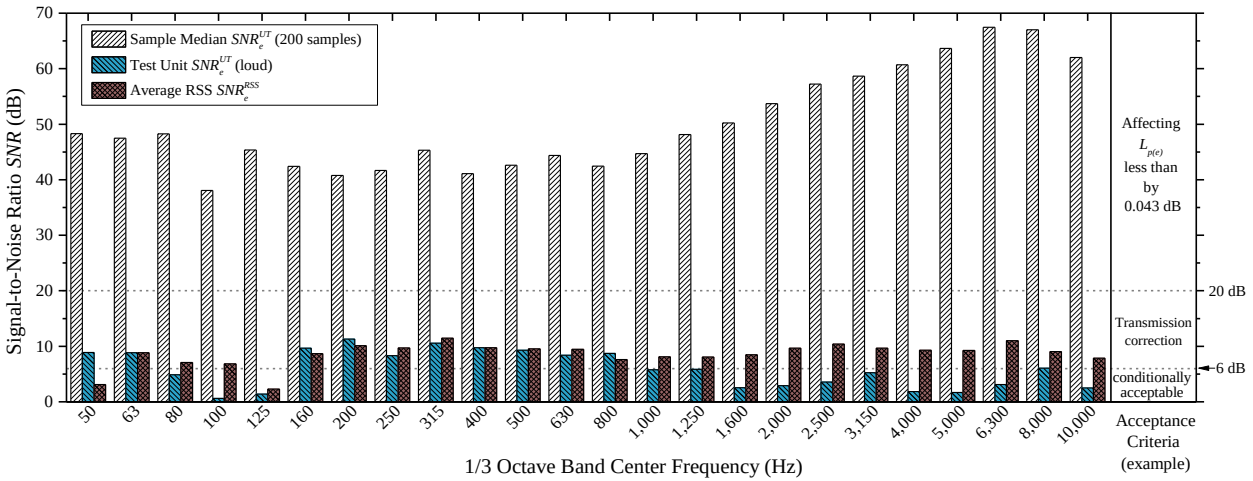

Figure 3-11 Signal-to-Noise Ratio (SNR) of the 200 test sample median, loud test unit, and average RSS

As previously discussed in the Description of Methods section, an example of the SNR criteria was set along the 6 and 20 dB SNR_e^{UT} boundaries. Specifically, when SNR_e^{UT} is larger than 20 dB, the correction is unnecessary, while SNR_e^{UT} between 6 dB to 20 dB requires the transmission correction as shown in Eq. (3-9). In addition, SNR_e^{UT} less than 6 dB means that the transmission correction can be at least 1.26 dB, which means there is a likelihood in a certain situation that the external background SPL $L_{p(e)}^{UT}$ may not represent the pure background even after the transmission correction expressed in Eq. (3-9). Of special importance, the criteria introduced herein is consistent to ISO/ANSI reverberant acoustic standards [10, 11], and it should be noted that the criteria introduced in this study serves as an example. Therefore, different criteria can be introduced based on the specific need, depending on the nature of test specimen.

In Figure 3-11, it is not surprising that the median SNR_e^{UT} in Figure 3-11 exceeds 20 dB by the great margin. Also, the SNR_e^{UT} becomes larger at higher frequency bands primarily because the insertion loss is larger at higher frequencies. In contrast, the RSS SNR_e^{RSS} is found to be smaller than 20 dB, which means the RSS transmission influenced the external background SPL $L_{p(e)}^{RSS}$ to the extent that the transmission corrections is necessary, if one attempts to evaluate the background steadiness by using the external microphones. Likewise, the test with the minimum SNR_e^{UT} in Figure 3-11 showed its SNR less than 20 dB, and even less than 6 dB in almost half of the overall frequency bands. Another interesting observation for the test with the minimum SNR_e^{UT} is several SNRs were almost similar to or even greater than SNR_e^{RSS} while other SNRs were less than the SNR_e^{RSS} by the significant margin. It was originally expected that the

SNR_e^{UT} for the test could be less than the SNR_e^{RSS} for the RSS because the measured SPLs $L_{p(i)}^{UT}$ were greater than the RSS $L_{p(i)}^{RSS}$ for each frequency band. However, it was found that the varying background noise dictated the trends of these SNRs, which again emphasizes that the background noise and its fluctuations can affect the transmission analytics.

By using the methods and the criteria introduced in the study, one can determine how much the external background SPLs $L_{p(e)}$ is affected by the transmission of the unit under test. As the next step, the background steadiness assessment by using the external signals will be discussed in the next volume.

Conclusions

The intrusion of the acoustic background noise results in background noise characterizations and treatment processes in different areas of the acoustic performance evaluations of sound sources (or unit under test) as demanded by various international standards. The treatment of the background noise has been extensively studied, and most of the efforts have focused on eliminating its effect on the signal emitted from the unit under test, such as background corrections that follows measurements of the unit under test. However, the assessment of the background steadiness has been less studied, and its implementations have been limited to the use of the measurement uncertainty and comparisons of the two different background noises.

As such, more studies to improve the process of evaluating the background noise steadiness is necessary. The study herein proposed the background steadiness assessment by monitoring the external background noise outside the semi-reverberant chamber,

while the signal of the unit under test is being measured. In order to monitor the external background noise, the background noise should not be influenced by the sound of the unit under test or the reference sound source (RSS) that can be transmitted through the chamber construction, which in turn demands the sound transmission characterization of the chamber as the unit is under test or as the RSS generates the sound.

As the first part of the background steadiness study, the two methods are introduced, namely the spatial background difference method and the insertion loss method, for evaluating the sound transmission through the semi-reverberant chamber. The spatial background difference method uses the spatial sound pressure level (SPL) difference inside and outside the chamber when neither the unit under test nor the RSS operates. Because the signal inside and outside the chamber are simultaneously measured, assumptions or statistical inference regarding the background steadiness are necessary. However, depending on the amount of the SPLs, there is a possibility of the overestimated sound transmission, which renders the method less useful for the frequencies that experienced the overestimation.

As a real world-example, the study herein analyzed 200 individual tests, and it was found that the average external background noise was 47.1 dB, which was quieter than the moderate residential background noise levels of 55-65 dB. Because of this relatively quiet background, multiple frequency bands are expected to experience the overestimated transmission when the spatial background difference method was used. In order to validate the overestimation, the propagation factor, which assumes the free-field propagation of the sound, and the slope or the first derivative of the spatial background

SPL differences at each band were used to determine the overestimated sound transmission.

As an alternative, the insertion loss method, which uses the acoustic signature of the RSS to evaluate the sound transmission characteristics, was necessary for the multiple bands that suffered from the overestimated transmission. Because the insertion loss method needs to determine the sound transmission of the RSS, the method may intrinsically involve either the statistical inference to predict the RSS sound transmission or the assumption that the background randomness can be substituted with the transmitted RSS signal. Despite these statistical inferences or assumptions, the insertion loss method does not result in the overestimation of the sound transmission. In addition, test results by using both methods revealed that each test requires the transmission characterization by using either of the methods, because the different setups of the unit under test, varying field characteristics, and meteorological conditions can result in different sound transmissions.

The fundamental motivation of these two methods is the assessment of the transmission of the unit under test or the RSS when monitoring the external background. The signal-to-noise ratio (SNR) analytics were also presented as an example for these methods. Depending on the value of the SNRs, the sound transmission can be considered negligible, or if the external SPLs are being significantly influenced by the transmission of the unit under test or the RSS, then the external background is conditionally acceptable for a further background steadiness assessment. As an example, the SNR criteria were set to over 20 dB the for the transmission effect being negligible, between 6

and 20 dB for the transmission correction being necessary, and less than 6 dB for the external SPLs being conditionally acceptable for the usage of the external background. A majority of the sound transmission of the unit under test did not readily affect the external background SPLs in terms of the SNRs, being larger than 20 dB. However, for 6 tests out of 200 tests showed the SNRs less than 20 dB, and even lower than 6 dB at the high frequency band (over 1,600 Hz band). It is a reasonable and intuitive fact that the lower SNR is expected as the louder the unit is; however, another interesting finding was that the background unsteadiness as well as the level of the background noise affected the variations in SNRs.

It should be noted that the analysis conducted herein for the 200 individual tests were a real-world example of using a testing laboratory with a relatively quiet background noise. As such, the outcome of the spatial background difference method and the insertion loss method can differ from the analytics presented in this study. Testing environment exposed to the moderate to loud background noise may need to use only the spatial background difference method or the insertion loss method. Likewise, the criterion for the sound transmission SNRs may vary with respect to the testing environment. However, the process along with the two methods introduced in this the study can be applied to the transmission characterization process irrespective of the testing environments, when one tries to use the external microphone to analyze the background noise. Specifically, the methodologies herein can be useful when the sound transmission from the inside of the acoustic chamber is suspected to affect the external signal measured outside the chamber.

CHAPTER IV

METHODOLOGY FOR EVALUATING BACKGROUND STEADINESS BY MONITORING EXTERNAL BACKGROUND SIGNATURES

Overview

The intrusion of background noises on acoustic measurements of a test subject is an inevitable process, and if not addressed it can make the acoustical evaluation of a test subject difficult or even an impossible task. The need for a study of background steadiness, defined as a background with change, variation, or interruption, as a result of the existence of noise in the measured signal is especially acute when the test subject's sound level is comparable to the background noise level, which is usually a characteristic of low Signal-to-Noise Ratios (SNR). Despite different methods to characterize the influences of the background noise on the acoustic rating, such as SNRs, comparisons of temporal average SPLs of two different background noises, etc., an assessment of background steadiness has not been extensively investigated or discussed. Therefore, the study reported herein proposes a method to assess the background steadiness by monitoring external background signals. Specifically, the study herein discusses assessments of the background steadiness by utilizing statistics from 200 fan tests that measured external background noise. Specifically, mean external background noise and most importantly variations of the external background noise during each measurement phase were analyzed in detail for 200 fans that underwent acoustical evaluations and tests following standard procedures. Major findings include that (1)

background differences between measurement phases were larger than the existing background steadiness criteria such as the HVI 915, and (2) sampling of variations or fluctuations in each measurement showed large fluctuations at high frequencies over 2,500 Hz. These findings lead to a conclusion that external background monitoring can be a useful methodology in order to capture unsteady acoustic signature when low-noise devices were testing for standard acoustical performance evaluations.

Introduction

The intrusion of background noises on acoustic measurements of a test subject is an inevitable process, and if not addressed it can make the acoustical evaluation of a test subject difficult or even an impossible task. A simplified spectral form of acoustic signal and noise can help to understand the significance of the background noise as expressed below.

$$Y(f) = X(f) + N(f) \tag{4-1}$$

, where $Y(f)$, $X(f)$, and $N(f)$ are the Fourier transforms of the noisy signal $y(t)$, the signal of test specimen ($x(t)$, and the background noise $n(t)$, respectively, while the f is frequency. Because a typical standard acoustic testing requires only the signal of test specimen $X(f)$, the background noise must be numerically removed from the noisy signal $Y(f)$. Therefore, while excluding the contributions of test specimen or unit-under test, a separate measurement is performed in order to obtain only the background noise $N'(f)$, where superscripted $N'(f)$ denotes estimate of the original background noise signal $N(f)$. In most cases, background noises are unsteady due to randomness of uncorrelated noise sources, such as traffic, wind, human activity, rotating machinery, etc.

A number of techniques and methodologies are developed to model the background noise in the study of signal processing [18, 54, 56]. However, a study for background steadiness itself, which is defined as a background with change, variation, or interruption, has not been done actively especially for standard acoustical testing. Part of the reason come from the fact that the background steadiness is not a significant when the acoustic separation of a test specimen signal $X(f)$ and the an independently measured background noise $N'(f)$ are sufficient enough [54]. However, testing a low noise sources may result in the low separation of the signal of interest and the independently measured background noise. As such, the study presented herein review background noise criteria and techniques to address unsteady background noises, and then introduce another methodology, namely external background monitoring, which can address limitation on the current criteria or methodologies.

Therefore, the following two subsections, namely 1. 'Background Noise Criteria in Acoustic Standards in General' and 2. 'Background Noise Criteria in Ventilation Fan Standards', discusses existing techniques in leading international standards. These subsections introduce and discuss background noise criteria existing in general acoustical testing standards and ventilation fan testing standards. Lastly, 3. 'Limitations on Conventional Criteria and Importance of This Study' discusses limitations of the existing methodologies and criteria for background steadiness, and then proposes the background monitoring process in order to address limitations along with its importance and implication.

Background Noise Criteria in Acoustic Standards in General

The study reported herein presents comparisons of external background signals at each phase of the test which is listed as follows.

- the measurements of unit under test (UNIT phase),
- background (BGD phase), and
- reference sound source (RSS phase).

These three measurement phases are universally accepted as standard procedures for standard acoustic testing [9-11, 42].

However, each protocol or standard may differ from each other in terms of the background steadiness criteria with this background steadiness. For example, ISO 3741 Precision Method Grade 1 sets as the minimum SNR, which is the arithmetic difference of the SPLs of the unit under test L_p^{UT} and the background L_p^B as follows.

1. 6 dB minimum for 200 Hz and below, and 6,300 Hz and above of the 1/3 octave band center frequencies (henceforth, band frequencies), and
2. 10 dB for the 250-5,000 Hz band frequencies.

In addition, this ISO standard suggests the use of measurement uncertainties by performing repetitive background measurements under the assumption of a normal distribution of the background noise [11, 14], where the standard uncertainty, *u*, is expressed as follows.

$$u = \sigma\left(L_p^B\right)\left|s_K\right| = \sigma\left(L_p^B\right)\left|\frac{1}{1-10^{0.1\left(L_p^{UT}-L_p^B\right)}}\right| \tag{4-2}$$

, where $\sigma(L_p^B)$ is the standard deviation of the measured background noise SPL (L_p^B), s_K is the sensitivity coefficient, and L_p^{UT} is the measured SPLs of the test subject or the unit-under-test. As can be seen in Eq. (4-1), the uncertainty values vary (1) proportionally with the variation of the background noises in terms of the standard deviations, and (2) inverse-exponentially with respect to the SPL difference between the test subject and the background noises. As the term uncertainty implies, background noise is assumed to be unsteady, and variations of the background noise impose certain window of measurement precision [17].

Background Noise Criteria in Ventilation Fan Standards

Because the test subjects used in this study are the residential ventilators such as range hoods, bathroom ventilation fans, and utility room ventilation fans, one should focus on the background noise criteria found in leading international/national standards specifically designed for the residential ventilating devices. Standard such as the ANSI/AHRI 220 and ANSI/AHRI 260 [11, 32, 79] specifies the minimum SNRs of 6 dB for the band frequencies of 315 Hz and below and for 6,300 Hz and above, while an SNR of 10 dB is specified for the band frequencies between 400 and 5,000 Hz. Comparing the previous standard to the ISO/ANSI standard shows that the minimum SNR for the frequency bands differs only at 250 and 315 frequency bands with values being lower than the ISO/ANSI Standard [11]. The AMCA 300 [42] specifies only a minimum 6 dB SPL throughout the entire 1/3 octave bands as the requirement. Lastly, the testing procedure HVI 915 demands two different background measurements for 30 sec before and after the RSS measurement, and then compares these two average

background SPLs by using specified criteria. Furthermore, HVI 915 has implemented more detailed SNR criteria considering the fact that most of the residential ventilation devices generate very quiet sound at high frequencies, between 6,300 and 10,000 Hz band frequencies, meaning that the SNR can be lower than 6 dB in many cases. Table 4-1 summarizes these minimum SNR for each of the standards mentioned above.

Table 4-1 Suggested minimum SNRs in different standards and guidelines

1/3 Octave Band Frequency (Hz)	ISO 3741/ANSI S12.51 SNR limit (dB)	AHRI 260 SNR Limit (dB)	HVI 915 SNR Limit (dB)	1/3 Octave Band Frequency (Hz)	ISO 3741/ANSI S12.51 SNR limit	AHRI 260 SNR Limit (dB)	HVI 915 SNR Limit (dB)
50	6	6	20	800	10	10	10
63	6	6	20	1,000	10	10	10
80	6	6	20	1,250	10	10	10
100	6	6	20	1,600	10	10	10
125	6	6	20	2,000	10	10	10
160	6	6	20	2,500	10	10	10
200	6	6	20	3,150	10	10	10
250	10	6	10	4,000	10	10	10
315	10	6	10	5,000	10	10	10
400	10	10	10	6,300	6	6	3
500	10	10	10	8,000	6	6	3
630	10	10	10	10,000	6	6	3

In Table 4-1, it can be observed that the lower frequency bands of 50 through 200 Hz shows the largest differences between the HVI and other two minimum SNR standards. These large difference occur at the lower frequencies where the background SPLs are low to moderate levels compared to other frequency bands [9, 74]. As previously noted,

many residential ventilation devices are not significantly loud at high frequency bands, which results in the HVI 915 having lower SNRs at high frequencies.

Limitations on Conventional Criteria and Importance of This Study

Background noise affects ventilation noise measurements, and despite the efforts for the treatment of background noise in the aforementioned standards, there are several drawbacks on the existing background noise criteria specified by these standards. As discussed earlier, background noise criteria are dependent on the usage of uncertainties and signal-to-noise ratio as discussed below.

Limitations on the Usage of Uncertainties

The usage of uncertainty method has several impractical concerns which are presented below.

1. Determining uncertainty by repeatedly measuring background noise may be impractical because background noise is continuously transient or unsteady. Specifically, the background noise while taking measurements in the UNIT phase can be significantly different from other repetitive background measurements required for obtaining uncertainty. Also, there is another concern as to how many measurements should be taken for obtaining the uncertainty of the background noise.
2. Even though the uncertainty is necessary for quantifying the reproducibility and repeatability of the acoustical testing, the consistently varying nature of the background noise is not sufficiently explained by the uncertainty itself. The background noise uncertainty assumes random noise with its average SPLs having a normal distribution

[11]. Therefore, some random but temporary noises, which may be prevalent at any given moments, would not be sufficiently explained by uncertainties.

3. Several studies reported issues of overestimated uncertainties or incorrect uncertainties by using inter-laboratory tests [14, 80, 81]. For example, Loyau pointed out that uncertainties of 1-8 dB(A) are typically obtained through inter-library measurements when the ISO 3741 and 3744 uncertainty calculation procedure is used. Also, a study by Payne and Simmons, which conducted uncertainty analysis for four national laboratories in the U.K., found that large a uncertainty associated with background noises resulted in invalid measurements in low frequency bands (50 through 125 Hz). As such, relying merely on uncertainties for addressing unsteady background noises might not be practical.

Limitations on the Usage of Signal-to-Noise Ratios

Similar to the usage of uncertainties, the usage of the SNR for evaluating background noise concerns also has its limitations.

1. As a measure of the separation of the signal of interest and the background noise, the SNR is likely to be prescreening process of standard acoustical testing. Furthermore, if series of measurements suffer from a low SNR, testing are considered to be invalid. In special cases, there are exceptions when the ISO/ANSI Precision Method is used, which requires further testing when the measured background SPLs is less than the tabulated minimum background noise. However, the minimum background noise in the ISO/ANSI standards does not guarantee background steadiness if the minimum SNR requirements are not met.

2. Lastly, the SNR method is only based on the time average of the measured SPLs. For example, significant fluctuations in the background, such as loud impulse noise from machinery operations, cannot be addressed for the averaged background steadiness. In this regard, a need to improve the methodology for the background steadiness assessment still exists.

Importance of This Study

As pointed out in the limitations above, the SNRs and the uncertainties focus on 'addressing' the background noise. However, for standard conforming acoustical tests, a process to tell that the background noise measured during given test is 'steady' and 'consistent' is necessary. Specifically, as pointed out in Eq. (4-1), the measured average background SPLs shall be the representative quantification for background noises in that 1) background noises while measuring the test subject are same to the background noises while measuring only the background noises without operating test subjects or reference sound sources, and 2) variations or fluctuations of background noises are not severe that the average SPLs can be representative for a given span of acoustical testing.

In order to address the aforementioned issues on the conventional background steadiness methods, it is necessary to develop a methodology to assess or evaluate background noise steadiness. Furthermore, a development of the methodology is particularly acute for standard acoustical testing of low-noise devices. By introducing monitoring technique of an external acoustic signature, this study presents the methodology of the external background steadiness evaluation. The following section introduces processes for this methodology.

Description of Methods

In this section, methodologies of the external background monitoring, which is the main topic of the study reported herein, are explained. The instrumentation and acoustic chamber setup is available in earlier chapters and the paper by Choi et al. [73].

In addition, a transmission characterization process, which was the main topic of the previous part of this study, is briefly explained. Of special importance, the necessity of the transmission characterization process is that the process is a qualification process to valid use of the background monitoring. Lastly, key parameter for the analysis and discussions of the background monitoring results are presented as an aid for understanding the entire process.

Methodologies of External Background Monitoring

As previously discussed, the proposed method uses the external microphone that is placed outside the acoustical testing space (or the chamber) where the unit under test is also being monitored and measured. Therefore, SPL measurements are performed concurrently both inside and outside the chamber. As a graphical illustration, Figure 4-1 presents a schematic diagram of the external background monitoring process along with the acoustic characterization of the unit under test.

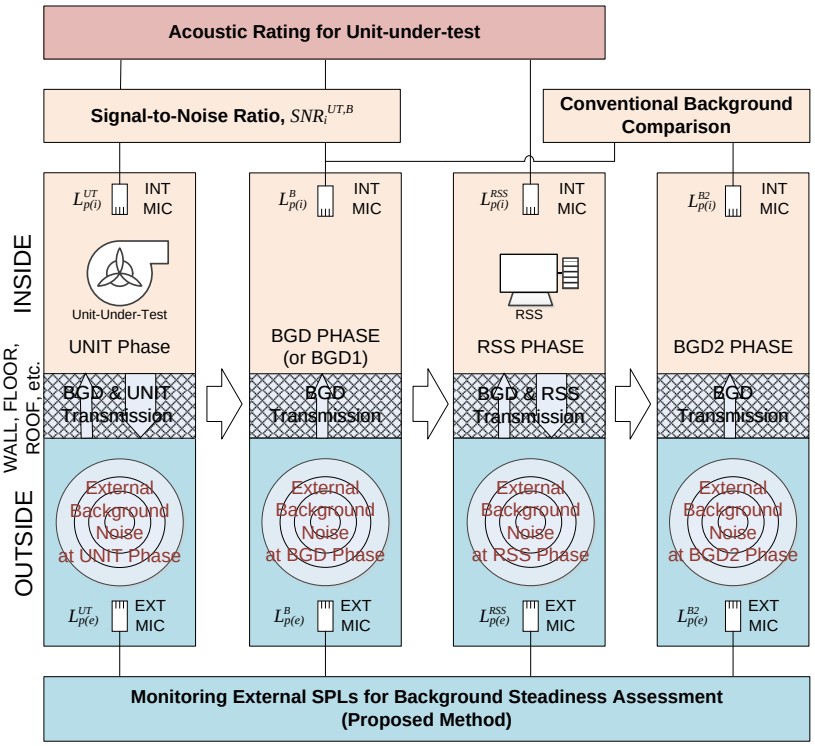

Figure 4-1 A schematic diagram of the external background monitoring process in this study

In the UNIT measurement phase, with microphones inside the chamber (internal microphones) measures the SPLs of the unit under test, the external microphone (or the microphone outside the chamber) measures the background noise along with the transmitted sound of the unit under test. In the BGD measurement phase, both internal and external microphones simultaneously measure the background noise. Because the source of background noise is located outside the chamber as a result of all devices and instruments inside the chamber being turned off, measured SPLs outside the chamber are larger than the SPLs inside the chamber. In the RSS measurement phase, the large broadband sound from the RSS is measured inside the chamber, and at the same moment

the external background noise and the transmitted RSS sound are measured outside the chamber. These three measurement phases comprise the acoustic rating of the unit under test and the proposed background steadiness assessment. As an additional scope to this study, the second background, BGD2, is measured primarily in order to compare the measured background in the BGD2 phase to the background measured at the BGD (or BGD1in order to make distinction). The background comparison process was originally intended to meet the HVI 915 background comparison criteria. It should be noted that the BGD2 is not a part of the proposed method of monitoring the external background, and the data analysis regarding the BGD2 is for comparison purposes.

Measurement Parameters for the Proposed Methodology

The important observations to be made for the proposed method are the time statistics of the signal, which is the sound pressure level (SPL) in this study measured at both locations, namely inside and outside the chamber. The signal can be decomposed into the signal mean and the fluctuation, in terms of standard deviation or coefficient of variation, and then analyzed separately. The comparison of the signal mean provides not only the transmission characteristic through the chamber foundation, wall and roof, which are covered in the previous chapter, but also the assessment of the steadiness. Specifically, the transmission can be characterized by comparing the signal means, i.e. between internal and external SPLs, at each measurement phase, and the steadiness can be assessed by comparing external SPLs at UNIT, BGD, and RSS measurement phases. The fluctuation measured at each point is the result of the randomness of the sound source and the transmission characteristic. Therefore, it is also necessary to compare the

fluctuation of each measurement phase in order to guarantee the background steadiness. The following is an outline of the measurement process.

1. The internal microphones or rotating boom microphone if that is the setup records the sound pressure of the unit under test (UT) or the sound pressure level $L_{p(i)}^{UT}$ and the background noise SPL $L_{p(i)}^{B}$, and the reference sound source $L_{p(i)}^{RSS}$ inside the semi-reverberant chamber under prescribed methods, following time and averaging processes with respect to the referring standards. For example in this study, SPLs are measured for 30 seconds and then linearly averaged per ANSI S12.51.

2. For UT, BGD, and RSS measurements, the external microphone records the signal of the external noise while performing the unit measurement, background noise measurement, and the reference sound source (RSS) measurement, where each SPL is $L_{p(e)}^{UT}$, $L_{p(e)}^{B}$, and $L_{p(e)}^{RSS}$.

3. Statistics of the measured sound signals, such as average, standard deviation, coefficient of variation, etc. of the internal SPL and external signals, are determined for the both internal and external signals in order to compare signal means and fluctuations.

The signal of the RSS is usually a large, broadband response as required by international standards [11, 72]. Furthermore, the sound power of the RSS is larger than other signals having large SNRs. Therefore, a comparison between the RSS signal and the other measurement signals is usually unnecessary. For example, the study herein has the RSS at about 83.7 dB SPL, with none of the background noise measurements observed with more than 60 dB SPL in the chamber. The large separation, between the

background and the RSS, results in negligible contributions of the background noise to the RSS signal. Therefore, a comparison is usually useful only between the UNIT and the BGD phases. However, the study herein discusses comparisons of RSS signals in conjunction with a broader coverage of the topic.

Results and Discussion

This section contains analysis of the results from external background noise measurements and other acoustic measurements explained and identified in an earlier section. Each subsection and their outline is presented below. All of the following sections provide real-world applications of the external background monitoring process based on utilizing a large 200 fan test database.

1. Signal-to-Noise Ratio Analysis: This section investigates challenges for standard-conforming acoustical testing for low noise sources, which are identified by the signal-to-noise ratio (SNR). Using the 200 fan test databank, further statistical evidence is provided that the same issues can frequently occur in a real-world acoustical testing.

2. Identification of Frequency Band of Interest: It was found that not all of the frequency bands suffer from unsteady background or low SNR issues. Through a statistical analysis of the test conditions (i.e., background noises), frequency bands of interest are identified.

3. Comparisons of External Background Acoustic Signatures between Measurement Phases: There are two major types of comparisons for the external background monitoring process. The first is comparisons of the external background between each measurement phase, namely the UNIT, BGD, and RSS phases. This section discusses

the results of the acoustic signatures of external background noises in these measurement phases.

4. Background Noise Variations during Measurement Phases: This section investigates the fluctuations or variations of the external background noises in each single measurement phase. Specifically, standard deviations of the external background noises that are sampled for 30 sec for each measurement phase is presented along with their statistical analysis.

Signal-to-Noise Ratio Analysis

The background steadiness becomes a more important concept when one attempts to study the noise sources in the presence of the background noise that is comparable to the noise sources in its sound levels. For example, a number of modern residential fluid moving devices such as heaters, air-conditioners, refrigerators, range hoods, etc. usually generates low to moderate level of sound (or noise) whose SPLs are usually less than the range of the typical commercial or industrial environmental SPLs [74]. Among the residential, fluid moving devices, the study herein utilizes residential ventilation devices including bathroom fans, utility-room ventilators, and kitchen range hoods as test subjects particularly because the sound of these ventilation devices has significantly improved in the last decade to barely noticeable sound levels. Furthermore, governing building codes have started demanding stricter guidelines in order to lower noise levels for fans [33, 64]. Therefore, the lower sound levels of these products have been impacting precise acoustic measurements, as an example, by suffering internal SPL

differences between the unit and the background measurement $SNR_i^{UT,B}$, which is defined below.

$$SNR_i^{UT,B} = L_{p(i)}^{UT} - L_{p(i)}^{B} \equiv \Delta L_{p(i)} \quad (4\text{-}3)$$

Figure 4-2 is an example of the $SNR_i^{UT,B}$ distributions of the 200 residential ventilation devices tested for this study. It should be noted that these 200 tests were conducted in accordance with the HVI 915, which requires the comparison of two backgrounds (30 secpmds each) before and after the RSS measurements. The $SNR_i^{UT,B}$ less than 6 dB, which is considered to be the lower limit for the background separation in both ISO 3741 and ANSI S12.51 [11], appears both at lower and higher bands, represented by the 1/3 octave band center frequencies 50 through 80 and 2,500 through 10,000 Hz. Also, the two extremes of the lowest $SNR_i^{UT,B}$ are observed at both ends of the octave bands.

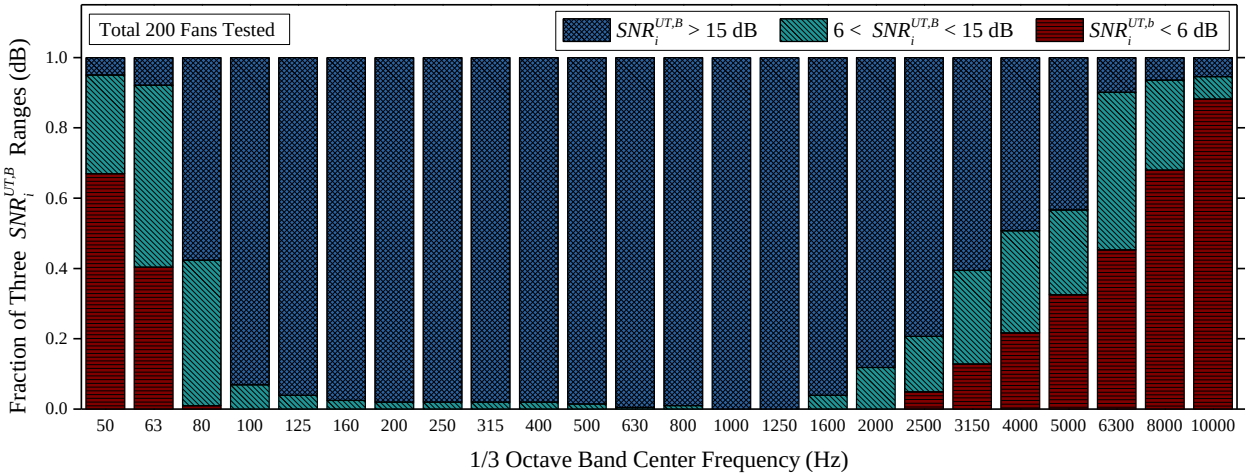

Figure 4-2 Fraction of three SNR ranges at each 1/3 octave band

Several insights can explain the reason of the low $SNR_i^{UT,B}$. First, the low acoustic emission of the test subjects (residential ventilation devices in this study) inflicts the low $SNR_i^{UT,B}$ when the same band is experiencing a similar level of a lower background noise. These low SPLs are usually observed in high frequency ranges over 3,150 Hz because residential fans tested in this study do not emit high frequency noises. Second, both the background noise and the sound of the testing unit may show similarly large amount SPLs. These large SPLs are particularly observed in low frequencies less than 200 Hz because low speed vibrations (less than 3,000 rpm) of the residential fans tested and the ground transmissions of the background noise are both prevalent.

Identification of Frequency Band of Interest

Although those two incidents exhibit similar precise signal separation issues in terms of SNR, different approaches can be made to assess the background steadiness depending on the governing nature of background noise sources. Figure 4-3 shows the SPL distribution of the internal background noise SPL, $L_{p(i)}^{U}$, of the 1/3 octave bands having a $SNR_i^{UT,B}$ less than 6 dB. The two frequency groups, the lower (50, 63, 80 Hz) and the higher bands (2,500 through 10,000 Hz), have distinctively different SPL distributions along with different SPL average trends. The lower bands show larger randomness characterized by the width of the boxes in each box plot, with elongated tails showing non-uniform randomness. In addition, the lowest two bands, 50 and 63 Hz of the center frequencies, showed relatively larger background noise SPLs compared to the other bands having $SNR_i^{UT,B}$ less than 6 dB. At the higher bands, 2,500 through 10,000 Hz, the background noise SPLs, $L_{p(i)}^{U}$, are distributed between 3 to 6 dB, as can

be seen in the inset in Figure 4-3, and they are relatively quiet being less than 6 dB, and less randomly dispersed within a 1 dB interval compared to the lower band SPLs (50, 63, and 80 Hz). Therefore, the background noises in the higher frequency bands are supposedly considered steadier than ones in the lower frequency bands despite the same low $SNR_i^{UT,B}$. Observations of the two different acoustic signatures result in useful insights in that the SNR evaluation and the background steadiness assessment can be decoupled even when the quiet sound source adversely affects the SNR.

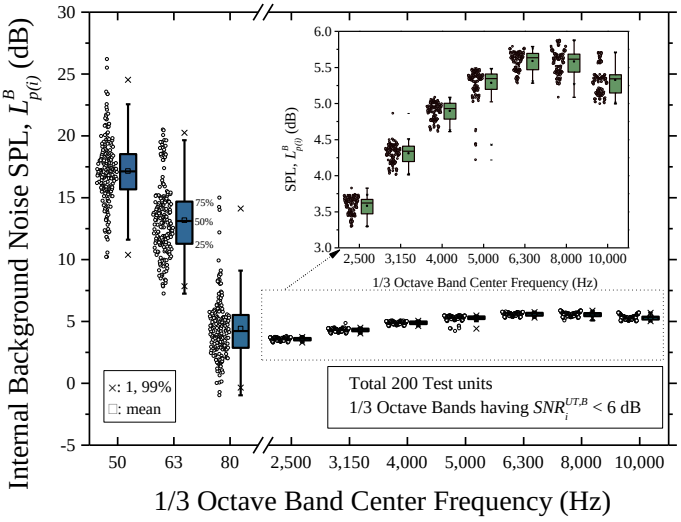

Figure 4-3 Sound-pressure-level distributions of the background noise ($L_{p(i)}^B$) inside the semi-reverberant chamber. The inset shows the enlarged distribution of the 1/3 octave band center frequencies 2,500 through 10,000 Hz

Based on observations, one can determine the frequency domain that requires the background steadiness assessment method discussed in the previous section. Although the method can be utilized on any spectrum, it is not necessary to apply the method for

the entire frequency domain. The reason is that the external background noise is not usually controlled at certain frequencies. For example, the method can be useful for the background steadiness assessment of the low frequency band (50, 63, and 80 Hz center frequencies) because of the random fluctuation of the low frequency background noise compared to the distribution of the higher frequency band noise. Furthermore, the external background noise might not provide useful insight when the internal background noise is well controlled and characterized. Figure 4-4 presents the external background noise fluctuations as evidence. There is a noticeably expanded, random uncertainty in the external (or outside the chamber) background noise SPL $L_{p(e)}^{B}$ in contrast to the less randomly dispersed SPLs in Figure 4-3. Of special importance, it should be noted that the measurements inside the chamber, e.g., $L_{p(i)}$, are only utilized for the acoustic characterization of the sound source. Provided that the acoustic signature inside the chamber is well controlled and established for a certain frequency range, then using method for the external signal on the same range is unnecessary. Because of the aforementioned observations, the external signal method will be used for the frequency range (or bands) upon the following criteria.

(1) Frequency range (or band) having significant SNR issues (e.g. $SNR_i^{UT,B} < 6$ dB)

(2) The background noise inside the testing space (e.g., inside the semi-reverberant chamber) are not controlled and shows a significant amount of fluctuations.

All of the bands shown in Figure 4-3 show the case of $SNR_i^{UT,B}$ less than 6 dB. However, only the lower bands of 50, 63, and 80 Hz have significant background noise SPL fluctuations inside the chamber as can be seen in Figure 4-3. Based on the above

criteria, the background steadiness assessment might not be necessary for the high frequency bands above 2,500 Hz. The study herein expands the frequency domain of interest up to 10,000 Hz although the background noise for the bands with center frequencies of 2,500 to 10,000 Hz do not show noticeable fluctuations. In contrast, the external background noise SPLs $L_{p(e)}^{B}$ for center frequencies of 5,000 through 10,000 Hz were found to have a larger uncertainty over 50% compared to the other high-frequency bands as can be seen in Figure 4-4. The large uncertainties of the external background SPLs in Figure 4-4 is in contrast to the small variations of the background noise SPLs $L_{p(i)}^{B}$ inside the chamber in Figure 4-3.

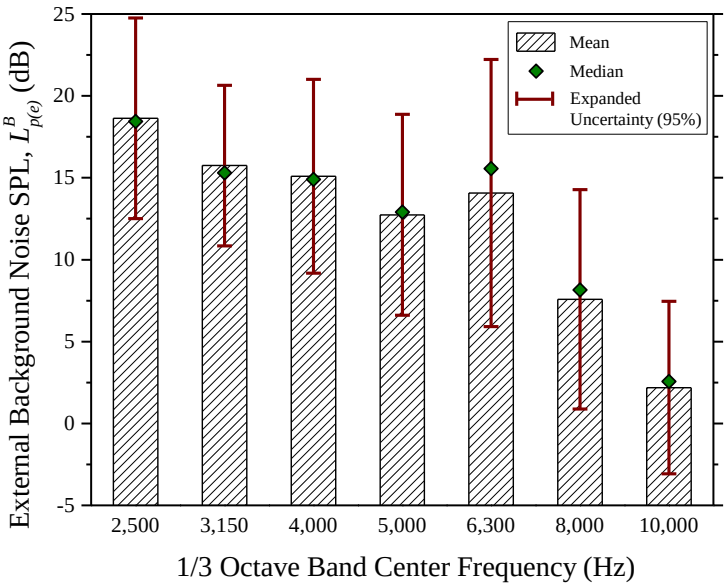

Figure 4-4 Sound-pressure-level distributions of the background noise $L_{p(e)}^{B}$ outside the semi-reverberant chamber at the high frequency bands, 2,500 through 10,000 Hz center frequencies

Based on these observations of the lower SNRs at both ends of the frequency bands in Figure 4-2, and the large variations of the external background SPLs with respect to the mean and median of the external background SPLs in Figure 4-4, a direct comparison can be made as to the similarity of external background SPLs in each measurement phase. Figure 4-5 through Figure 4-7 present the distribution of the 30-second averages of the external background SPLs in each measurement phase, namely the UNIT, BGD, and RSS phases, of the 200 fan tests, which met the HVI 915 background comparison criteria.

Comparisons of External Background Acoustic Signatures

Of special interest, the transmission correction, which is discussed in the Part 1, was performed on the external background SPLs in both the UNIT and the RSS phases. In these distributions, the 1/3 octave frequency bands are divided into three groups based on the SNR trends shown in Figure 4-2. The frequency bands up 80 Hz band frequency showed a lower $SNR_i^{UT,B}$ for several tests. This frequency group can be characterized by the largest external background SPLs and by lower transmission losses as discussed in the Chapter III. Furthermore, most residential ventilating devices are designed to avoid large sound power emissions at these frequencies because the noises at these frequencies are usually generated because of the mass imbalances [43], which might result in fatigue damage to the devices as well as the noise. Thus, the low $SNR_i^{UT,B}$ shown in Figure 4-2 can be understood as a combining effect of the background noise, sound transmission characteristic, and the sound of device, with all three components significantly affecting the $SNR_i^{UT,B}$. In contrast, the next frequency group (medium-to-high frequency bands)

between 100 and 2,000 Hz band frequencies have an overall larger $SNR_i^{UT,B}$ over 15 dB because most of the sound emission from the test subjects were focused on this frequency band. Therefore, the least influence of the external background unsteadiness to the internal background during the test is expected in the medium-to-high frequency bands among the three frequency band groups. The last frequency band group, between 2,500 and 10,000 Hz, experiences a lower $SNR_i^{UT,B}$ as shown in Figure 4-2 similar to the first frequency group. However, the external background SPLs in Figure 4-5 through Figure 4-7 in the high frequency band are less than the other frequency bands. Of special importance, the external background SPLs shown in this study are generally lower than typical background noise SPLs in residential, commercial, or industrial environments [74], hence the frequency groups or boundaries can significantly differ when the same analysis is performed in other environments.

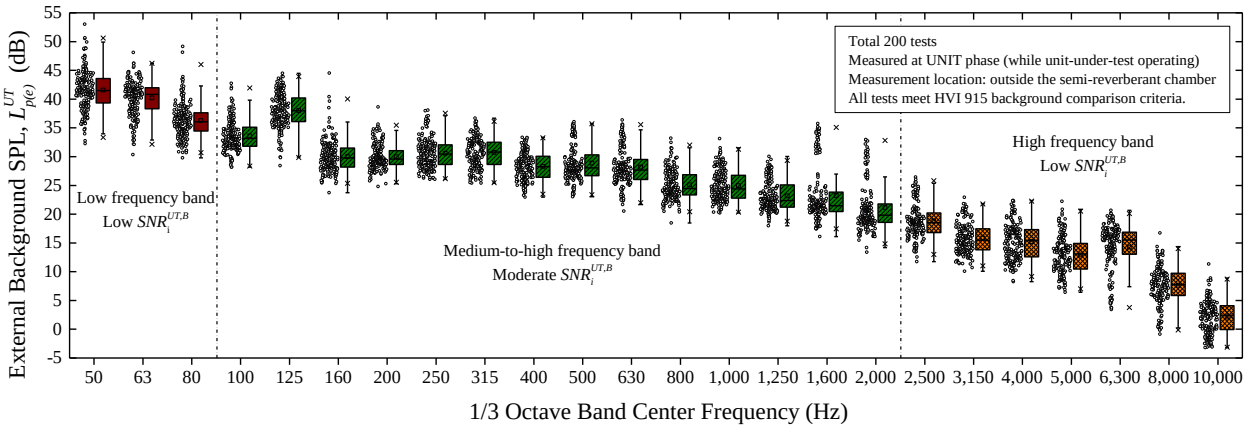

Figure 4-5 Distributions of the external background SPLs $L_{p(e)}^{UT}$ at the UNIT measurement phase

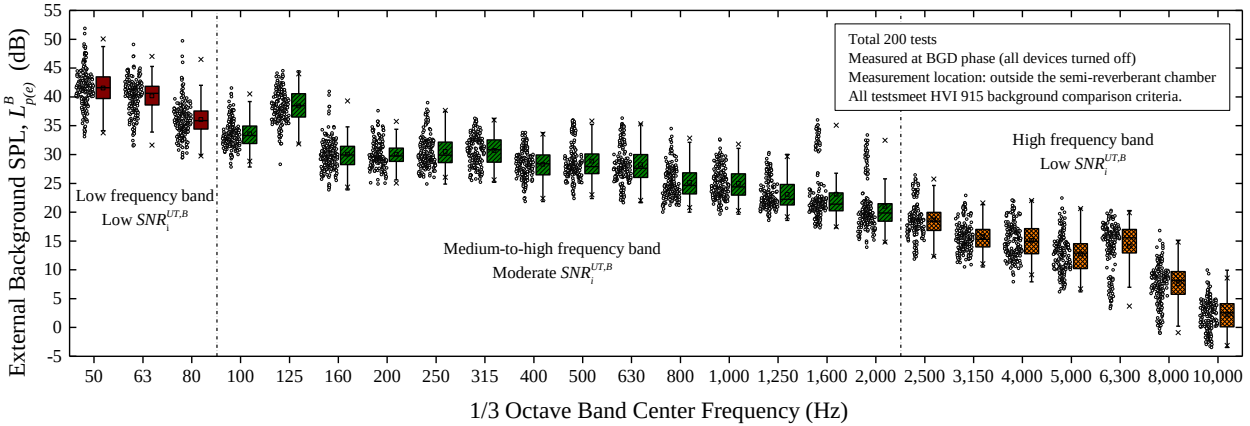

Figure 4-6 Distributions of the external background SPLs $L_{p(e)}^{B}$ at the BGD measurement phase

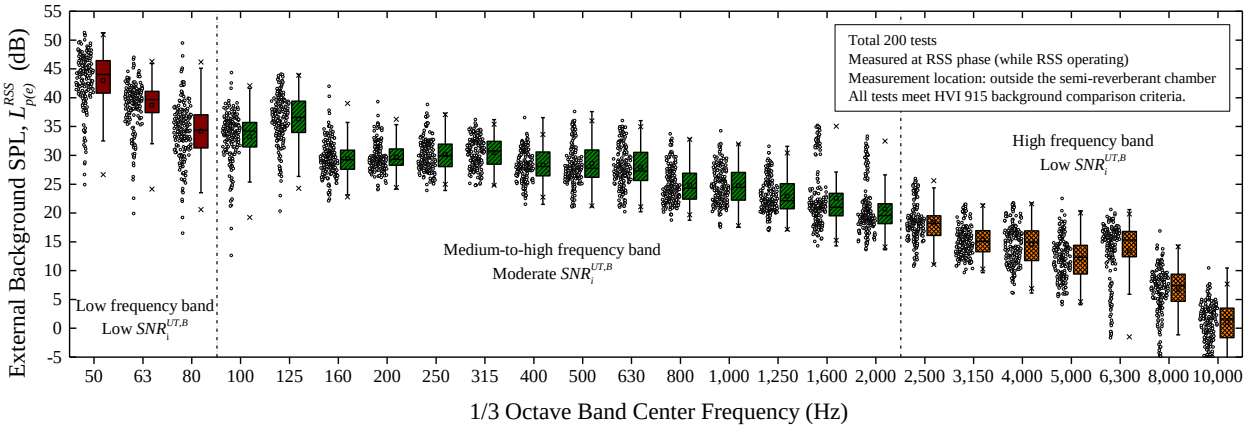

Figure 4-7 Distributions of the external background SPLs $L_{p(e)}^{RSS}$ at the RSS measurement phase

One interesting finding in Figure 4-5 through Figure 4-7 is that the amount of the spatial background variations in each band do not significantly differ from other bands. The interquartile range (IQR), the length of the box of the box plots or the SPL range of the fifty percentiles from the median, in Figure 4-5 through Figure 4-7 are about 4 to 5 dB in most of the frequency bands. The length of whiskers, the vertical lines across each box plot, however, are slightly different from each other. As noted in Figure 4-5 through Figure 4-7, differences are hardly noticeable except for the external background SPLs in the RSS phase at several frequency bands. Specifically, the $L_{p(e)}^{RSS}$ in Figure 4-7 were found to be more sparse than the $L_{p(e)}^{UT}$ in Figure 4-5 and the $L_{p(e)}^{B}$ in Figure 4-6 in several low frequency bands for the first and the last frequency groups, such as the 50, 125, and 6,300 through 10,000 Hz band frequencies. The reason can be found in the sound transmission characteristics discussed in the Chapter III of this study. It was pointed out in the Chapter III that more sound transmission was found at lower frequencies equal to and below 125 Hz, which resulted in a lower SNR between the external background and the transmitted RSS sound. Also, at the higher frequencies, quiet external backgrounds affected the lower SNRs although the transmission of the RSS sound inside the chamber was less than at the lower frequencies. Although the same transmission correction, which was done for the UNIT phase, was applied to the external background in the RSS phase, several lower SNR_e^{RSS} values, which is defined below, caused the sparse distributions in Figure 4-7.

$$SNR_e^{RSS} = L_{p(e)}^{RSS} - L_{p(e)}^{R^*} \quad (4\text{-}4)$$

, where $L_{p(e)}^{R*}$ are the transmitted SPLs of the RSS from inside the chamber to the outside through the chamber construction, which is determined by the methodology presented in the Chapter III. In the SNR analytics of the Chapter III, it was found that several bands, such as 50 and 125 Hz, had SNR_e^{RSS} values less than 6 dB. Although the 200-test-average SNR_e^{RSS} values were over 6 dB, where the transmission correction is readily available, for bands above 6,300 Hz, not a negligible portion of about 32%, of the SNR_e^{RSS} values were found to be less than 6 dB, which resulted in the large distribution in the high frequency bands. However, it should be noted that a significant similarity of external backgrounds was found. Aside from exceptions of the RSS, an interpretation can be made that the tests that met the background comparison criteria of the HVI 915 also showed similar external background trends in most of the frequency bands.

Background Variation between Measurement Phases

Another observation to be made is how much of an external background difference exists in a given testing set. The analysis of this question can be performed by looking into the SPL difference between each measurement phase, such as UNIT versus BGD, RSS versus BGD, etc.

The SPL difference can provide the clue as to how constant the external background is throughout a given test. As the first external background difference, Figure 4-8 shows the external background SPL difference between the UNIT phase and the BGD phase, $L_{p(e)}^{UT} - L_{p(e)}^{B}$. The measured external background in the UNIT phase are adjusted by the transmission correction. In addition to the distributions expressed by the open-circle symbols (o) and the box-plots, the box drawn with the dash lines delineate the

background difference limit proposed by HVI 915 (henceforth, background difference limit). It should be noted that the limit is originally for the comparison of the two different backgrounds (BGD1 and BGD2) measured inside the chamber. The representative, external background in this study is taken while the first background (BGD1) is being measured (i.e. superscript B corresponds to BGD1).

In Figure 4-8, the SPL differences are within ±10 dB for the maximum, and more importantly the difference is aligned at zero along with minor deviations from the zero, which are not frequency specific, presumably. As can be seen from the different lengths IQRs at each frequency band, the varying degree of the distributions are observed in the external background SPL differences in Figure 4-8. These variations in the IQRs are in contrast to the lengths of the IQRs in Figure 4-5 through Figure 4-7, which were rather similar throughout the frequency bands. In Figure 4-8, the lengths of the IQR are between 0.5-5 dB, and the lower frequency IQRs are generally larger than the higher frequency IQRs, such as the 125 Hz band that showed the largest IQRs (about 5 dB). An interpretation can be made for these IQRs in Figure 4-8 in that the lower frequency bands are more susceptible to the background unsteadiness in terms of the external SPL average. This interpretation can also mean that each measurement phase can be influenced by the background randomness, which may differ for frequency bands or frequency groups. Because the measured SPLs in Figure 4-8 excludes the effect of the sound transmission from inside the chamber, the different background randomness is sorely from background noise sources.

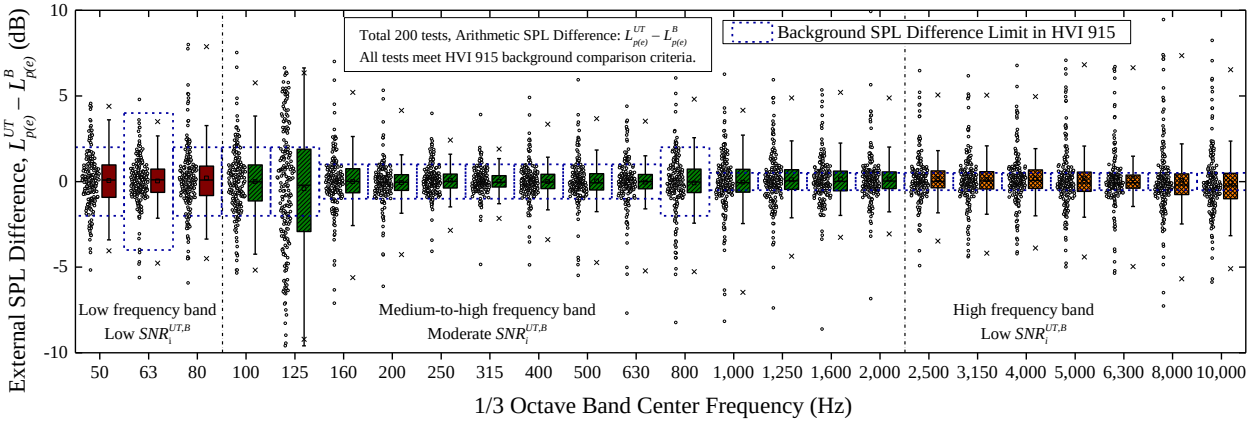

Figure 4-8 External background SPL differences between the UNIT phase and the BGD phase, $L_{p(e)}^{UT} - L_{p(e)}^{B}$

The measured external background differences in Figure 4-8 can be compared to the background difference limit (rectangles in dash). The IQRs of most of the low to medium frequency bands fall into the range of the background difference limit, while the IQRs in the high frequency bands over 2,000 Hz start to be larger than the background difference limit. This observation for Figure 4-8 is of no surprise when considering that two different internal background SPLs, $L^{B}_{p(i)}$ and $L^{B2}_{p(i)}$, inside the chamber were close to just being within the limit, and if so, it is more likely that the background is steady. However, it should be noted that there is still is a possibility that it does not necessarily mean the external backgrounds in the UNIT and BGD1 (or BGD) phases are similar to the same extent, although two backgrounds BGD1 and BGD2 are close to each other.

Figure 4-9 presents the external background SPL differences between the BGD1 (or BGD) phase and the BGD2 phase, $L^{B}_{p(i)} - L^{B2}_{p(i)}$, as a supporting example. It is again noticed that the most IQRs are within the background difference limit (rectangles in dash) in Figure 4-9. However, more of the external SPL differences are found inside the background difference limit compared to Figure 4-8. Furthermore, the length of the whiskers in Figure 4-9, which represent overall distributions along with the extremes, are diminished compared to the length of the whiskers in Figure 4-8. In this regard, noticeable distinctions that are found in the SPL difference distributions especially at the low frequency bands (up to 125 Hz) can be interpreted as evidence that there is also a likelihood that the background comparison criteria in HVI 915 may not predict the background steadiness precisely because the two sets of the SPL differences, $L^{UT}_{p(e)} - L^{B}_{p(e)}$ and, $L^{B}_{p(i)} - L^{B2}_{p(i)}$ could be different.

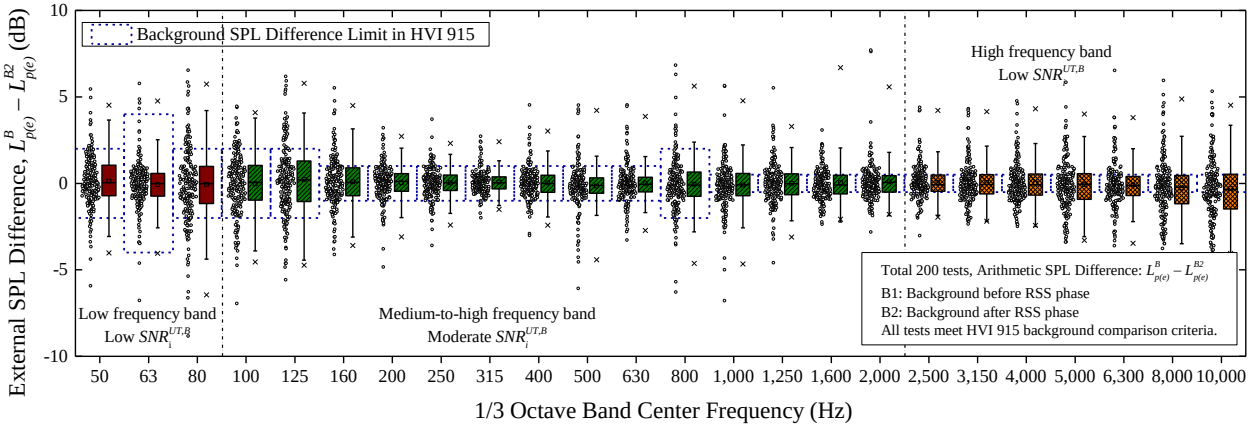

Figure 4-9 External background SPL differences between the BGD1 phase (before the RSS phase) and the BGD2 phase (after the RSS phase), $L_{p(e)}^{B} - L_{p(e)}^{B2}$

In both Figure 4-8 and Figure 4-9, a considerable number of the external background differences exist outside the background difference limit. For example, large spans of the outliers are observed in several frequencies such as the 125, 160, 1,250, and 8,000 Hz bands, and about 50% of the external background differences in 10,000 Hz band are outside the limit.

Correlations between Internal and External SPL Differences

It should be noted that all internal background SPL differences $L^{B}_{p(i)} - L^{B2}_{p(i)}$ were within the limit set by HVI 915. As such, it was found that the internal background difference $L^{B}_{p(i)} - L^{B2}_{p(i)}$ tends to be less than the external background difference $L^{B}_{p(e)} - L^{B2}_{p(e)}$ based on the comparison of the measured differences and the background difference limit in Figure 4-9. To provide insight on the comparisons of the internal and external backgrounds, Figure 4-10 presents four scatter plots of the internal and external background differences, namely $L^{B}_{p(i)} - L^{B2}_{p(i)}$ and $L^{B}_{p(e)} - L^{B2}_{p(e)}$, for the selected frequency bands, 125, 160, 1,250, and 8,000 Hz, which were mentioned above. In each scatter diagram, the Pearson product-moment correlation coefficients with respect to variables *X* and *Y*, $\rho_{X,Y}$, are presented, which is calculated as follows [65].

$$\rho_{X,Y} = \frac{E\left[\left(X - \mu_X\right)\left(Y - \mu_y\right)\right]}{\sigma_X \sigma_Y} \tag{4-5}$$

, where E, μ_i, and σ_i are the expectation, the mean of variable *i*, and the standard deviation of variable *i*.

Table 4-2 is the calculated Pearson product-moment correlation coefficients for the entire 1/3 octave bands. An interpretation of Pearson correlation $\rho_{X,Y}$, which is determined between -1 and 1, is that the positive relationship between the variables X and Y is expected for the positive value of the $\rho_{X,Y}$, and the variables X and Y tend to have an opposing relationship for the $\rho_{X,Y}$ less than 0. In addition, the $\rho_{X,Y}$ being close to either 1 or -1 means that a stronger relationship is expected.

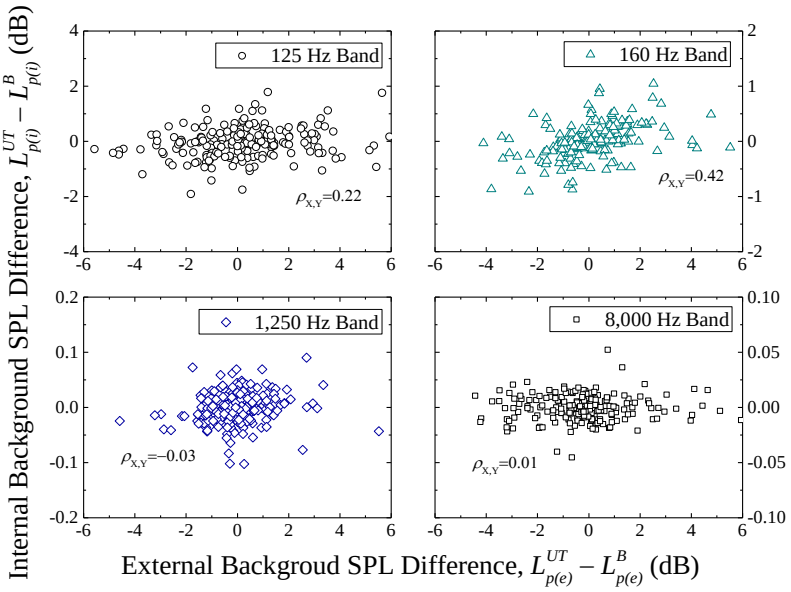

Figure 4-10 Comparison of the external and internal background SPL differences along with Pearson product-moment correlations

Table 4-2 Pearson product-moment correlations of the measured internal and external background differences, $L^{B}_{p(i)} - L^{B2}_{p(i)}$ and $L^{B}_{p(e)} - L^{B2}_{p(e)}$, respectively, for the 1/3 octave frequency bands

1/3 Octave Band Frequency (Hz)	Pearson Correlation, $\rho_{X,Y}$	1/3 Octave Band Frequency (Hz)	Pearson Correlation, $\rho_{X,Y}$
50	0.53	800	0.21
63	0.62	1,000	0.11
80	0.60	1,250	-0.03
100	0.57	1,600	0.14
125	0.22	2,000	0.20
160	0.42	2,500	0.16
200	0.39	3,150	-0.01
250	0.27	4,000	-0.03
315	0.27	5,000	-0.05
400	0.50	6,300	-0.01
500	0.40	8,000	0.01
630	0.04	10,000	0.02

It should be noted that no certain criteria exist for the strong or the weak relationships for the Pearson correlations. Rather, presumptions for relationships can be made based on the sign (+/-) of the value and the value itself. Both in Figure 4-10 and Table 4-2, positive relationships are expected between the internal and external background difference in the low-to-medium frequencies up to 500 Hz band frequency; however, any relationship is barely recognized in the higher frequency band over 630 Hz. The findings in Figure 4-10 and Table 4-2 emphasis the need to track down the background steadiness near the locations of background sources, i.e. outside the chamber.

Comparisons of External Acoustical Signature with RSS Sounds

As discussed in the Description of Methods section, the background steadiness assessment at the RSS measurement phase may not be necessary for the most of the tests because the SNR of the RSS signal versus the internal background noise, $L_{p(i)}^{RSS} - L_{p(i)}^{B}$, is large, such as over 15 dB [10, 11, 68], thus affecting the resulting SPL only by 0.135 dB, or 20 dB used in this study, which in turn affects to the resulting SPL only by 0.043 dB. However, depending on the situation, further research on the background steadiness assessment may be necessary. In order to provide a broader scope to the background steadiness study, the study herein presents the background steadiness assessment for the RSS phase. Figure 4-11 and Figure 4-12 are the external background SPL differences between the RSS phase and the BGD phase, $L_{p(e)}^{RSS} - L_{p(e)}^{B}$ with the transmission correction being applied (Figure 4-11) and not applied (Figure 4-12). It was noted in Figure 4-7 that the transmission correction could lead to sparser and wider distributions of the external background SPLs, especially when the SNR_e^{RSS} is less than 6 dB. Although the transmission characteristics presented in Part 1 can be useful to investigate the transmission of the unit under test and the RSS to the external SPL measurement, the use of the transmission correction for the background steadiness assessment when the SNR_e^{UT} or SNR_e^{RSS} causes a deprecation of the reproducibility of the measured data, it may not be appropriate to use the transmission correction for the background analysis. The same postulation holds true to the external background difference analysis for the RSS phase.

Because of the aforementioned reasons, delving into the transmission-corrected external SPL difference might not provide useful insights into background steadiness. In Figure 4-11, the lower frequencies (up to 100 Hz band frequency) are widely dispersed, along with more extremes than the other external background differences in Figure 4-12.

Next, the external SPL differences at the higher frequencies over 5,000 Hz in Figure 4-11 are deviated from zero by amounts up to 2-3 dB, which is in contrast to the other external background differences. Meanwhile, Figure 4-12 shows distinctive positive values at lower frequencies, which is believed to be the effect of the RSS transmission, while maintaining the length of the distribution comparable to the distributions in Figure 4-8. In addition, it should be noted that the background difference limit by HVI 915 is not applicable in Figure 4-12 because the transmission could affect the overall bias of the background signature.

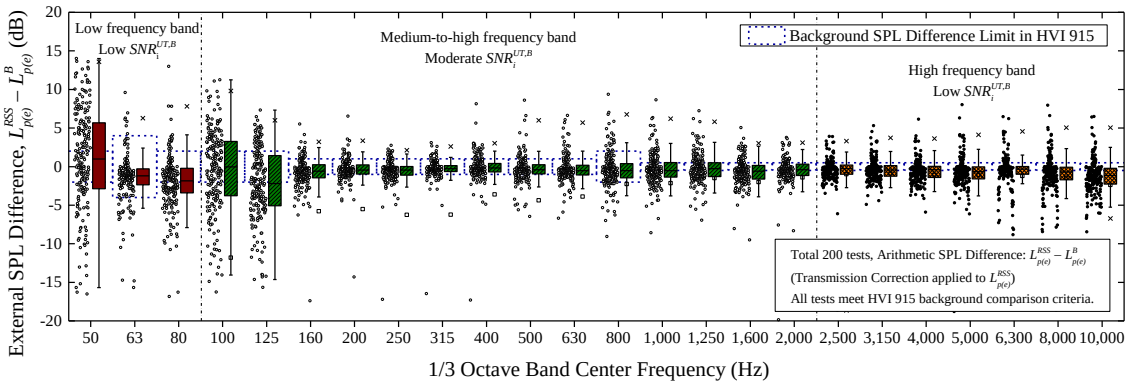

Figure 4-11 External background SPL differences between the RSS phase (transmission correction applied) and the BGD phase, $L_{p(e)}^{RSS} - L_{p(e)}^{B}$

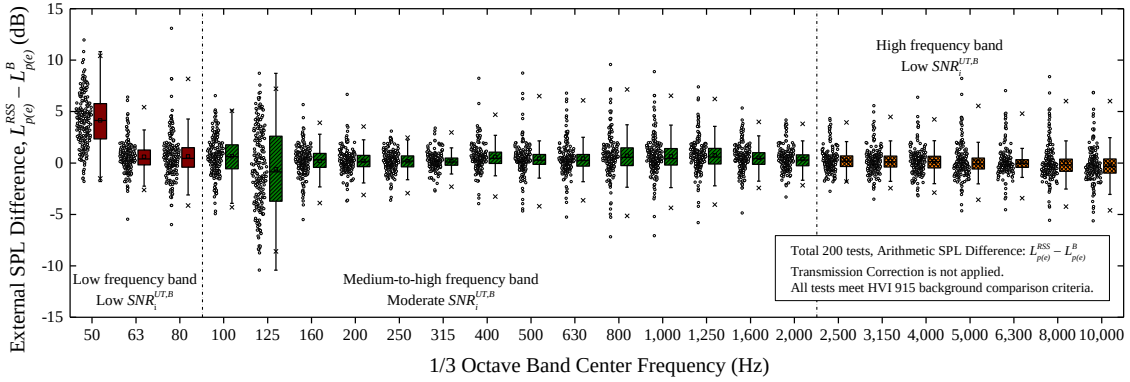

Figure 4-12 External background SPL differences between the RSS phase without the transmission correction and the BGD phase, $L_{p(e)}^{RSS} - L_{p(e)}^{B}$

The external background SPLs and their differences between the individual measurement phases show how the background can differ from another measurement phase in the average sense. The fundamental motivation of the comparisons of the background at the different phases is primarily because the internal background SPLs at the BGD phase $L^{B}_{p(i)}$ are used for the background corrections

$$K = -10\log\left(1-10^{-0.1\left(L_{p(i)}-L^{B}_{p(i)}\right)}\right) \tag{4-6}$$

, where K is a background correction factor, and $L_{p(i)}$ (without superscripts) is the measure SPL of a measurement phase (e.g. the UNIT or RSS phases). In this regard, the background SPLs measured at the BGD phase needs to be close to the background noise of the UNIT and the RSS phases.

Background Noise Variations during Measurement Phases

Once the comparisons of the external backgrounds at the different measurement phases have been performed, it is necessary to evaluate how the backgrounds change or fluctuate while the measurement is being taken for a specific phase. As an example, Figure 4-13 shows time variations of the external background SPLs for the four frequency bands, namely 50, 250, 800, and 8,000 Hz, measured at the BGD phase.

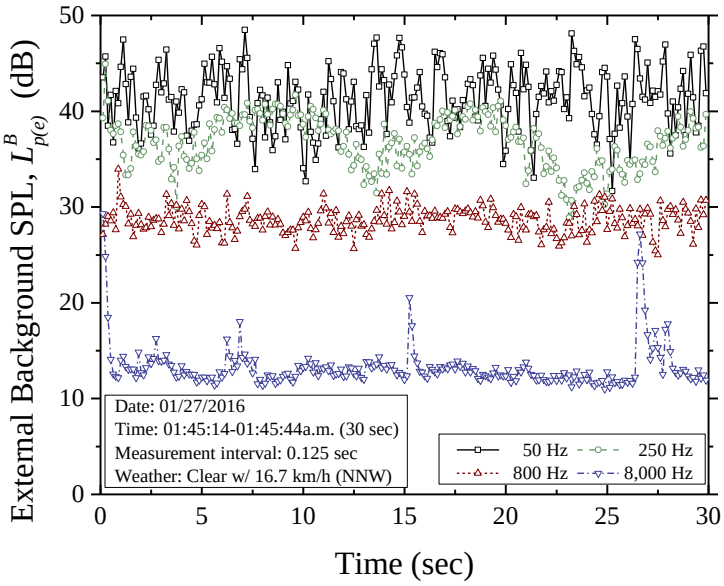

Figure 4-13 Time variations of the external background SPLs of a test conducted at the quiet environment

The four frequency bands were chosen based on the largest standard deviations of the three frequency groups, 50 through 80 Hz (50 Hz chosen), 100 through 2,000 Hz (250 and 800 Hz), and 2,500 through 10,000 Hz (8,000 Hz), which are used throughout this study. As noted in Figure 4-13, the measurements were taken at midnight when the weather was clear with winds less than usual. Of special interest, the test site was located in a rural area with quiet environmental backgrounds, which were also discussed in the Chapter III. Therefore, the time variation presented in Figure 4-13 is a typical or quieter-than-usual background rather than an example showing an extreme case. Despite the quite background condition, the external background SPLs are in flux along with irregular variations. For example, the two lower bands, 50 and 250 Hz bands, show constantly moving backgrounds. Furthermore, the external background SPLs at the

8,000 Hz band show several impulses although the fluctuation is relatively suppressed than the other frequency bands. Based on these observations two discussions can be made. First, based on the different time averaging scheme, the measured average background SPLs can differ, as can be seen in the consistently changing background (50, 250 Hz bands) and the impulse noises (8,000 Hz). Next, as can be seen from the case example in Figure 4-13, the background steadiness needs to be assessed during measurement if a fluctuation is expected.

Standard Deviations of External Background Noise

Figure 4-14 through Figure 4-16 present the distribution of the standard deviations of the external background SPLs measured in the UNIT, BGD, and RSS phases, respectively. In Figure 4-14 through Figure 4-16, it is easily noticeable that the distributions are the same when the standard deviations of the three different measurement phases, namely the UNIT, BGD, and RSS phases, are compared. Based on the similarity between the measurement phases, the sound transmission of the unit under test or the RSS do not significantly affect the standard deviations of the external noises.

When the background comparison limit set by HVI 915 is taken into consideration with standard deviations, it is noticed that the majority standard deviations are outside the limits. It should be noted that the background difference limit was originally set to compare two difference background measurements. Furthermore, the limit cannot account for the background fluctuations during a specific measurement phase. As such, the background steadiness at a specific measurement phase should be analyzed in a

different context to the background comparison or difference criteria by having different sets of limits or criteria.

Another findings in the distributions of the standard deviations in Figure 4-14 through Figure 4-16 is that the mean or median values for the standard deviations vary along with the frequency bands, in contrast to the previous findings on the average external background SPL shown in Figure 4-5 through Figure 4-7, and the external background differences at the two measurement phases discussed in Figure 4-8 through Figure 4-12. Specifically, both lower frequency bands up to about 125 Hz band and the higher frequency bands over 2,500 Hz show larger standards deviations over 2 dB while the medium-to-high frequency bands show lesser standard deviations.

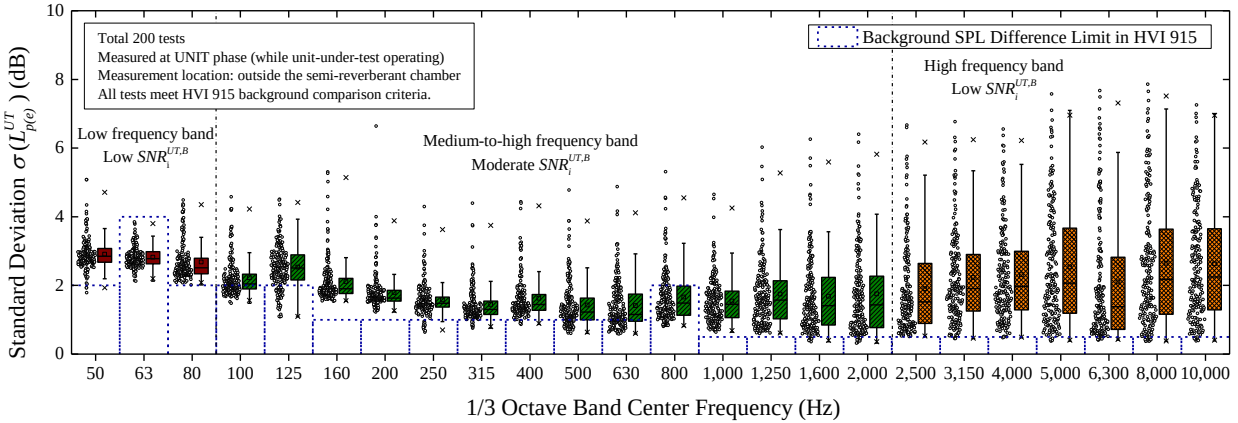

Figure 4-14 Distributions of the standard deviation of the external background SPLs at the UNIT phase

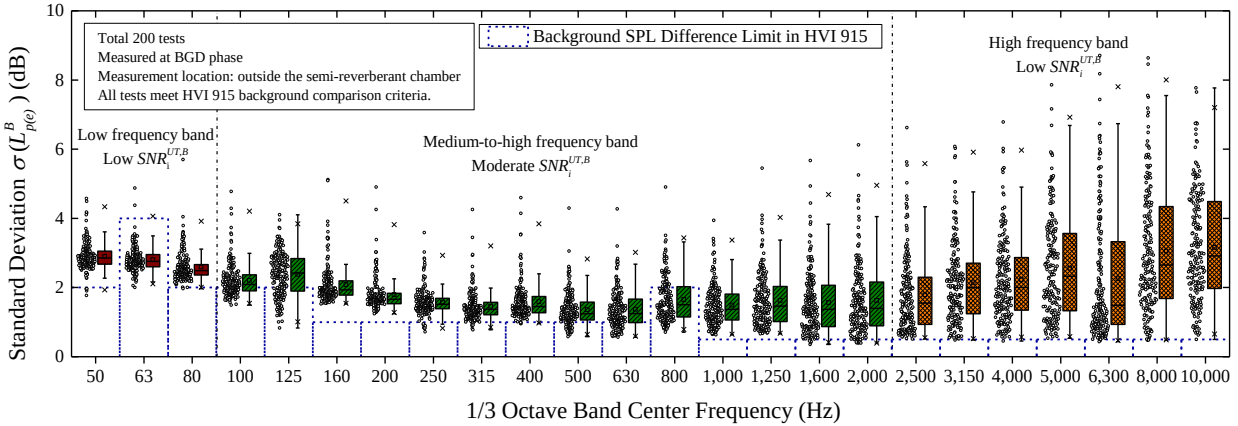

Figure 4-15 Distributions of the standard deviation of the external background SPLs at the BGD phase

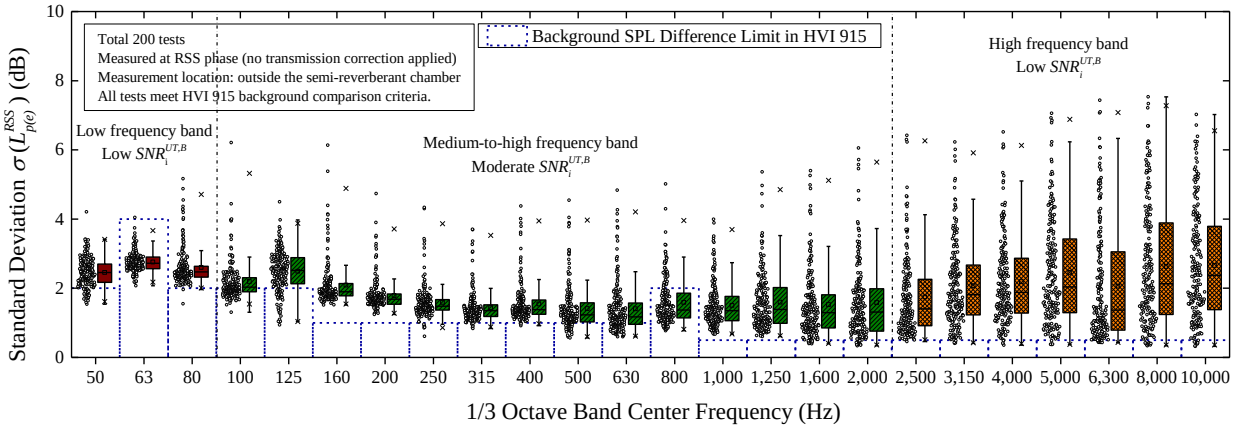

Figure 4-16 Distributions of the standard deviation of the external background SPLs at the RSS phase

Also, the larger extremes, characterized by the long whiskers, is observed in the high frequency bands in Figure 4-14 through Figure 4-16. Of special interest, the large extremes spanning 4 to 6 dB of the standard deviations can be even detrimental to the background steadiness when it comes to the low background noise SPLs of about 3-20 dB observed in Figure 4-5 through Figure 4-7.

Coefficient of Variations of External Background Noise

Because the standard deviations of the high frequency bands are of the potential concern, another metric showing the relative standard deviation or the coefficient of variation, which is the ratio between the standard deviation and the mean, is useful to expand understanding. Figure 4-17 shows the distributions of the coefficients of the variations (CV) of the external background SPLs taken at the UNIT phase for the frequency bands of 2,500 through 10,000 Hz. It should be noted that the CV of the 10,000 Hz band was distributed over a large span of values, so the different range of the vertical axis was presented in the right hand side of Figure 4-17. First thing to notice in Figure 4-17 is the large CVs that is caused by the larger standard deviations along with the relatively lower external background SPLs. For example, the last two frequency bands, namely 8,000 and 10,000 Hz bands, have large portions (at least a quarter of the tests) of the CVs over 0.5, which is interpreted as the standard deviation being more than 50% of the measured average SPLs. Of special importance, it should be noted that dispersion (or distribution) of the external background of these two last bands were similar in Figure 4-5, while the extremes of these two frequency CVs in Figure 4-17 were exceedingly large. The large extremes in the last two frequency bands, which is

longer than the IQRs, can be a clue to the presence of the highly random background noises which are intermittently measured as the large intensity noise, such as impulses in the 8,000 Hz band in Figure 4-13.

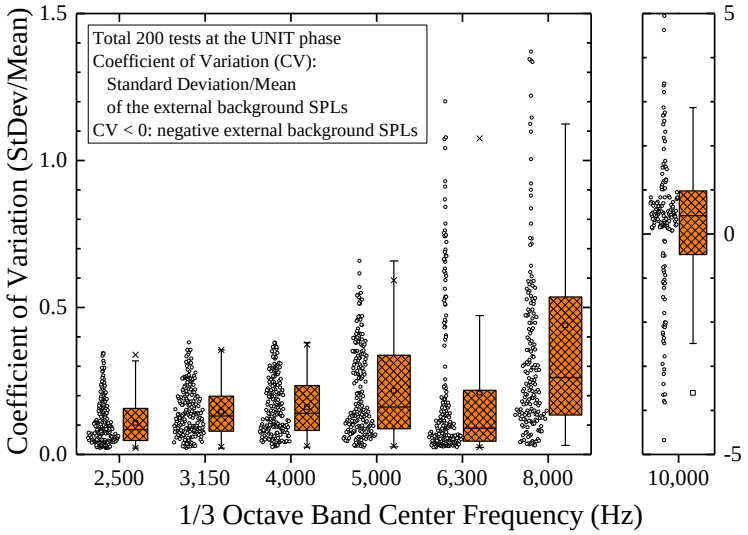

Figure 4-17 Distributions of the coefficient of variations (CV) of the external background SPLs taken at the UNIT phase

Considering the large coefficient of variations in these frequency bands, it is possible to assume the background noise in these bands is the combination of the impulse noises, having larger sound pressure level, and the other noise sources, forming a basis background noise at the frequency band, which again emphasis the uncorrelated nature of the background noise sources. In the light of the background steadiness assessment, the exceedingly large standard deviations in the higher frequency bands can be interpreted as the unsteadiness of the background noise, which might affect the precision

of the acoustic rating of the unit under test. Of special importance, the low $SNR_i^{UT,B}$ was found to potentially compromise the background steadiness in the low frequency band and the high frequency band as previously discussed in Figure 4-2. As such, unsteady background noises are forecasted in these two groups by means of the overall larger standard deviations and the large extremes observed in the group 3.

Based on the discussions made with the standard deviations and the coefficient of variables, a practical guideline for the comparison can be made. First, the comparison of the standard deviations determined during each phase can lead to the assessment of the background variations at each measurement phase. If the standard deviations of the external background SPLs are found to be the same, the similar pattern of the background variation is expected. Then, one can consider that the background variation is consistent throughout the test. Next, one can assess the background steadiness for a single measurement phase, the UNIT, BGD, or RSS phase, by analyzing the absolute amount of the standard deviation as well as the amount relative to the average external background SPLs. It was found that exceeding the amount of the standard deviation with respect to the average SPLs, characterized as the extreme CVs in Figure 4-17, can be caused by the random impulse noises, which can intermittently appear during the measurement. In this case, the background is not considered to be steady.

Of special importance, it should be noted that the results presented in this study is an example of the possible results of the reverberant acoustics along with quiet to moderate backgrounds with some degree of variation. The background noise and the acoustic facility vary along with different test specimen and test locations. For example, many

urban, industrial and commercial testing sites can suffer from louder background noise, especially in terms of the poor SNRs of the sound emission of the test specimen in the presence of the louder background. However, the approaches and the methodologies for the analysis and the assessments of the background steadiness covered herein can be applied similarly. As such, based on the background characteristics along with the transmission characteristics, one can set criteria of the background steadiness, such as the difference limit of the average external background SPLs or the standard deviations limit.

Conclusions

Various testing protocol and code have demanded the qualification or assessment of the background in different details such as an SNR metrics or the comparison of the two different background measurements. Despite the equal motive of guaranteeing the background steadiness for the acoustic rating, each method has its own disadvantages due to the limitation that the background noise while measuring the unit-under-test is not identified. In order to address this issue, the study herein implemented the measurement of the external background noise, while conducting acoustic testing.

The fundamental motivation of the need of the background steadiness assessment is that a number of the test subject (unit-under-test) have sound emissions that are not easily separated from the background noise. For example, the residential ventilation devices tested in this study show low signal-to-noise ratios (SNRs), e.g. under 6 dB, at the two frequency groups, namely at the low frequencies (up to 80 Hz 1/3 octave frequency band) and the high frequencies (over 2,500 Hz band). Despite the same lower

SNRs, the poor SNRs of the two frequency groups were caused by a different nature of the sound emission. The low frequency group (up to 80 Hz band frequency) showed large variations in the background noise along with more sound transmission as characterized in the Chapter III of this study. Also, relatively larger background noise levels are also coupled with a similar amount of the unit noise. In contrast, the high frequency group (over 2,500 Hz band frequency) showed relatively less variations in the background noise inside the measurement space, namely the semi-reverberant chamber, along with lower background noise levels compared to the lower frequency background noise.

Comparisons of the average external (or outside-the-chamber) background SPLs in the UNIT, BGD, and RSS phases revealed that the interquartile range (IQR) of the external background SPLs remain similar with IQR being 4 to 5 dB throughout the entire 1/3 octave frequency bands. Meanwhile, each frequency band showed different mean and median SPLs. In addition, the comparison of each measurement phase, UNIT, BGD, and RSS, have shown that the distributions of the external background SPLs are similar in general. It should be noted that the 200 tests analyzed herein met the background difference criteria, which compares the two background signals taken before and after the RSS phase with a certain limit. Therefore, similar patterns of the external background distributions were found among the measurement phases. In this light, the proposed external background monitoring is potentially a better background comparison methodology in that the wider coverage of the measurement phases including the UNIT and the RSS phases.

The fluctuation of the background while taking measurements is also important as the consistent background throughout a test set (e.g. UNIT, BGD, and then RSS) because the different fluctuation at each measurement phase may result in different backgrounds. Our preliminary study on the time variations of the external background noises has explicitly shown the presence of continuously changing backgrounds along with impulse noises that is predominant especially at high frequencies, such as 8,000 Hz and over. In order to expand the background fluctuation study, the distributions of the standard deviations of each external background measurement phase were presented. Comparisons of the standard deviations of the measurement phases led to the findings that the distributions were similar to the measurement phases irrespective of the transmission characteristics, which enables a more convenient comparison. Also, this finding led to a methodology of another background steadiness assessment with similar standards deviations being a clue to the background steadiness in that the background can be considered to be steady once the same background fluctuation as well as the similar average background were identified.

Unlike the average external background SPLs, the standard deviations varied along with the different 1/3 octave frequency bands. Specifically, the overall large standard deviations were observed at the low frequency group and the high frequency group. As previously noted, these two frequency groups were of special importance in that the low SNRs of the test subjects to the background noise were focused on these groups. The coefficient of variations (CVs), the ratio of the standard deviation to the average external background SPLs, presented the relative variation of the external background with

respect to the measure external background SPL. The CVs of the 8,000 and 10,000 Hz were found to be exceedingly large, which can be interpreted as a large potential for unsteady background.

Based on the findings in the external background study herein, several points can be made. First, it is necessary to identify how much the sound transmission of the unit under test or the RSS affects the external background before assessing the background steadiness. It was found that the sound transmission can affect the average external background SPLs, especially in case of the level of the transmitted sound is not significantly different from the external background. Second, despite the wide applicability of the external background monitoring method, the background steadiness assessment can be done effectively in the range of frequencies where the poor SNR can be an issue. By selecting the frequency of interest, one can reduce the demand of the sampling, which can often be a challenge for the large frequency ranges along with the short sampling intervals. Third, the average external background signals can provide a clue to the validity of the usage of the internal background signal for the background correction purposes. Lastly, fluctuation of the external backgrounds such as in terms of the standard deviations, can provide an insight that how much background fluctuation or s occurred, and how similar are their fluctuations and variations between measurement phases periods, such as the UNIT, the BGD, or the RSS phases.

CHAPTER V

UNCERTAINTY AND SIGNAL-TO-NOISE RATIO FOR UNSTEADY BACKGROUND NOISE

Overview

This paper presents methodologies that can be to evaluate the impact of unsteady background noise for standard acoustic tests. When the sound or noise emitted by a test subject is measured following standards and codes in the presence of background noise, then a background correction is necessary. However, the use of a background correction factor is valid only when the signal-to-noise ratio (SNR) of the sound source being evaluated is above the lower-limit specified in the acoustic test standard. Therefore, the testing of increasingly quiet devices is becoming a problem because a poor SNR is significantly affected by background noise variations (i.e. unsteadiness, defined as a background with change, variation, or interruption). This study investigates and introduces two methodologies that address the negative effects of background variations that produce poor SNRs when following standard testing procedures. The first methodology evaluates and discusses the uncertainty in the background correction. The second methodology introduces a SNR metric, namely the zero loudness SNR, in order to provide some more acceptable tolerances during standard acoustic tests that use loudness as a rating method. The application and the usefulness of implementing the two above methodologies is presented with the result showing that the combined use of the

zero loudness SNR and the uncertainty of the SNR can overcome the negative effect of background unsteadiness, when acoustical tests of devices suffer from low SNRs.

Introduction

Addressing random, uncorrelated fluctuations of background noises, which is an extraneous signal coexisting with a signal of interest, is important when measuring and signal processing acoustical signatures from mechanical devices during their operations. Presently, either of two approaches are generally used to account for background noise variations, namely reducing the background noise or evaluating the potential impact of the background variations. The first approach of reducing the background noise usually involves structural considerations such as adding mass, springs, and damping controls to the testing space, along with using acoustic insulations, resonators, and anechoic chambers [13, 68]. Although anechoic chambers equipped with heavy acoustic insulations can minimize the impact of the background unsteadiness [82], the anechoic chamber may not be suitable for the entire scope of acoustic measurements and characterization techniques because of space limitation, budget concerns, or limitations of auxiliary device (environmental conditioning, pressurizing, etc.) integrations. Likewise, certain limitations can exist for reducing background noises in that construction-wise approaches may not be cost effective when a setup must adhere to acoustic standards such as ANSI, IEC ISO, etc. [10, 11, 83]. Furthermore, not all of the frequency ranges may benefit from the use of the structural improvements, especially at lower frequencies with their lower sound transmission losses [68] because of the limitations of reducing the background noise. The second approach of evaluating the

impact of the background noise variation has been widely adopted for a wide range of practices and applications during acoustical testing with noisy signal measurements.

Signal processing extensively deals with the influence of the background variations [18, 54]. For example, one of the simple but frequently used methods is the spectral subtraction method, based on treating the measured signal as a combination of the signal of interest and the undesirable background. A simplified spectral form can be written as follows.

$$Y(f) = X(f) + N(f) \tag{5-1}$$

, where $Y(f)$, $X(f)$, and $N(f)$ are the Fourier transforms of the noisy signal $y(t)$, the signal of interest (or original signal) $x(t)$, and the background noise $n(t)$, respectively, while the f is frequency. More sophisticated variations of the spectral subtractions method are based on incorporating Eq. (5-1) with statistical methods [84], extended mathematical dimensions [16], or different averaging schemes [85], to name a few. Additional approaches to background noise modeling have been studied and utilized in disciplines, being the non-convolution, colored-noise-based modeling [55], dynamic-and-static background modeling [86, 87], etc.

The objective of signal processing is to improve of the quality of the signal and yield of any measured signal of interest. Because modeling schemes require that assumptions be made regarding the inputs (or noise in Eq. (5-1)), the output signal after processing is influenced by biased information from these assumptions such as under- or over-estimations of the input noise or neglecting phase properties of the output in the frequency-domain [18, 54]. Even though there are numerous methods to evaluate an

effectiveness of the aforementioned noise processing methods, such as signal-to-noise ratio (SNR) and perceptual evaluation of speech quality (PESQ) [16, 18], the evaluation can vary according to purposes and applications of the processing methods. For standard testing, a logarithmic variation of Eq. (5-1) is used, which is called the background correction factor.

$$K = -10\log\left(1-10^{-0.1\left(\Delta L_p\right)}\right) \tag{5-2}$$

, where K is a background correction factor, and ΔL_p is defined as follows.

$$\Delta L_p \equiv L_p^{UT} - L_p^B \tag{5-3}$$

, where L_p^{UT} is a sound pressure level of a test subject or a unit under test (UT), and L_p^B is a sound pressure level of background or ambient noise with the absence of the acoustic emission of the unit under test.

Of special interest, Eq. (5-3) is also defined as the signal-to-noise ratio (SNR) of the test subject and background sound pressure levels (SPLs), $SNR^{UT,B}$. As the term SNR implies, the major concern with respect to the background is whether there is enough separation of the signal of interest and the background noise. The ISO/ANSI Precision Method (Grade 1) [11] under reverberation conditions requires $SNR^{UT,B}$ being at least 6 dB in one-third octave bands represented by the center frequencies of 200 Hz and below, and 6,300 Hz and above, and $SNR^{UT,B}$ being at least 10 dB for 250-5,000 Hz center frequencies.

If the $SNR^{UT,B}$ does not meet the criteria above, additional procedures to qualify the background are required, such as the maximum background SPLs or identifying partial fulfillments of the criteria [10, 11].

Despite the stringent requirements of SNRs, frequently experienced during actual acoustical testing is that the sound emission of the test subject is not significantly larger than the background steadiness. For instance, Figure 5-1 shows a histogram of the number of the 1/3 octave bands violating the SNR limit set by ISO 3741 Precision Method. The data in Figure 5-1 comprises 200 tests for residential bath fans, utility room fans, and range hoods performed during the period 2013-2016 at the Texas A&M University Riverside Energy Efficiency Laboratory (REEL).

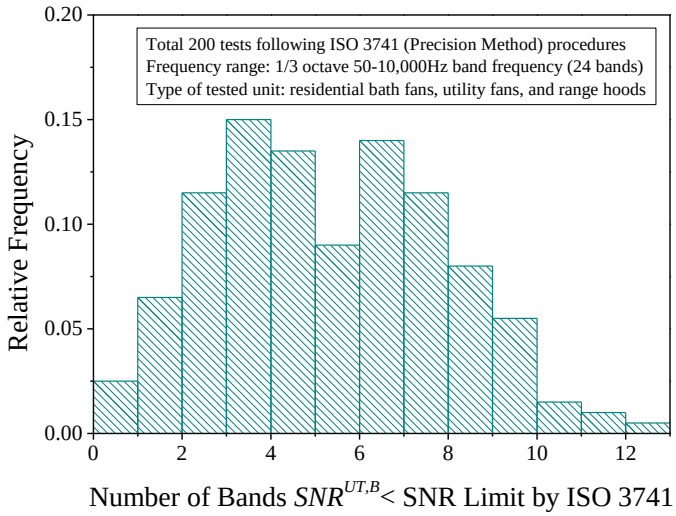

Figure 5-1 Histogram of the number of 1/3 octave bands having $SNR^{UT,B}$ less than the SNR limit by ISO 3741 Precision Method for 200 residential ventilation device tests

In Figure 5-1, only five out of two hundred residential-ventilation-fan tests (2.5 percent) met the minimum SNR criteria of the ISO Precision method, and the other 97.5 percent of the tests (195 tests) had at least one band violating the SNR limit. It should be noted that the background noise SPL or environmental noise SPL in the test site were relatively lower (47 dB) than the typical environmental noises in industrial or commercial sites [74], and all 200 tests were conducted in the late evening or at night after the normal work day in order to minimize background sound levels. Therefore, the background SPLs were not severer than any testing site. Instead, the sound emissions of the test subjects in Figure 5-1 were not loud enough to overcome the background noises, which are relatively low (47 dB).

The examples shown in Figure 5-1 comprise only a fraction of the issues related low $SNR^{UT,B}$. It has been observed that residential ventilation devices have become quieter [88] since the introductions of building ventilation codes and regulations [2, 23, 33]. As noted before, more issues are associated with the low $SNR^{UT,B}$. Likewise with time, other acoustic test subjects, not only the ventilation devices in Figure 5-1, are likely to suffer from poor SNRs. In this light, the impact of the background noise variations must be investigated and evaluated so as to quantify it when a standard acoustic test suffers from the low $SNR^{UT,B}$. Therefore, the study herein investigates approaches for evaluating the impact of the unsteady background noises by using statistical methods. Also, for practical applications, the assessment methodologies of the unsteady background noise are investigated by using the psychoacoustic term loudness [8, 20, 89, 90] along with the loudness calculation procedures.

Description of Methods

Sensitivity Coefficient and Uncertainty

Before discussing the methodologies in this study, it is useful to provide additional information on Eq. (5-2). The two minimum SNR limits for the ISO Precision Methods are 10 dB (250-5,000 Hz bands) and 6 dB (50-200 Hz and 6,300-10,00 Hz bands) as previously discussed. When these two SNR limits in dB are converted to the background correction factor in Eq. (5-2), the results are

- The 10 dB of the $SNR^{UT,B}$ corresponds to about 0.46 dB of the background correction in Eq. (5-2), which means the SPL of the pure signal is expected to be about 0.46 dB less than the noisy signal.
- Likewise, 6 dB of the $SNR^{UT,B}$ corresponds to about 1.26 dB of the background correction.

The impact of the above background correction values of 0.46 and 1.26 dB can be interpreted arbitrarily depending on the sound emission of the subject and the testing condition. However, it is intuitively understood as the $SNR^{UT,B}$ becomes lower, the larger background corrections are necessary. Likewise, background noise variations strongly affect the reproducibility of the test results at the lower $SNR^{UT,B}$. As such, the variability of the background needs to be taken into consideration for the analysis of the background impact. In addition to the calculated background corrections of 6 and 10 dB $SNR^{UT,B}$, the first derivative of Eq. (5-2), or the sensitivity coefficient of the background correction factor *K*, s_K plays an important role for the background impact analysis.

$$s_K = \frac{1}{1-10^{0.1\Delta L_p}} \tag{5-4}$$

By applying values of the measured ΔL_p or $SNR^{UT,B}$ to Eq. (5-4), one can determine the sensitivity of the background corrections. For example, when the $SNR^{UT,B}$ is found to be 6 dB, the sensitivity coefficient is -0.34 dB, which can be interpreted to mean that the variation of the background correction can be 0.34 dB per 1 dB of the $SNR^{UT,B}$ variations. When the sensitivity coefficients are multiplied by the quantitative measure of the background variability, the impact of the background unsteadiness can be evaluated. For example, the standard background uncertainty u_K is a representative of this multiplication, which is defined in Eq. (5-5). [17].

$$u_K = \sigma\left(L_p^B\right)\left|s_K\right| \tag{5-5}$$

, where $\sigma(L_p^B)$ is the standard deviation of the measured background SPLs. It should be noted that the absolute value of the sensitivity is taken because its value is usually $s_K < 0$. The use of the uncertainties in Eq. (5-5), along with comparisons to other approaches, is discussed in the next section, namely Result and Discussions.

Zero Loudness SNR

Although sound levels in dB are ubiquitous in acoustical applications, the psychoacoustic term loudness, which is defined as a "human perception" quantitative measure of sound loudness, is increasingly used in many standards and codes [8, 9, 20, 33, 89]. For example, the standard tests used the study herein conform to AMCA 301 and HVI 915, in addition to ISO 3741, in order to determine sound power levels and loudness.

The detailed evaluation procedure for loudness can be found elsewhere in another paper [88]; however, an overview of the calculation process is presented below.

1. First, based on the sound power level of a test subject, L_w^{UT}, determined by standards, such as ISO 3741 [11], the SPL at the spherical free field, $L_{p(sf)}^{UT}$, is obtained at a 1.52 m (5 feet) distance from the noise source by subtracting 14.65 dB [8, 9].
2. Next, loudness for each one third octave band are determined by using the human equal loudness contours and table [9, 20, 90].
3. Lastly, the total loudness *N* is determined by using the summation rule developed by Stevens [9, 20].

Figure 5-2 is a contour mapping of loudness converted for the one-third octave band frequencies used herein [9]. It should be noted that the loudness contour in Figure 5-2 is one of the loudness contours used in the standard testing of residential ventilation devices, such as in AMCA and HVI testing protocols [8, 9]. As noted, the loudness starts to have nonzero values at different SPLs per each frequency, which means the perception of the sound differs from each frequency band. In addition, the 8,000 Hz band shows the lowest loudness threshold; however, the gradient of the loudness does not in fact significantly differ from the adjacent bands.

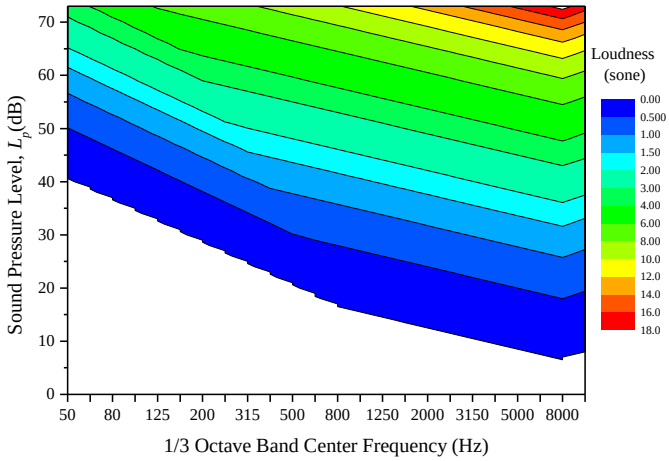

Figure 5-2 Contour mapping of the 1/3 octave band loudness used in this study (HVI 915) [9]

Based on the loudness calculation procedures, one can suggest a measure of another SNRs, namely zero-loudness SNR, which is the signal-to-noise ratio of the zero loudness threshold at the measured background SPLs. Before introducing the formulation of the zero loudness SNR, it is important to note two major findings.

1. First, the zero-loudness, which presumably is the threshold of the perception, is larger than 0 dB SPL in most frequency bands.
2. Second, the poor SNRs is usually caused by low to moderate sound emissions from the test subject, and some bands can actually show zero-loudness for the low to moderate sound emissions.

The following is the calculation procedure of the zero-loudness SNR.

1. First, spherical-free-field zero-loudness SPL L_p^{zl} in each band is identified by using either tabulated values or contour diagrams.
2. Then, the obtained zero-loudness SPLs are converted back to the zero-loudness sound power level (SWL) L_w^{zl} by using the following formula.

$$L_w^{zl} = L_p^{zl} + \left| 10\log\frac{Q}{4\pi r^2} \right| \tag{5-6}$$

, where Q is a directivity factor, which corresponds to 1 for the spherical free field, and r is a distance in meters from the sound source. As previously noted, the distance r was chosen to be 1.52 m for the standard testing [9].

3. Next, the zero-loudness SWL is converted to the SPL of the acoustic field used for testing, such as anechoic fields, reverberant fields, etc., by using a conversion method prescribed in standard for use. For example, because the study herein uses the semi-reverberant chamber for standard acoustic testing, the comparison method, which utilizes the calibrated SWL, L_w^{RSS}, and measure SPL, L_p^{RSS}, of a reference sound source (RSS), is used in order to convert the zero-loudness SWL to the zero-loudness SPL in the reverberant field $L_{p(r)}^{zl}$ [11], which is expressed as follows.

$$L_{p(r)}^{zl} = L_w^{zl} - L_w^{RSS} + L_p^{RSS} \tag{5-7}$$

Of special importance, the last two terms in the right hand side is also called the room characteristic ratio (RCR), because the logarithmic ratio of the SWL and the SPL contains the field character of the test site. The zero-loudness reverberant SPL $L_{p(r)}^{zl}$ does not contain information of the background noise. Therefore, the measured background is logarithmically added to make a zero-loudness-reverberant SPL, $L_{p(r)}^{zl,B}$, in the reverberant field.

$$L_{p(r)}^{zl,B} = 10\log\left(10^{L_{p(r)}^{zl}/10} + 10^{L_p^B/10}\right) \tag{5-8}$$

4. Lastly, the zero loudness SNR, SNR_{zl} is determined as follows.

$$SNR_{zl} = L_{p(r)}^{zl,B} - L_p^B \tag{5-9}$$

It should be noted that the zero loudness is a function of the background noise, RCR, and the human loudness perception (or model implemented), not the sound level of the unit. Therefore, the zero loudness SNR can be different from $SNR^{UT,B}$ in its value.

The application of the zero loudness SNR and comparisons to other approaches are discussed in the following section.

Results and Discussion

Background Correction Factor Uncertainty

Before developing an analysis on the sensitivities and uncertainties of the measured backgrounds, it is important to describe the test data that is used herein for this study. For the sensitivity and uncertainty study, the test results for 200 different fans were randomly chosen between the test period 2013 and 2016 in order to avoid temporal bias. The subjects of these 200 tests consists of residential bath fans, utility room fans, and range hoods whose sound emissions are not exceedingly large but rather in the mainstream, which was also revealed by the several SNR violations in Figure 5-1 discussed in the Introduction section. All tests of these 200 units were performed by using the procedures of ISO 3741, AMCA 301, and HVI 915. Of special importance, each tests consists of two different background measurements, namely BGD1 and BGD2, and the two BGDs were compared to address the background steadiness as required by the background comparison criteria in HVI 915 [9].

Sensitivity and Standard Uncertainty

Before a discussion of results is presented herein, it is useful to note values and trends of the background correction factor *K* in Eq. (5-2) and the sensitivity coefficient s_K in Eq. (5-5) because values of *K* and s_K provide useful insight to the uncertainty analysis. Figure 5-3 shows *K* and s_K plotted against the ΔL_p (or $SNR^{UT,B}$). Because these factors and coefficients are exponential functions, the vertical axis is

logarithmically scaled, while the inset in Figure 5-3 is plotted in a linear scale. As an aside, it should be noted that the sign of the sensitivity coefficients is negative.

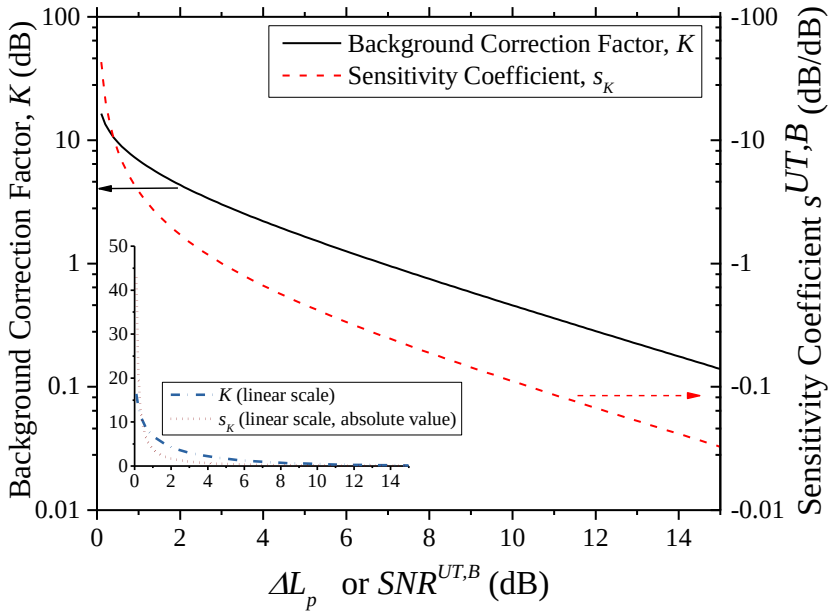

Figure 5-3 Background correction factors and sensitivity coefficients plotted against ΔL_p (or $SNR^{UT,B}$)

Based on these values in Figure 5-3 and the standard deviations of the background SPLs, $\sigma(L_p^B)$, the standard uncertainties of the 200 background measurements were determined. Figure 5-4 and Figure 5-5 show distributions of the uncertainty of the standard background correction factor, u_K, which is defined in Eq. (5-5). The range of the uncertainty distributions were distinctively different between two groups, namely

1. low (up to 80 Hz) and high bands (4,000-10,000 Hz) in Figure 5-4, and
2. mid-frequency bands (100-3,150 Hz) in Figure 5-5.

An interpretation and comparison of Figure 5-4 and Figure 5-5 results in the following observations.

1. The uncertainties u_K of the frequency groups in Figure 5-4 (i.e., low and high bands) spans over 30 dB.
2. In contrast, none of the uncertainties of the frequency groups in Figure 5-5 (i.e., mid-frequency bands) are larger than 0.4 dB.
3. Of special interest, the standard deviations of the background SPLs $\sigma(L_p^B)$ were between 0.11 and 2.9 dB throughout the 1/3 octave bands.

Therefore, such large separations of the uncertainties u_K in Figure 5-4 and Figure 5-5 were primarily driven by the sensitivity coefficients s_K, which means the extremely large or small uncertainties u_K is usually caused by exceedingly larger or smaller sensitivity coefficients s_K. Further insight can be obtained by focusing on the sensitivity coefficients s_K and the background correction factors *K* in Figure 5-3. That is, the absolute values of s_K and *K* shows similar trends in that both s_K and *K* are larger as the test subject sound emissions become less separated from the background noise, i.e. lower ΔL_p or $SNR^{UT,B}$. Furthermore, the exponential term in Eqs. (5-4) and (5-5) have s_K and *K* maintaining the same trends in Figure 5-3. This finding is interesting in that the poor $SNR^{UT,B}$ results in significantly larger uncertainties not only because of the background variation in terms of the standard deviation, but also because of the sensitivity of the background correction factor.

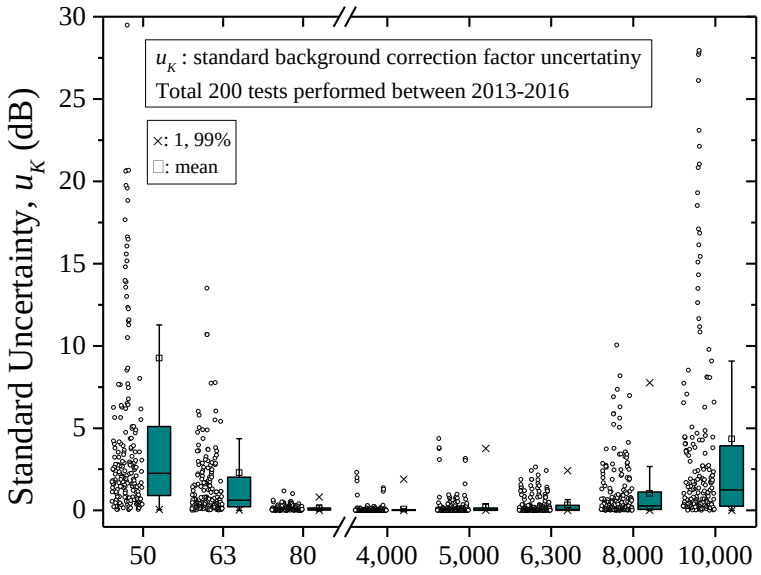

Figure 5-4 Distributions of the standard background correction factor uncertainties at low (up to 80 Hz bands) and high (4,000-10,000 Hz bands) frequency bands

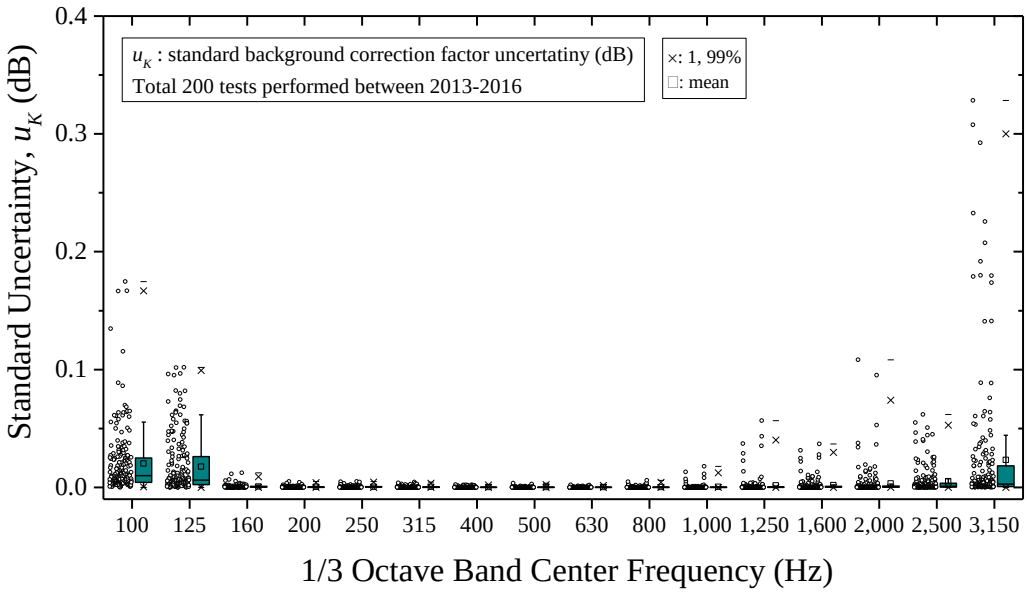

Figure 5-5 Distributions of the standard background correction factor uncertainties at mid frequency bands between 100 and 3,150 Hz bands

Expanded Uncertainty of SNR Limit

The average standard uncertainty can also be useful to evaluate the background impact on measurements, especially when the measured $SNR^{UT,B}$ is equal to the minimum SNR required by the ISO Precision Method. Figure 5-6 is a graphical digest for various 1/3 octave-band center frequencies of background noise standard deviations for all 200 measurements, the standard uncertainties u_K, and the expanded uncertainties of the 95% confidence level $U_{K,95\%}$. In Figure 5-6, the standard deviation was calculated by combining the 200 background SPL measurements. Also, two different uncertainties were determined for the background correction factors, based on assuming when the $SNR^{UT,B}$ equals to the minimum SNRs required by the ISO 3741 Precision Method. The expanded uncertainty, which is practically used for most uncertainty budgets, is obtained by multiplying the standard uncertainty u_K by the coverage factor for a 95 % confidence level [17].

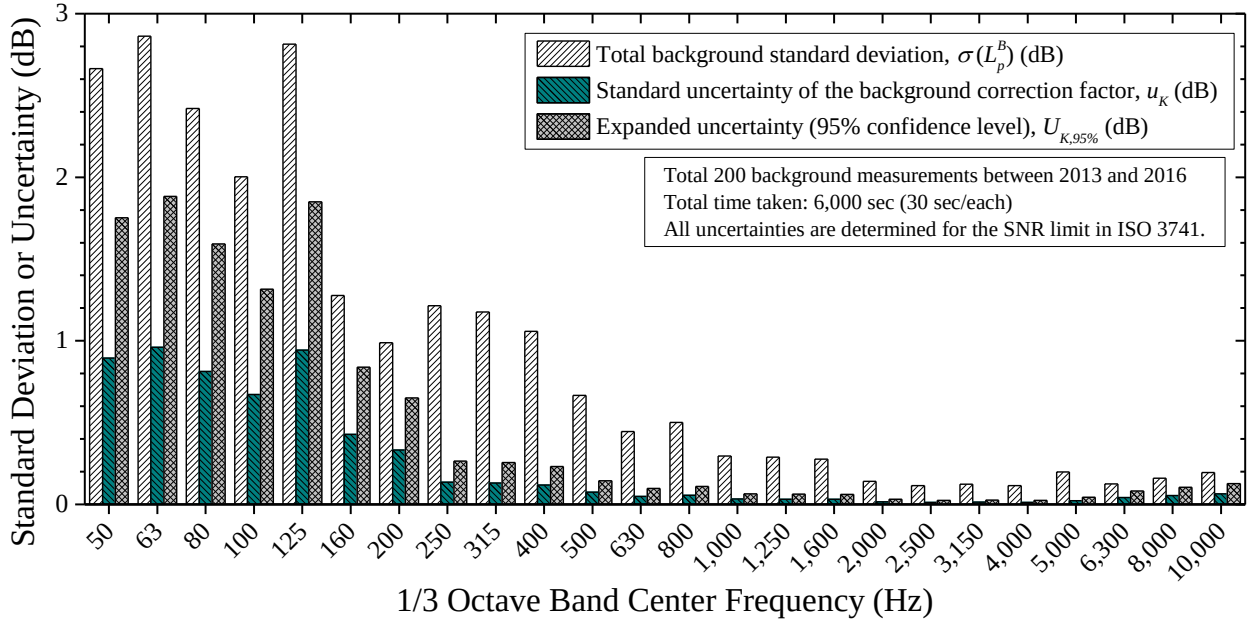

Figure 5-6 Background noise standard deviations, standard uncertainties u_K, and expanded uncertainties of 95% confidence level $U_{K,95\%}$ for the SNR limit in ISO 3741

In Figure 5-6, the expanded uncertainty is larger at lower frequency bands (up to the 200 Hz). In contrast, the expanded uncertainties are relatively small in these frequency bands even though the standard deviations are observed in the mid frequency ranges (250-800 Hz).

An interpretation of the standard uncertainty u_K can be arbitrary depending on SPLs of the test subject. The standard uncertainty u_K can be converted to the relative scales of the sound power by taking the power of ten after dividing the standard uncertainty by ten, i.e. $u_K/10$. For example, 0.5 dB corresponds to 12% of the relative uncertainty of the sound power, in Pa, psi, etc. As such, the standard uncertainties u_K for the low and high frequency bands in Figure 5-4 can be considered as a significant amount when the uncertainty budget requires lower uncertainty limits than the reported uncertainties. As noted previously, the 200 test subjects shown in Figure 5-4 and Figure 5-5 are low-to-medium noise residential ventilation devices, and these subjects were specifically tested and evaluated for loudness.

Zero Loudness SNR

Background SPL and Zero Loudness Threshold

The sound pressure levels for zero loudness means a person of the normal hearing [89] does not recognize the noise when subjected to this sound pressure level. In most cases, the background SPLs in the testing environment, i.e. inside the reverberant chamber, were determined to be zero loudness because the measured background SPLs were less than the zero loudness thresholds. For comparisons between the measured SPLs and the zero loudness SPL threshold, Figure 5-7 shows the measured background

SPLs plotted by the color contour surface and the zero loudness SPL threshold plotted by the mesh surface. It can be seen in Figure 5-7 that the measured background noise inside the reverberant chamber is in fact inaudible according to the loudness model used herein. In addition, the small variations in the zero loudness SPL threshold can be observed in Figure 5-7. As discussed in Eq. (5-7), for the minor variations in the zero loudness threshold are caused by the varying RCRs, which is outcome of different field characteristics due to meteorological conditions, such as air density, humidity, etc., and the configuration inside an acoustic testing space.

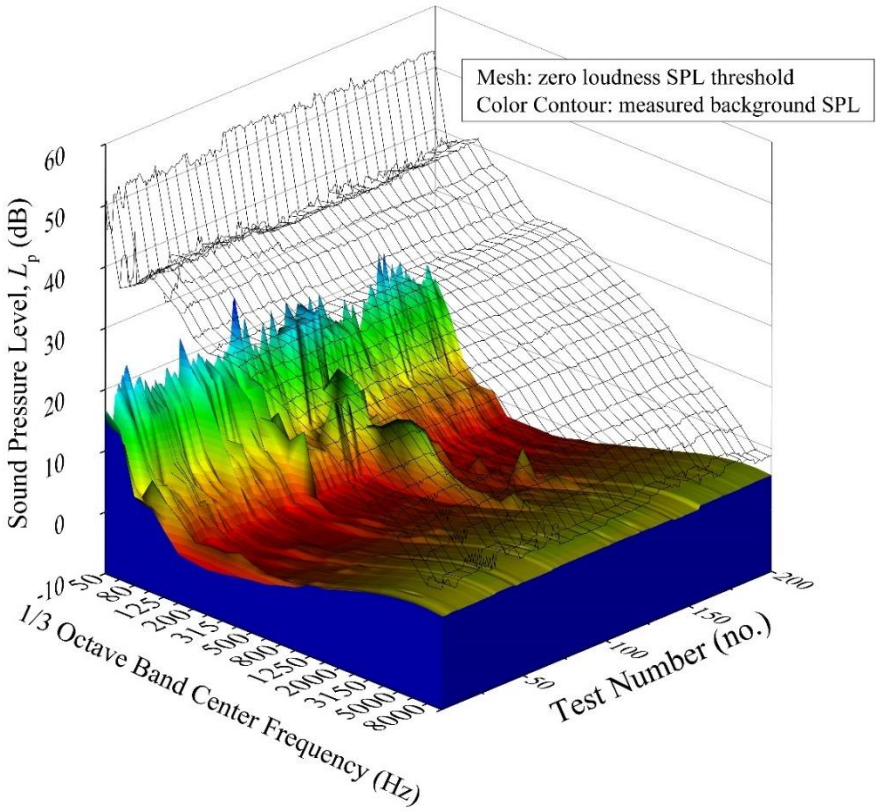

Figure 5-7 Mesh and contour diagram of the zero loudness SPL threshold (mesh) and the measured background SPLs (color contour)

Zero Loudness SNR

Based on the values plotted in Figure 5-7, along with Eqs. (5-8) and (5-9), the zero loudness SNR, SNR_{zl}, was determined. Figure 5-8 through Figure 5-10 are the distributions of $SNR^{UT,B}$ and SNR_{zl} for three 1/3 octave band groups along with the box plots. It is clearly noticeable in Figure 5-8 that the SNR_{zl} is larger than the $SNR^{UT,B}$ by a large margin, being more than 40 dB in the 50 Hz band. The large differences in these two SNRs are due to the sound emission of the test subject at a frequency band that is less than the loudness threshold. In contrast, the two SNRs overlap in frequency bands over 125 Hz band. Furthermore, most of the SNR_{zl} between the 250 Hz and 1,600 Hz bands in **Error! Reference source not found.** were distributed under the first quartile of t he $SNR^{UT,B}$. The SNR_{zl} distributions in the mid frequency band (250-1,600 Hz) mean most test subjects, i.e. residential ventilation devices, are emanating sounds perceptible to humans with normal hearing, and the loudness is over the threshold.

The SNR distributions in Figure 5-10 show $SNR^{UT,B}$ being lower than the SNR_{zl} for more than 75% of the tests, which means the sound emission of the test subjects are less than the loudness threshold. Another difference in the SNR distributions in Figure 5-8 through Figure 5-10 is the size of the distribution. The SNR_{zl} has narrow spans of variations in its values compared to the $SNR^{UT,B}$, which spans over 10 to 40 dB from the medians. These different sizes come from the variability of the inputs used in the calculations. Specifically, the RCR and the background measurements are variables for the calculation of the SNR_{zl} while the SPLs of the test subjects and the backgrounds are variables in order to determine the $SNR^{UT,B}$.

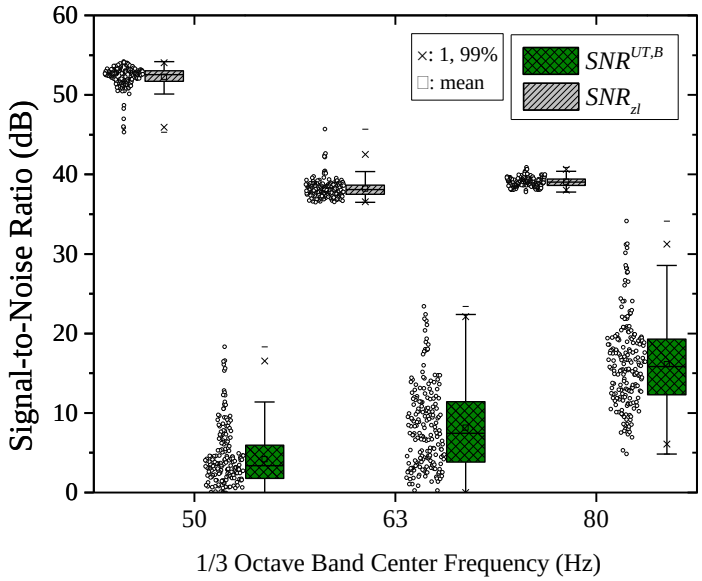

Figure 5-8 Distributions of $SNR^{UT,B}$ and SNR_{zl}, at the low frequency bands (up to 80 Hz band)

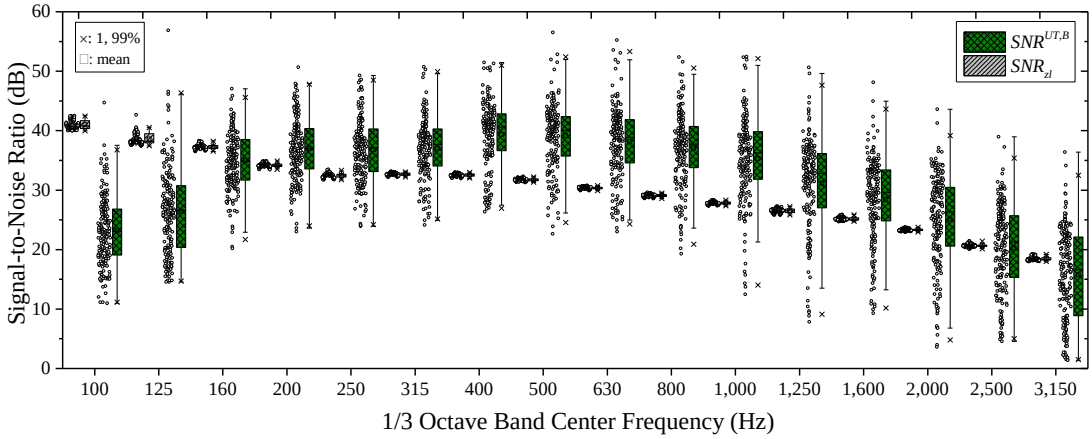

Figure 5-9 Distributions of $SNR^{UT,B}$ and SNR_{zl}, at the mid frequency bands (between 100 and 3,150 Hz bands)

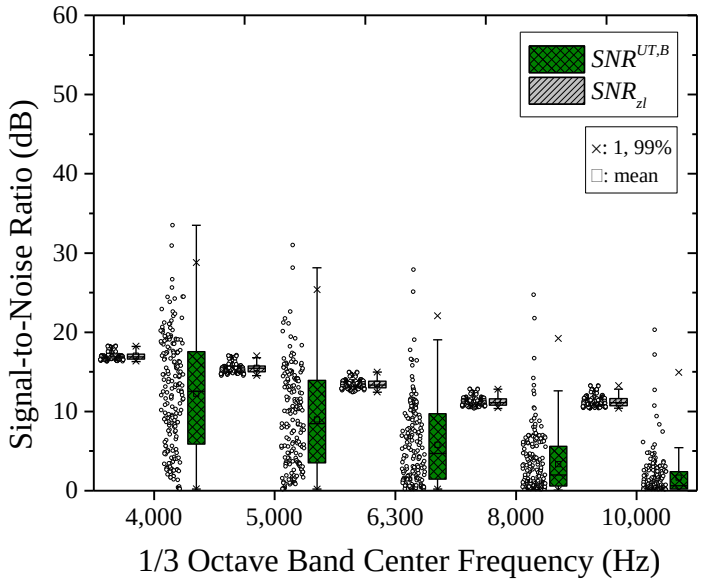

Figure 5-10 Distributions of $SNR^{UT,B}$ and SNR_{zl}, at the high frequency bands (between 4,000 and 10,000 Hz bands)

Combined Use of Zero Loudness SNR and Uncertainty

In Figure 5-8 through Figure 5-10, it is useful to note implications of the zero loudness SPLs and SNR_{zl} . The zero-loudness-reverberant SPL, $L_{p(r)}^{zl,B}$ in Eq. (5-8) implies an imaginary test subject whose loudness is exactly at the threshold of the zero loudness after performing the background correction in Eq. (5-2). As such, the SNR_{zl} represents the signal-to-noise ratio of the imaginary zero loudness test subject, or a measure of the background impact to the sound rating of the imaginary test subject. Based on these implications, the SNR_{zl} can be used as another measure of the impact of the background unsteadiness. For instance, having large SNR_{zl} can be interpreted as the signal of interest being separated from the given measured background by the amount of the zero loudness threshold. Therefore, if the SNR_{zl} is large enough or meets certain

criteria, the background impact can be minimal as long as the loudness is utilized as a measure of the acoustic rating.

Previously, it was noted that large uncertainties that can significantly affect the test results were observed in Figure 5-4 and Figure 5-5. However, the use of the SNR_{zl} can in fact provide another perspective of the testing data in terms of its precision, if the loudness is used for the acoustic rating. If the SNR_{zl} is larger than $SNR^{UT,B}$ by a sufficient amount, such as an amount equal to the expanded uncertainty of the $SNR^{UT,B}$, the measurement can be considered to be valid for a loudness rating. Of special importance, the uncertainties associated with the SNR should differ from the uncertainties of the background correction factor, u_K, because the dimension of the uncertainties must be of the SNRs. Therefore, the sensitivity coefficient of the background correction factor *K*, s_K is not used for the SNR uncertainty. Instead, the sensitivity coefficient of the $SNR^{UT,B}$, s_{SNR}, is used for the expanded uncertainty, U_{SNR} of the background impact to the SNRs.

$$U_{SNR} = k\left|s_{SNR}\right|\sigma\left(L_p^B\right) \tag{5-10}$$

The coverage factor *k* is 1.96 for a 95% confidence, and if the sample size is insufficient, then the *k* value can be determined from other statistical distributions such as a Student's t-distribution [65]. The sensitivity coefficient of the $SNR^{UT,B}$, s_{SNR}, is unity because the first derivative of the $SNR^{UT,B}$ with respect to the background SPL, L_p^B, becomes 1. By using the standard deviation $\sigma(L_p^B)$ in Figure 5-6, the expanded uncertainty for the U_{SNR} can be obtained.

It can be concluded from the above discussions that the background impact can be negligible in Figure 5-8 in that the SNR_{zl} is larger than the expanded uncertainty U_{SNR}. In other words, the loudness of the measured sound emission of the test subject remains zero by the 95% confidence. In Figure 5-8, the first two bands show SNR_{zl} value larger than $SNR^{UT,B}$ value by varying amounts; however, the $SNR^{UT,B}$ were found to be larger than the prescribed limit, i.e. ISO 3741 minimum SNRs (6 dB). Therefore, the background correction factors *K* are not significantly affected by the background unsteadiness. Likewise, the frequency bands between 160 and 1,600 Hz band frequencies would not be affected by the background because of the sufficient $SNR^{UT,B}$, i.e. above the minimum SNR limit. In addition, non-zero loudness can be observed in these frequency bands. In contrast, at 1/3 octave bands between 2,000 and 10,000 Hz band frequencies, more incidents of having the SNR_{zl} larger than the $SNR^{UT,B}$ can be observed, and the differences between the two SNRs are relatively smaller (0-15 dB) than the SNR differences (up to 50 dB) in Figure 5-8. However, the measurements can still be valid for the loudness metric because the expanded uncertainty is usually less than 0.5 dB.

It should be noted that the data from the 200 fan tests presented herein serve as a real-world application example of using the methodologies investigated herein. As noted, challenging situations arising from poor SNRs are likely to happen in any field of acoustic testing. Implementation of the loudness metrics can be useful not only for the acoustic rating of sound sources operating closely associated with human occupants, but also useful for addressing issues from poor SNRs because of the zero loudness SNR.

Conclusions

This study investigated the impact of background noise variations on acoustical ratings by using a combination of test data from 200 fan units and test standard guidelines. When the sound of a test subject is measured in the presence of a background noise, the measured signal has to be corrected so as to eliminate background noise contribution. In order to correct the signal affected by the background noise, a logarithmic subtraction is performed by using an individually measured background noise which is the approach used in most standard acoustic protocols. However, when a testing environment experiences variations or fluctuations of background noises, the precision of the acoustic rating can be compromised. Therefore, the impact of background unsteadiness has to be addressed, which is the subject of the study herein.

Two methodologies are presented herein for evaluating the impact of the background variations, namely uncertainties and zero loudness SNRs. With regards to the first methodology, the uncertainty is determined from the sensitivity coefficients of the background corrections and standard deviations of the measured background noise. Using data from 200 fan units, it was found that the uncertainty becomes exceedingly larger when an SNR of a test subject and a background noise, $SNR^{UT,B}$, is low. For example, the expanded uncertainty increased over 4 dB when the SNR satisfied the minimum SNRs in the ISO Precision Method. Furthermore, low frequencies (50-80 Hz 1/3 octave bands) and high frequencies (over the 4,000 Hz band) were found to have large uncertainties over ±10 dB, for the 200 tests presented herein.

When loudness is used for the acoustic rating, another SNR metric, namely zero-loudness SNR, SNR_{zl}, can be used to evaluate the background impact on the acoustic rating, which is the second methodology. The zero-loudness SNR, SNR_{zl}, is defined as an SNR of imaginary sound source whose sound emissions is at the zero loudness threshold. Using data from 200 fan units, the SNR_{zl} at the low frequency bands (50, 63, and 80 Hz bands) were found to be larger over 35 dB, which means that background noise variations would not affect the loudness at these low band. Also, mid-frequency bands of 100-3,150 Hz showed decreasing trends of the SNR_{zl} ranging from 20-40 dB, which can still exceed the SNR limit set by the ISO Precision Method. Lastly, the SNR_{zl} at high bands (exceeding a 4,000 Hz frequency band) were in most cases between 10 and 20 dB, which is significantly lower than the low frequency SNR_{zl}.

The combined usage of both of the above methodologies, namely the uncertainties and the zero loudness SNRs, can be useful, especially if a test suffers from a low $SNR^{UT,B}$. Based on the results of tests of 200 fan units discussed in this study, the impact of the background was found to be negligible in the following scenarios.

1. When the uncertainties of the measured background is within the gap between the zero loudness SNR and the $SNR^{UT,B}$, and
2. When the zero loudness SNR is sufficiently large.

For example, the 200 fan test results presented in this study showed that the zero loudness SNRs were larger than the $SNR^{UT,B}$ by up to 40 dB, and the expanded uncertainty was less than 6 dB at low frequencies (up to the 80 Hz band). Furthermore, the uncertainty was reduced down to 0.5 dB at high frequencies over the 2,000 Hz band.

Based on the above discussions, the combined usage of both the uncertainty and the zero loudness SNR can provide more useful estimations of background variations and its impact on acoustic ratings, especially for low-to-medium sound emissions of test subjects.

CHAPTER VI

AN IMPACT OF AN IMPROVED PSYCHOACOUSTIC MODEL ON FAN LOUDNESS AND ACOUSTIC RATINGS

Overview

Loudness has been increasingly used as an acoustic rating for the built environment since its adoption in industrial standards and rating programs such as ASHRAE and Energy Star. The increasing usage of loudness is based on the fact that occupants in buildings are exposed to noise from ventilating fans in operational proximities. The current loudness calculation procedure based on ANSI S3.4-1980 is widely considered to be outdated because of its limited accuracy on equal-loudness contours, loudness-level-to-loudness conversions, and tonal components. This study investigates the real-world usage of a revised model introduced by Moore et al., which forms the foundation for the recent ANSI S3.4-2007, and the potential impacts from adopting this revised model by acoustic rating and certification programs. The major findings include: (1) a majority of tests under 2 sone have a larger loudness under the revised model, (2) for tests over 3 sone, the revised model resulted in either similar or less loudness, and (3) for Energy Star V4.0 for ventilating devices, about 0.5 sone differences are expected between the two models. Overall, this study suggests that improvements and revisions can be made to the current fan loudness protocol by replacing the conventional model with the revised model.

Introduction

The psychoacoustic terminology of loudness is defined as an auditory sensation on a scale extending from quiet to loud [91], and it has been widely used in the built environment sector since its introduction in the early 1990s as a methodology for acoustic rating in industrial standards [8, 9, 12, 92-94]. Moreover, loudness ratings, which are a numerical designation of sound strength measured in sone, are increasingly included in international and regional building codes and requirements in the U.S. [33, 95-97]. For example, the American Society of Heating, Refrigerating, and Air-Conditioning Engineers (ASHRAE) Standard 62.2 places a limit on sound emissions from mechanical ventilation devices with the most recent version specifying an upper limit of one sone for continuous ventilation devices (e.g., whole house fans) and 3 sone for demand-controlled mechanical exhaust fans (e.g., local fans in bathrooms and kitchens) [33]. Also, International Residential Codes, along with several U.S. state local guidelines, demand similar loudness limitations [95-97]. Of special importance for the U.S., Energy Star V4.0, in effect since October, 2015 demands no more than 2 sone for kitchen range hoods and 3 sone for bathroom ventilation fans [64].

Although loudness has been primarily used by audiologists and psychologists in the last century, the usage of the psychoacoustic quantity loudness (i.e., sone) for ventilation devices is acceptable as evidenced by being promoted by governmental and industry sectors in codes and guidelines [9, 33, 64, 95-97]. Typical residential air-conditioning fans or duct in-line blowers are somewhat isolated from humans making loudness less important; however, range hood fans and bathroom fans are neither concealed inside of

buildings nor isolated outside the building envelope. In fact, these two fan types are often installed and mounted within a few feet of human occupants so that limits on loudness are imperative. The reason for these installation practices is that fans of this type operate on demand with short fluidic entrance lengths between the fan and its inlet so as to provide instantaneous ventilation. Therefore, occupants in residential buildings are certainly susceptible to fan noise, at least for these two applications.

Until recently, the control of loudness has not been emphasized in residential ventilation standards and codes, with one of the reasons being that most of these residential ventilation fans are not capable of causing severe hearing damage. Nevertheless, fan noise can be tonal, discomforting, and disturbing to human communications and productivity. Therefore, fan evaluation and analysis studies in terms of loudness or psychoacoustic measures, which account for both acoustical noise emission and the human perception of them, are necessary in order to control fan sound quality or performance. In fact, the control of fan noise is an important issue for promoting Indoor Environmental Quality (IEQ).

Conventional loudness rating procedures for residential ventilation devices as presented and described in AMCA 301, HVI 915, the Energy Star Program, etc., are based on ANSI S3.4-1980 [8, 9, 19, 92], which is based on a psychoacoustic study conducted by Stevens [20, 98] almost five decades ago. Long before developing the above conventional procedures, Stevens proposed the unit sone for quantifying loudness in 1936, and suggested the fundamental concepts of loudness predictions by using power

law and equal loudness contours designated as the Mark VI and VII models, respectively [20, 98, 99], which in turn later became the foundations of ANSI S3.4-1980.

The procedures proposed by ANSI S3.4-1980 have proven to be effective for predicting broadband homogeneous spectra, especially in the mid-frequency region [21]. However, limitations on using this conventional procedure have been found over the several decades since the ANSI procedure was first implemented [22]. First, ANSI S3.4-1980 fails to give accurate calculations of tonal components, which are relatively prevalent in rotating machineries, such as air moving devices and fans [93].

Second, the loudness calculation procedure in ANSI S3.4-1980 is not based on the state-of-the-art human equal-loudness contours as found in ISO 226:2003 [100]. The use of outdated equal-loudness contours in ANSI S3.4-1980 has a broad impact on accurate and precise loudness determinations, especially because the equal-loudness contour is the backbone of the loudness calculation procedure.

Third, ANSI S3.4-1980 does not provide relationships between "loudness levels" in terms of a "phon and "loudness" in "sone" at least for the loudness levels less than 20 phon. Of special importance, "loudness levels" in terms of a "phon" refers to a sound level designed to describe sounds that are equally loud to the human-hearing perception. For example, a sound pressure level of 60 dB at 1,000 Hz is defined as 60 phon, and then equally loud sounds at other frequencies are measured as 60 phon [89]. Also of note, "loudness" in "sone" is different from "loudness levels" in phon in that the "loudness" is based on a linear scale of human loudness perception, which means 4 sone is twice as loud as 2 sone.

It should be noted that the 20 phon mentioned above, which is a lower limit of the loudness-level to loudness relationship in ANSI S3.4-1980, is far louder than the human hearing threshold of 2 phon (≈ 0.003 sone) [89], which means the conventional relationships are not suitable for near human hearing threshold.

Considering the fact that noise emissions of the modern residential ventilation devices have been reduced in recent years, the lack of a relationship between sone and phone near the hearing threshold is a critical issue. In order to address the lack of lower-loudness-range relationships between "sone" and "phon", AMCA 301 and HVI 915 have extrapolated the equal-loudness contours down to -0.02 sone. However, along with the revised equal-loudness contours in ISO 226:2003, the extrapolated equal-loudness contours in AMCA 301 and HVI 915 need revisions.

In order to address these deficiencies and discrepancies, Moore et al. developed the revised loudness models that are applicable to tonal components of sounds while providing more accurate "loudness-to-loudness level" conversions [101, 102]. More importantly, these modified models show good agreement with the modern equal loudness contours of ISO 226:2003 [103]. Because of these advantages, the newer loudness standard, ANSI S3.4-2007 is primarily based on the work by Glasberg and Moore [101], meaning a revised loudness model.

However, of special importance, the implementation of using ANSI S3.4-2007 in acoustic ratings of ventilations devices has not been considered to date by certification bodies or by the Energy Star Program. Likewise, the usage of this revised loudness

model by Moore et al. has not been completely accepted by many acoustic applications [104].

The reluctance of various entities from adopting the revised loudness model, even with its obvious improvements, is the prime motivation for the study reported herein. It is hoped that a real-world comparison of the two models that emphasizes and reveals the advantage of the revised model will promote the adoption of the revised model. Therefore, the focus of the research reported herein is to fully investigate the real-world differences between the new state-of-the-art revised loudness model and the conventional loudness model presently used for rating residential ventilating devices, such as fans.

In order to accomplish this task, a review of the two psychoacoustic loudness models is performed along with an analysis of their limitations, especially for the acoustic rating of fans. Because the loudness calculation procedure consists of psychoacoustic processes employing a series of filters dealing with human hearing perceptions, a review and evaluation of physiological and psychological models is provided herein. Finally, because fan loudness has been widely used for acoustic rating of fans by organizations, such as Energy Star, ASHRAE, etc., based on outdated ANSI S3.4-1980, which is based on the conventional loudness model. The impact of this new psychoacoustic model on acoustic ratings is also investigated and presented herein, based on acoustical test data from 394 fans.

The acoustic measurement and rating study herein are based on several standards, codes, and requirements, which were introduced and discussed above. These standards and codes are listed in Table 6-1, along with their name and purpose.

Table 6-1 List of codes and standard referred in the presented study

Code/Standard Designation	Code/Standard Title	Category	Description/Purpose	Reference
AMCA 301	Methods for Calculating Fan Sound Ratings from Laboratory Test Data	Standard (Procedure)	Acoustic testing standard for ventilation devices	[8]
ANSI S12.51	Acoustics - Determination of sound power levels of noise sources using sound pressure - Precision methods for reverberation rooms	Standard (Procedure)	Acoustic testing standard for reverberation method in general	[12]
ANSI S3.4-1980	Procedure for the computation of loudness of noise	Standard	Conventional loudness (sone) calculation procedure	[19]
ANSI S3.4-2007	Computation of Loudness of Steady Sound	Standard	Revised loudness (sone) calculation procedure	[93]
ASHRAE 62.2	Ventilation and Acceptable Indoor Air Quality in Low-Rise Residential Buildings	Code (Requirement)	Ventilation requirements for residential buildings	[33]
Energy Star V4.0 (Ventilation)	ENERGY STAR® Program Requirements for Residential Ventilating Fans V4.0	Code (Requirement)	Certification and verification program for ventilation devices	[64]
HVI 915	HVI® Loudness Testing and Rating Procedure	Procedure	Certification and verification program for ventilation devices	[9]
ISO 226:2003	Acoustics -- Normal equal-loudness-level contours	Standard	Standard for the revised equal loudness level contours	[100]

Overview of Loudness Calculation Procedures

Before comparing the loudness calculation procedures in each loudness model, it is necessary to identify model inputs. Free-field sound pressure levels, SPLs in a sound field region in which there are no adjacent reflecting surfaces, are obtained by either measurements in anechoic chambers or if using the reverberation method, then in reverberant chambers. The study herein utilizes the reverberation method by using measurements taken in a semi-reverberation chamber that was specifically built for HVAC device testing according to ANSI S12.51 [12]. The required test-setup and procedures are described in detail in HVI 915 [88, 105] with equipment, specifications, and uncertainties listed in Table 6-2. Of special importance, up-to-date certified calibrations are maintained for every instrument so that the uncertainty of the resulting sound data can be analyzed.

Table 6-2 Sound test instrumentation with uncertainties

Equipment Name	Description	Uncertainty
Microphones with preamplifiers	Sound pressure measurement in dB (15 – 148 dB(A), 3.15 – 20000 Hz)	±0.35dB
Reference Sound Source (RSS)	Generating reference sound (sound pressure level at 83.4 dB(A))	±0.54 dB
Data analyzer and data acquisition device	Performing frequency domain analysis (0 – 25.6 kHz, 5mV – 5 V RMS)	±0.10 dB
Voltage meter	Measuring and monitoring voltage (0-1000 V)	±0.068 V (up to $300V_{AC}$)
Tachometer	Measuring Fan RPM (5 – 999990 RPM)	±0.50 RPM

Because measured sound pressure levels in the semi-reverberation chamber can be characterized as combinations of free-field and diffuse-field sounds, the fan sound-power level (SWL) must be determined in order to obtain the free-field SPLs by following procedures in ANSI S12.51 and HVI 915 [9, 12, 88]. The comparison method, also known as the reference sound source method, for obtaining SWLs is characterized by the usage of a reference sound source (RSS) that generates broadband flat and loud noise spectrum along with a calibrated sound power levels. Using data input, the following Eq. (6-1) is then used to obtain SWLs for the test subjects (i.e., fans), L_{wf}.

$$L_{wf} = L_{pf} + L_{wr} - L_{pr} \tag{6-1}$$

where L_{pf} is the SPL of the test subject, L_{wr} is the SWL of the test subject RSS, and L_{pr} is the SPL of the RSS. Next, the SWL of the test subject is converted to the free-field SPL by using Eq (6-2) that follows.

$$L_{p'} = L_{wf} - \left| 10 \log \frac{Q}{4\pi r^2} \right| \tag{6-2}$$

where $L_{p'}$ is a representative sound pressure level of a fan at a1.52 meter (5 feet) distance, Q is a directivity factor, which corresponds to 1.0 for the spherical free field and 2.0 for the hemispherical field, and r is a distance in meters from the sound source, where r=1.52m (5 feet).

Of special note, AMCA 301 and HVI 915 differ from each other with regards to the assumption used for the free-field. The procedures of AMCA 301 assumes a hemispherical free-field, while HVI 915 and Energy Star V4.0 assume a spherical free-field with all having the same representation length of 1.52 m (or 5 ft). For the study

reported herein, the hemispherical representation of SPLs as presented in AMCA 301 for the free field is used as mandated by the AMCA standard.

Based on the free-field SPL calculations in Eqs. (6-1) and (6-2), an evaluation comparison of the two loudness models is performed and presented herein [98, 102] with each model designated as follows.

- The Conventional Loudness Model refers to the model by Stevens, specifically Mark VI [98], introduced in 1961, and used in AMCA 301, ANSI S3.4-1980, ASHRAE 62.2, Energy Star V4.0 (Ventilation), and HVI 915 [8, 9, 19, 33, 64] as listed in Table 6-1.
- The Revised Loudness Model refers to the model by Moore et al. [102] introduced in 1997, and used in ANSI S3.4-2007 as listed in Table 6-1.

The procedures and methodologies for both the Conventional and Revised Loudness Models will later be used to obtain fan loudness ratings for 394 residential ventilation fans including bathroom fans, range hoods, and utility fans. All measurement data was processed through data-mining and post-processing by using custom-made programs in Matlab and R (a statistical programming language).

Conventional Loudness Model by Stevens and ANSI S3.4-1980

As noted in the Introduction, the Conventional Loudness Model for ventilating devices, which is widely used to date is based on the Steven's model and ANSI S3.4-1980. The procedure to determine loudness takes place in two major steps, namely looking up loudness-indices, N, and then summing them for the total loudness, N_t. The first step, looking up loudness-indices, is obtained by looking up equal-loudness

contours for each SPL in 1/3 octave bands. Figure 6-1 is a color contour of the HVI 915 equal loudness contour used for the study presented herein [8, 9, 98]. Of special interest, the contour in Figure 6-1 reflect data points presented in HVI 915 [9], which is originally 1/3 octave tabulations ANSI S3.4-1980 [19]. Specifically, the 1/3 octave band loudness indices are obtained by looking up the equal-loudness contours for each 1/3 octave band (abscissa) and each SPL (ordinate) obtained from Eq. (6-2).

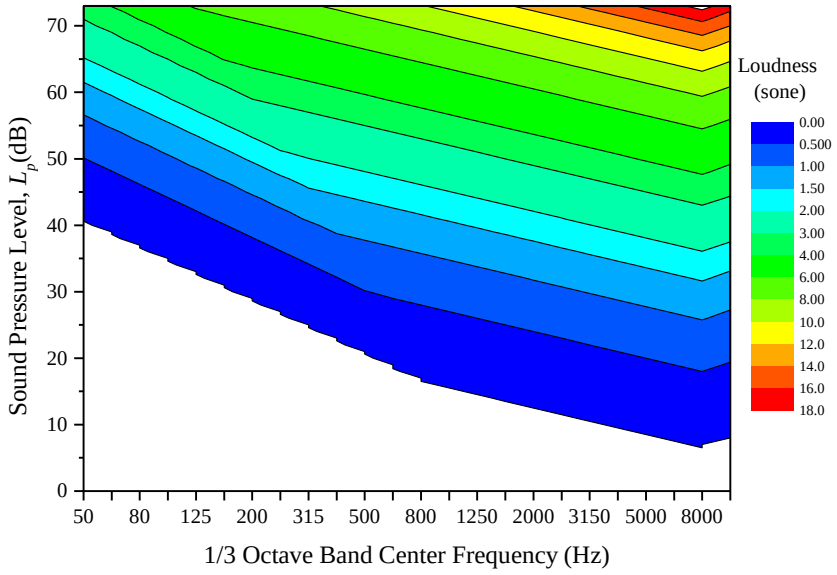

Figure 6-1 Contour mapping of the 1/3 octave band loudness (Conventional Model) used in the study reported herein [8, 9, 19]

Then, the total loudness is determined by a summation of loudness, which is expressed by the following expression.

$$N_t = N_m + F\left(\sum N - N_m\right) \tag{6-3}$$

, where N_t is the total loudness rating in sone, F is a loudness weighting factor, N is a loudness index for each frequency spectrum, and N_m is the maximum loudness index. The loudness weighting factors, F, depends on the bandwidth used in the analysis of the noise, namely, F=0.15 for one-third octave bandwidths, F=0.2 for half-octave bandwidths, and 0.3 for octave bandwidths.

Revised Loudness Model by Moore et al. and ANSI S3.4-2007

An obvious difference between the Revised Loudness Model by Moore et al. compared to the Conventional Loudness Model is that the Revised Model is mathematically more sophisticated in that several steps of iterations required to determine loudness. Another important difference is that equal loudness level contours are replaced by a series of mathematical expressions. Before presenting mathematical formulations, it is useful to introduce the four major processes that characterize the loudness model by Moore et al. [93, 101].

1. Modeling signal transfers from the outer ear to the middle ear by two transfer functions, namely an outer-to-eardrum transfer function and an eardrum-to-middle ear transfer function
2. Transformations from the middle-ear sound spectrum to excitation patterns of basilar membrane in the human cochlea.
3. Transformations from excitation patterns to specific loudness.
4. Determinations of total loudness by integrating specific loudness over the measurement frequencies.

Detailed calculation procedures representing each of the above four processes are covered in detail by ANSI S3.4-2007 and other literatures [93, 101, 102] with highlights presented for the purposes of this study in subsections that follows.

Modeling Outer-ear to Middle-ear Transfer Functions

The first two steps are easily implemented by applying two predetermined transfer functions, where inputs are the sound pressure levels reaching the human ear (or a microphone). One of the functions of the human outer ear is gathering sound (or noise) impinging on human ears and then amplifying the sound. As such, the sound reaching an eardrum (the tympanic membrane) has a signal gain of about 15 dB at 2,500 Hz. Then, sound experiences attenuations through the eardrum and auditory ossicles, which consists of three tiny bones, namely the malleus, incus, and stapes. Figure 6-2 shows the signal gains or the attenuations through these two transfer functions in the free field. It should be noted that the net output gain of SPL at 1,000 Hz is set to zero as a reference, which also means that the 1,000 Hz tone presented in the free field will have the same effective SPL that reaches the cochlea, which is the sensory organ of hearing inside the human inner ear [106].

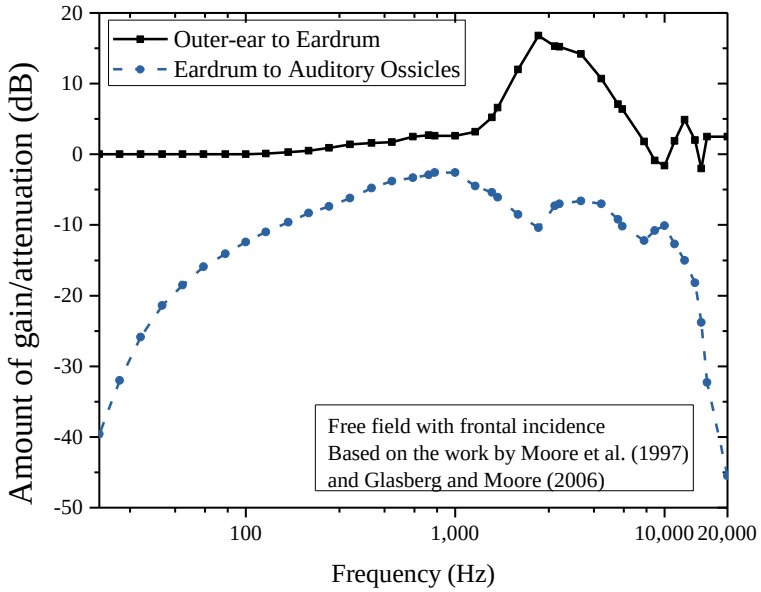

Figure 6-2 Transfer functions of the outer-ear-to-eardrum (solid line) and the eardrum-to-auditory ossicles (dashed line) at acoustic free field with frontal incidence condition [101, 102]

Transformations from the Middle-ear Sound Spectrum to Excitation Pattern

It is known that the sensitivity of the human hearing is non-linear over the entire audible frequency range [89, 107] even though the conventional loudness model assumes linearity, and the implementation of this non-linearity for the revised loudness model is achieved by introducing of auditory filters, which is a set of filters having specific bandwidths. The general concept of auditory filters is that two different tones can interfere with each other if these two tones overlap their filter bandwidths [89]. In order to model the auditory filter, Glasberg and Moore introduced an equivalent rectangular bandwidth (ERB), which is formulated as a function of the center frequency f_c of the frequency band as follows [101, 102].

$$ERB = 24.673\left(0.004368 f_c + 1\right) \tag{6-4}$$

The transformation process from the middle ear sound spectrum to an excitation pattern is triggered by the sensory selectivity of sounds primarily due to the shape of the basilar membrane [108], which is referred to as masking. The masking process is implemented in the revised loudness model discussed by introducing weighting functions, *W(g)*, for the auditory filters.

$$W\left(g\right) = \left(1 + pg\right)e^{-pg} \tag{6-5}$$

where g and p are determined by

$$g \equiv \frac{f - f_c}{f_c} \tag{6-6}$$

$$p \equiv \frac{4 f_c}{ERB} - 0.01155\left(x - 51\right) \qquad \text{if } f < f_c \tag{6-7}$$

$$p \equiv \frac{4 f_c}{ERB} \qquad \text{if } f > f_c \tag{6-8}$$

where f is frequency for entire input spectrum, and x is the SPL per each ERB, which is obtained by integrating SPLs for a given bandwidth of ERB. As can be seen in Eqs. (6-7) and (8), p is a dependent variable in terms of independent variables f_c and x. Once the weighting function *W(g)* is determined for each f_c, then the weighting function *W(g)* is applied to entire domain of ERBs, which results in the excitation pattern E for each *ERB*. Of special interest, the process of obtaining excitation patterns by using the weighting function essentially means a masking effect in a psychacoustical sense, which is defined as concealment or screening of one auditory sensation by another.

Transformations from Excitation Patterns to Specific Loudness

The excitation pattern E is transformed to a specific loudness N'. Because the conversion process inherently incorporates the mathematical expressions of the equal loudness contours [101], several sets of equations in terms of the non-linear coefficients are necessary. For example, the Revised Model consists of three different equations, which are chosen by the amount of the excitation pattern E obtained from the previous step at each ERB, with E being in units of linear power rather than in dB units. Equations are presented for three different E regions characterized as follows.

1. E is smaller than human hearing threshold E_{THRQ} (i.e., $E< E_{THRQ}$)
2. E is larger than the human hearing threshold E_{THRQ} but smaller than 10^{10} sone/ERB (i.e., $E_{THRQ}< E <10^{10}$)
3. E is larger than 10^{10} sone/ERB (i.e., $E >10^{10}$)

Moore et al. and ANSI S3.4-2007 provides mathematical formulations in detail [93, 102]; however, the study herein presents only the general mathematical formulation to determine the specific loudness N'.

$$N' = 0.046871F(E)\left[(GE + A)^{\alpha} - A^{\alpha}\right]^{\beta} \tag{6-9}$$

where G represents the low-level gain of the cochlear amplifier, which is determined by the ratio of E_{THRQ} at 500 Hz and E_{THRQ} at the given center frequency. The parameter $F(E)$ in Eq. (6-9) is defined as a function of E for the three different regions presented earlier as follows.

$$F(E) \equiv \left(\frac{2E}{E + E_{THRQ}} \right)^{1.5} \quad \text{if } E < E_{THRQ} \tag{6-10}$$

$$F(E) \equiv 1 \qquad \text{if } E_{THRQ} < E < 10^{10} \tag{6-11}$$

$$F(E) \equiv \left(\frac{E}{1.0707} \right)^{0.2} \qquad \text{if } E > 10^{10} \tag{6-12}$$

In Eqs. (6-10) through (6-12), two empirical parameters, α and A, need to be determined by tabulated relationships along with the low-level gain G of the cochlear amplifier as found in Moore et al. [93, 102]. Lastly, the exponent β is 1 if E is less than 10^{10}, and 0 if E exceeds 10^{10}.

Determinations of Total Loudness by Integrating Specific Loudness

As a final step, the total loudness N_t is obtained by the integration of the specific loudness N' over the ERB number N_{ERB} domain (i.e. summation of $N' \cdot \Delta N_{ERB}$), where N_{ERB} is defined below.

$$N_{ERB} = 21.366 \log_{10} (0.004368 f_c + 1) \tag{6-13}$$

Comparison of Loudness Contours for the Two Models

As noted earlier in the Introduction, the two models are based on fundamentally different equal-loudness contours. The contours of the Conventional Model are based on the Stevens Mark VI model, which is also used for conventional fan acoustic ratings [98, 109, 110]. In contrast, the Revised Model by Moore et al. does not explicitly provide the equal loudness contour; rather, a series of mathematical expressions in Eqs. (6-4) through (6-13) that are inherently based on a set of revised equal loudness contours are used. Glasberg and Moore pointed out that the model reflects the most recent equal

loudness contours, namely the ISO 226 [101]. Therefore, in this study, using a reference source containing contours, namely ISO 226, is appropriate for the comparisons of equal loudness contours.

As a graphical comparison, the two equal loudness contours, namely ISO 226:2003 (revised) and the Stevens Mart VI (conventional) used in ANSI S3.4-1980, HVI 915, AMCA 301 are shown in Figure 6-3 [8, 9, 19, 100].

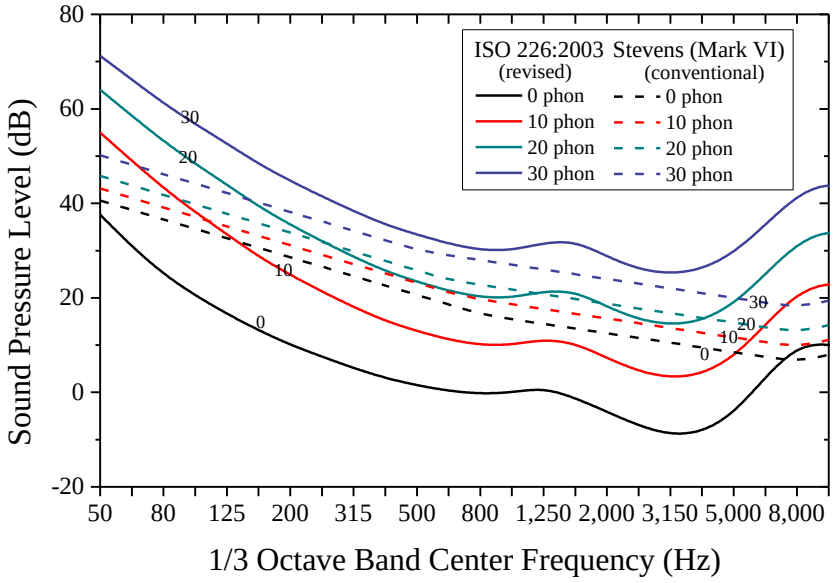

Figure 6-3 Equal loudness level contour for ISO 226 and Stevens Mark VI

Of special importance, the unit for comparisons in Figure 6-3 is the phon, representing a loudness level, rather than a sone, representing loudness, because the ISO 226 contour is plotted with the unit phon rather than sone. The comparisons by using the loudness level in phon is justifiable because the loudness in sone can vary with different

types of acoustic fields (free field, diffuse field, etc.) and listening/measurement conditions (monaural or binaural and head or microphone, etc.) [93, 101]. The differences are clear in Figure 6-3, which includes linear (Stevens, conventional) and non-linear (ISO 226, revised) shapes of the contours, the thresholds of zero loudness level, and the slopes. As such, several observations that illustrate major differences between the two contour maps in Figure 6-3 are as follows.

1. Zero-loudness-level threshold: the zero-loudness-level threshold of the Stevens Mark VI are generally higher than the threshold of the ISO 226, except for high 1/3 octave bands exceeding the band frequency of 8,000 Hz. The difference can be about 10 dB in a majority of bands and even up to 20 dB. Therefore, major discrepancies in calculated total loudness based on each model are expected near the zero-loudness or zero-loudness-level.

2. Shape of the contours: Because the Stevens Mark VI model was developed based on the power law proposed by Stevens [98, 110], the shape of the contours are linear in the decibel scale. In contrast, slopes of the ISO 226 contours represent the highly non-linear nature of the human hearing perception, so that there are local maxima or minima in multiple points around 1,250 and 10,000 Hz. In contrast, the contour by Stevens are generally linear having three different slopes. These different shapes result in overlaps and intersections of the two contours. For example, two 20 phon contours from ISO 226 and Stevens Mark VI overlap each other between 315 and 3,150 Hz because of nonlinearities.

3. Contour spacing: for loudness levels from 0 to 30 phon, the spacing of ISO 226 is significantly wider than the spacings of the conventional fan loudness contour. This can result in i) increases in loudness levels in mid-frequency ranges from 160 to 6,300 Hz for loudness levels lower than 10 phon, and ii) overall loudness-level reductions for loudness levels over 30 phon, if the ISO 226 is implemented instead of the Stevens Mark VI.

As an aside, it is worth noting that loudness levels in phon are similar to associated SPLs at 1,000 Hz for the ISO 226 while the Stevens are slightly off by 3 dB. Therefore, overall discrepancies over 3 dB are expected when the loudness level in converted from SPLs for the two models.

Loudness Level (phon) and Loudness (sone) Conversion Comparisons

Another important comparison to be made between the models is conversions between loudness levels (phon) and loudness (sone). The loudness level is more useful for comparing the equal loudness contours and SPLs of pure tones [111] because loudness (sone) can vary depending on underlying assumptions. Specifically, loudness can be different for the same loudness level with respect to the acoustic field measurement/listening conditions, etc. Traditionally, the relationship between the loudness level (phon) and the loudness (sone) was determined based on a power law, where a 10 phon increase results in a loudness increase twice as much [89, 98] as formulated below.

$$N = 2^{(M-40)/10} \tag{6-14}$$

, where *N* and *M* are loudness (sone) and loudness level (phon). As can be seen in Eq. (6-14), the reference loudness level is 40 phon, and the relationship is expected to be precise around 40 phon and over. However, a number of researchers have pointed out that the power low may not provide precise relationship for human hearing perceptions especially below 20 phon while the relationship asymptotically converges to the power law around 40 phon [111-113]. More precise relationships have been suggested by groups of researchers including Moore et al., which was also adopted by the revision of ANSI S3.4 [106]. Figure 6-4 shows these two relationships, namely the relationship from Stevens Mark VI (ANSI S3.4-1980) and the relationship from the collective work by Moore et al. (ANSI S3.4-2007), for loudness level (phon) and loudness (sone) [19, 89, 93, 106, 111-113].

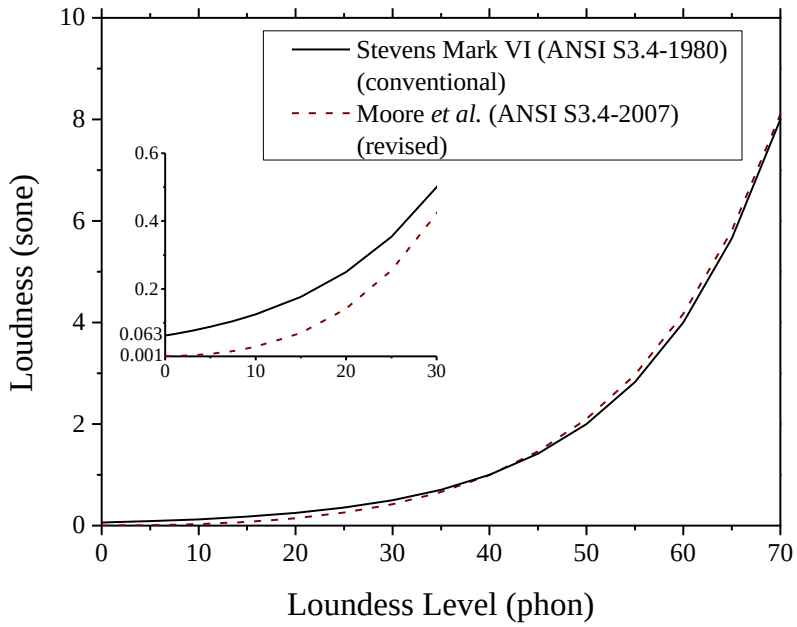

Figure 6-4 Comparisons of relationships between loudness level (phon) and loudness (sone) with inset showing zoom-in for lower loudness levels of 0-30 phon

As noted, these two relationships intersect each other at 40 phon, which is a reference point for the loudness level and loudness conversions, however, relationship trends are different from each other. For loudness levels less than 40 phon, the relationship by Moore *et al.* shows lower loudness for the same loudness level compared to the relationship from the Stevens Mark VI. Of special importance, the two relationships at values less than 15 phon, which is highlighted in the inset of Figure 6-4, show the largest discrepancies with the ANSI S3.4-2006, which is up to 0.1 sone. When considering the fact that the psychoacoustic term loudness represents a linear scale to human hearing perception, having about 0.1 sone at such low loudness levels (less than 15 phon) may not be a negligible discrepancy. However, the loudness level is a secondary output while loudness is directly obtained from the calculation procedure in Eqs. (6-4) through (6-13) of the Revised Loudness Model. Therefore, when it comes to the acoustic rating for ventilation devices (i.e., fan loudness), the conversion from the loudness level to loudness should not be a critical issue.

Comparisons of Loudness Models by Using Fan Testing Data

Because sound emissions from fans are characterized as broadband noise with tonal components, the equal loudness contours presented in the earlier section can only reveal limited information when calculating total loudness. It is primarily because of a physiological process that the human cochlea transforms input sound spectrums transmitted from a middle ear into a bundle of excitation patterns. In the Revised Model, the entire sound spectrum affects a single excitation pattern at each *ERB*, which is a function of center frequencies f_c as implemented in Eqs. (6-4) and (6-5). In contrast, the

Conventional Model by Stevens incorporate equal loudness contours, which results in a limited capability for incorporating excitation patterns compared to the Revised Loudness Model [22, 114]. The above differences between the two models are made more obvious as sound test data from 394 fans are used to determine acoustic ratings and the results from the two methods are compared.

Statistical Makeup of Fan Testing Data—Conventional Method

Before conducting a direct comparison of two loudness models with measured data, the fan database for the 394 fans tested herein was analyzed for the conventional method, which is appropriate considering that this is the accepted approach presently used in acoustic rating standards, codes, and guidelines. Figure 6-5 shows histograms of loudness (sone) determined by using the Conventional Loudness Model and measured SPLs for the 394 fans experimentally tested in the reverberation room for this study.

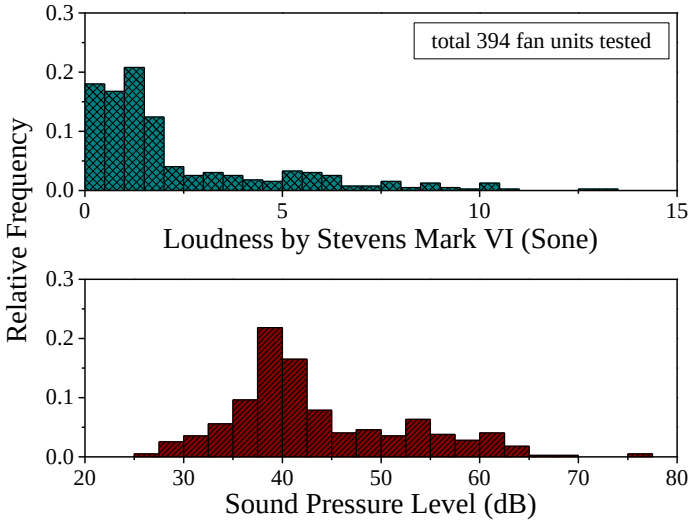

Figure 6-5 Histograms of loudness determined by the Conventional Model and measured sound pressure levels

As can be seen in Figure 6-5, about 70% of the fans tested had a loudness of less than 2 sone and less than 45 dB SPL. This conventional loudness range of less than 2 sone is an important range for bath fans and range hoods because 1). most modern residential ventilation fans have begun to generate fan noise values of less than 2 sone in only the last decade with decreasing loudness in each year [88], and 2). the loudness range of 0-2 sone is the allowable loudness range for Energy Star V4.0 certification for ventilation devices [64]. Therefore, a loudness range less than 2 sone is critical and relevant for this analysis.

Fan Data Loudness Comparisons for the Revised and Conventional Models

Just as the Conventional Model was used in the previous section, the Revised model was used to acoustically rate the 394 fans where sound test data was available. A direct comparison of the two loudness models is presented in Figure 6-6 with the diagonal line representing the cases where the two loudness models produce the same results. As observed previously in Figure 6-5 for the Conventional Model, most of data points are located in the low loudness region, with the number of data points becoming fewer with increasing loudness. At first glance, it would appear that the overall data points in Figure 6-6 are distributed along with diagonal line, which represents similar loudness despite a few deviations from the diagonal line. However, some differences exist as discussed below.

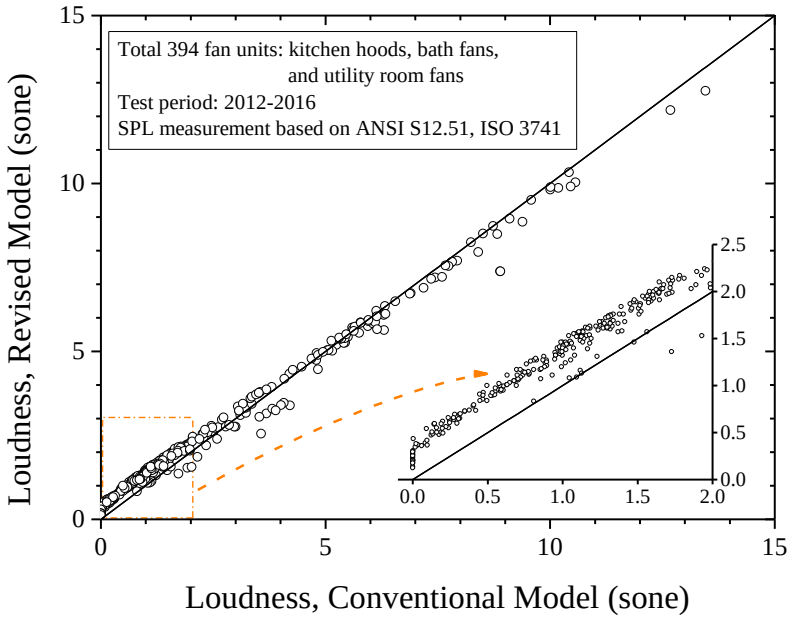

Figure 6-6 Comparison of the calculated loudness based on two loudness models, the Conventional Model by Stevens and the Revised Model by Moore et al

It should be noted in Figure 6-6 that fan loudness has been plotted up to 15 sone, which can be considered to be a large loudness for residential ventilation devices [88]. Even though data points in Figure 6-6 show a similar calculated loudness between these two models, meaning an alignment along the diagonal line, the scale up to 15 sone may distort this observation. In order to aid the understanding of differences between the two models, Figure 6-7 is a plot of loudness differences with respect to the loudness calculated by the Conventional Model for the 394 fans tested herein. The differences plotted in Figure 6-7 is simply an arithmetic loudness difference between the Revised Model by Moore et al. and the Conventional Model by Stevens. As an aside, a linear

regression line and its associated R^2 value is determined for the data plotted in Figure 6-7 as follows.

$$y = 0.40 - 0.086x$$
$$R^2 = 0.55 \tag{6-15}$$

, where R^2 is defined below.

$$R^2 \equiv 1 - \frac{\sum (y_i - f_i)^2}{\sum (y_i - \bar{y})^2} \tag{6-16}$$

with y_i, $\bar{y}_i$, and f_i mean revised loudness, average revised loudness, and estimated revised loudness by the regression, respectively.

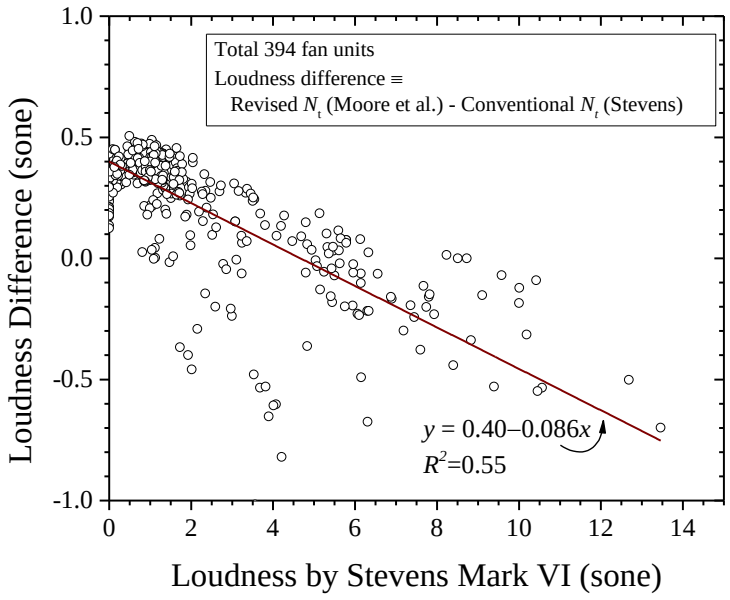

Figure 6-7 Loudness differences between the Conventional Model and the Revised Model for 394 fans tested

It should be noted that even though the regression line in Figure 6-7 shows an overall linear trend, the low R^2-value represent a significant amount of deviations from the regression line for many data points. Furthermore, different trends can be locally observed with respect to several ranges of conventional loudness in Figure 6-6 and Figure 6-7 as follows.

1. For data points having 0 sone by the Conventional Model, the loudness based on the Revised Model by Moore et al. shows a larger (i.e., non-zero) loudness of over 0.1-0.5 sone.

2. For data points less than 2 sone for the conventional loudness, which was pointed out earlier as a critical loudness range for acoustic ratings, the plots show a relatively consistent increase in the Glasberg and Moore loudness of about 0.4 sone. A few instances of the same or lower revised loudness can occasionally be observed in Figure 6-6.

3. Between 3 and 6 sone, loudness calculated by these two models are more aligned to the diagonal line, which means similar loudness between the two models. In Figure 6-7, about 40 percent of the data points are found to exhibit a lower revised loudness than the conventional loudness between 3 and 6 sone.

4. Over 7 sone, about 90% of the revised loudness values were lower than the loudness calculated by the Conventional Model.

All of these observations are consistent with the major findings from the earlier comparison of the equal loudness-level contours in Figure 6-3. Because the improved

equal-loudness-level contour (i.e., ISO 226:2003) has lower zero loudness-level threshold, increases in loudness were anticipated near hearing thresholds when the Revised Model by Moore et al. is implemented. Also, it was originally noticed in Figure 6-3 that the narrower spacings of the Stevens equal-loudness-level contours have resulted in revised loudness level being less than the conventional loudness level over 30 phon. This observation is consistent with the negative loudness difference shown in Figure 6-7, which means loudness by the Revised Model is generally less than loudness by the Conventional Model at values over 4 sone based on the conventional loudness.

Variations in Loudness Due to Tonal Components

As noted in Figure 6-7, considerable amounts of revised loudness variations exist for the same conventional loudness. The loudness variations are responsible for the different excitation patterns developed for each test, which is not readily achievable for the Conventional Model.

If fan sound is either a flat spectrum or highly tonal, which represent the two extremes of sound patterns, then these may result in a different loudness because the human ear perceives the characteristics of the sound differently. As previously noted in the Introduction, the Conventional Loudness model fails to explain tonal components over wide range of sound spectrum. In order to investigate the influences of different acoustic signatures, Figure 6-8 shows comparisons of two different flat or tonal acoustic signatures, namely Test A (flat) and Test B (tonal) with each having a similar loudness of 2 sone when the Conventional Model is used.

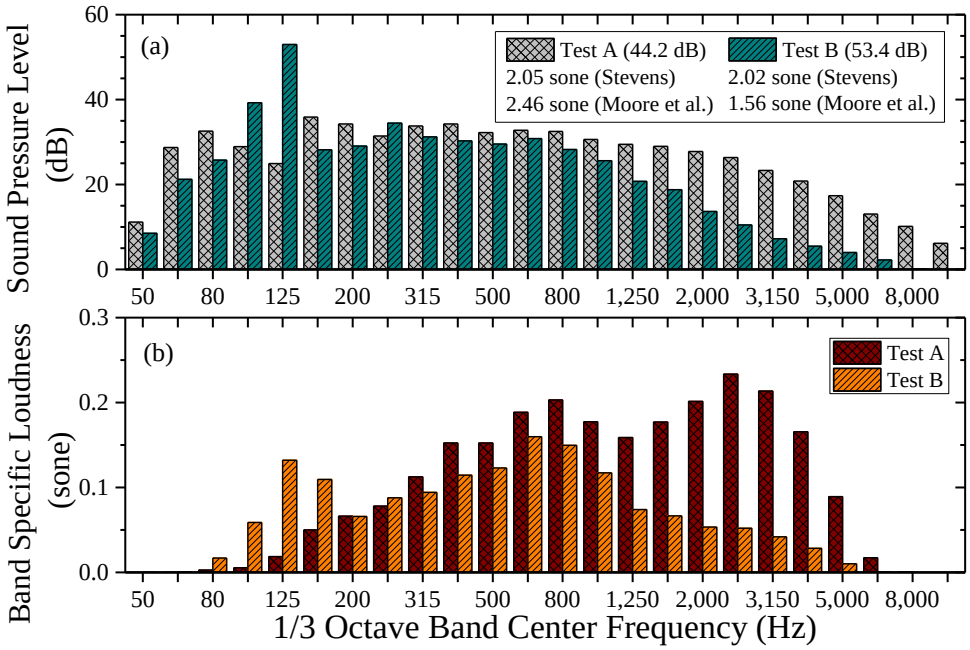

Figure 6-8 Acoustic signatures of the two different tests having the similar Stevens loudness in terms of (a) sound pressure levels and (b) 1/3 ocatve band specific loudness

The upper figure in Figure 6-8 presents the sound pressure levels for the two different tests, and the lower figure presents the band specific loudness for the same two different tests. As can be seen in Figure 6-8(a), the Test A shows relatively continuous noise spectrum while tonal components are prevalent in the Test B. When the Revised Loudness Model is implemented for Test A and Test B, the resulting total loudness are 2.46 and 1.56 sone for Test A and Test B, respectively, even though these two tests showed similar loudness, 2.05 and 2.02 sone, respectively, by the Conventional Model. These differences are clear evidence that the revised model can account for tonal components in a way that the conventional cannot.

The 1/3 octave band specific loudness in Figure 6-8(b) provide further insight to the loudness difference in the two tests. As noted, the Test A, which has a relatively flat spectrum compared to Test B, has an overall larger specific loudness at high frequency bands over 1,000 Hz, which caused the larger loudness than the loudness of Test B when the Revised Model is used. Even though the tonal components at 125 Hz band are prominent in the sound pressure scale in Figure 6-8(a) for Test B, the impact to the overall loudness was limited to the lower frequency range, which also has a lower sensitivity to the human hearing perception as can be seen in Figure 6-3 [89, 100].

The finding in Figure 6-8 with regards to the tonal components is consistent with aforementioned limitations of the Conventional Model, which was discussed earlier in the Introduction section [22, 114]. Specifically, despite the overall increased loudness trend near around 2 sone as seen in Figure 6-6 and Figure 6-7, the loudness of the tonal components (i.e., Test B) showed lower loudness by the Revised Model compared to the Conventional Model. Because the total loudness is a function of multiple variables including frequency, ERB, input noise spectrums, etc., as noticed in Eq. (6-9), it is difficult to ascertain that the tonal components can either over-predict or under-predict the total loudness when the Conventional Model is used. However, large discrepancies can exist when the tonal components are prevalent in measured sound signatures.

Potential Impact to Acoustic Rating Programs

For residential ventilation devices, two major acoustic rating requirements are used nationwide in the U.S., namely in ASHRAE 62.2 and Energy Star V4.0 [33, 64, 95-97]. The following outlines loudness requirements of these two programs.

- ASHRAE 62.2-2013: loudness should be no more than 3.0 sone for ventilation devices operating on-demand whose volume flow rates are equal to or less than 400 ft^3/min (or 200 L/s). Also, the loudness of whole-building ventilation devices should not exceed 1.0 sone.
- Energy Star V4.0: range hood ($\leq$ 500 ft^3/min or 236 L/s) loudness should be a maximum of 2.0 sone while bathroom and utility room fan loudness should be less than 2.0 sone ($\leq$ 200 ft^3/min or 95 L/s) and 3.0 sone (over 200 ft^3/min or 95 L/s).

As an aside, several U.S. state regulations include residential-building ventilation requirements that are the same as ASHRAE 62.2-2013 [95-97]. As can be seen for these loudness requirements, loudness ratings of 1.0, 2.0, and 3.0 sone representing critical points are of great importance. However, the bathroom fans and the utility fans in the study herein do not exceed 200 ft^3/min or 95 L/s, and the 2 sone was considered as the Energy Star limit.

Interpretation of the Variation Based on Codes and Criteria

The earlier sections showed that larger loudness values were observed with having relatively constant differences between the Conventional and Revised Model, especially between the 0 and 2 sone range. In order to investigate possible impact on the acoustic rating by implementing the new loudness model, it is necessary to look into the statistics of the distributions of the loudness in Figure 6-6. As such, Figure 6-9 shows distributions of the Glasberg and Moore loudness deviations from the conventional fan loudness. The right hand side of Figure 6-9 shows the box plots of the loudness by the Revised Model for 0.1 sone increments on the vertical axis, and the figure on the left

hand side shows the overall distributions of the loudness differences between two models for the conventional fan loudness under 2.0 sone.

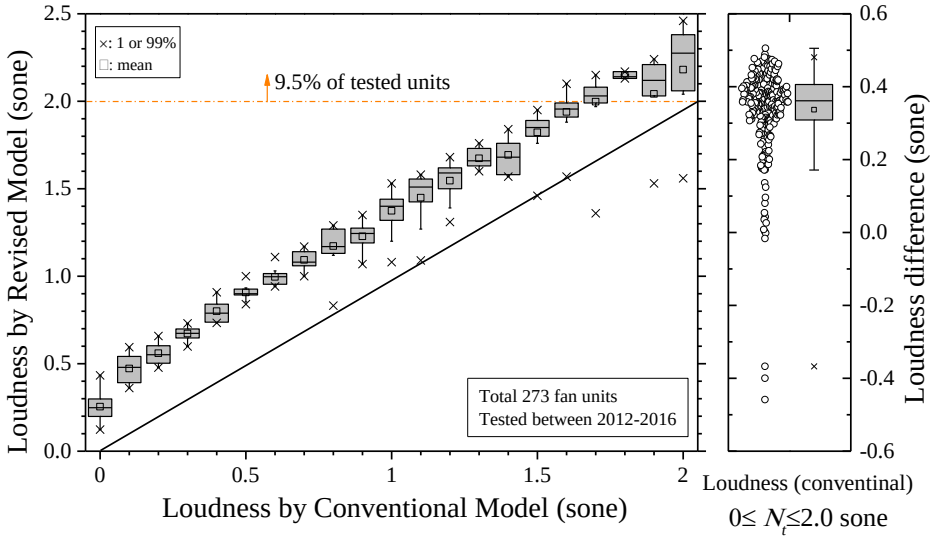

Figure 6-9 Box plots of the revised loudness between 0 and 2 sone of the conventional loudness (left), and distributions of loudness differences between the two models under conventional 2 sone (right)

Before relating the results in Figure 6-9 to impacts on acoustic rating programs, it may be useful to point out several statistical observations in Figure 6-9. For example, the medians (horizontal lines inside the box) and the averages (small squares) are generally increasing as presented earlier in Figure 6-6 discussions. It is also interesting to note is that the 99 percentiles marked as 'x' in Figure 6-9 are on the upper whiskers, which are vertical lines outside of each box representing data points away from the third quartile (Q3) by the amount of the interquartile range (IQR), i.e., Q3+IQR. This trend is unusual considering the fact that regions outside of whiskers are usually considered as outliers

[115], and therefore the largest loudness in each box plot in Figure 6-9 cannot be considered as outliers. In contrast, outliers can be observed at the lower end of box plot in Figure 6-9. As discussed in the previous section, different acoustic signatures that contain tonal components may result in these data points outside of a majority of the data.

Energy Star Loudness Requirement Based on Revised Model

When it comes to acoustic rating programs, any fan loudness that exceeds the current requirements mandated by ASHRAE, Energy Star, and local state regulations can is of concern for those that design and manufacture fans in that fan models that exceed specified loudness limits are considered to fail certification. In Figure 6-9, about 9.5% of fan tests that satisfied the conventional 2.0 sone limit were then found to be over 2.0 sone when the Revised Loudness Model was implemented. This result can be interpreted to mean that for this fan database about 10% of the fans tested would be found to fail the specified criteria if the Revised Model were added to codes and standards.

An important question is that if the Revised Model is implemented, would it be necessary to change loudness limits in the codes and standards. The largest revised loudness in Figure 6-9 was found to be 2.46 sone while the largest conventional loudness was 2.0 sone. Considering that even the largest differences in Figure 6-9 are not considered to be outliers based on previous discussions, it would seem that acoustic rating programs can accommodate a limit increase to requirement for the Revised Model. For example, the current requirement of 2.0 sone in the Energy Star Programs might in fact be equivalent to a revised requirement of 2.5 sone for kitchen range hoods

and bathroom fans. However, a mismatch might still exist in that some fans could meet the revised requirements of 2.5 sone while exceeding the conventional loudness limit of 2.0 sone. For the 394 fan tests herein, five (5) tests were found to have less than 2.5 sone with the Revised Model although their Stevens loudness ratings exceed 2.0 sone, which means 1.25% of the fans are in this category. Table 6-3 shows these five test results that exceed 2.0 sone for the acoustic rating (i.e., conventional loudness) while still satisfying the revised loudness being less than 2.5 sone.

Table 6-3 A list of tests which exceeded the conventional 2.0 sone (Stevens), with the revised loudness being less than 2.5 sone

Test designation	**Type**	**Conventional Loudness (sone)**	**Revised loudness (sone)**	**Sound Pressure Level (dB)**
C	Bath	2.2	1.9	43.2
D	Bath	2.3	2.4	45.5
E	Range hood	2.2	2.4	46.2
F	Range hood	2.3	2.2	47.8
G	Range hood	2.6	2.4	47.0

One way to view these 5 tests is that fans that fail the certification based on the conventional loudness criteria of 2.0 sone would in fact pass a revised loudness criterion of 2.5 sone. Another observation of Table 6-3 is that three tests out of five tests resulted in lower revised loudness than the conventional loudness when the Revised Model was implemented. These three tests are in contrast to data seen in Figure 6-7 where a majority of tests were observed to have positive loudness differences for the

conventional loudness between 2 and 3, meaning the tests in Table 6-3 represent a minority of the data points in Figure 6-6 and Figure 6-7 by having smaller positive differences (Tests D and E) or even lower loudness with the Revised Model (Tests C, F, and G).

It can be said with certainty that the revised model by Moore et al. overcomes several aforementioned limitations of the Conventional Model by incorporating sophisticated modeling of the human hearing perception, which resulted in variations of the loudness along with trends observed in Figure 6-6. However, a clear delineation between the models is not readily available in that some overlap or disagreements are likely to exist, such as data points in Table 6-3. This lack of a well-developed relationship between conventional loudness and revised loudness means that the limits of 2 and 2.5 sone discussed above are for illustration purposes only, and setting actual limit values would require a more detailed study.

As a final note, it is important to recognize that psychoacoustic loudness is based on the fundamentals of human hearing unlike weighted sound ratings such as dB(A) or NC [62, 68]. As a result, growing number of studies [116-119] have supported the fact that psychoacoustic loudness explains and quantifies noise and its impact to humans better than weighted SPLs. Based on this scientific consensus, the usage of the revised loudness model for fan acoustic rating is widely supported by various sectors as discussed in the Introduction section, which is signified by recent revisions of ANSI S3.4 being based on the Revised Loudness Model by Moore et al. [93, 106] In this light,

it is recommended that the Conventional Model be replaced by the Revised Model for fan loudness rating in programs such as ASHRAE, Energy Star, etc.

Conclusions

This study uses 394 fan testing data which comprises kitchen range hoods, bathroom fans, and utility room fans to investigate the implementation of a state-of-the-art loudness model as an update to Conventional Loudness Model found in codes, standards, and regulations. The psychoacoustic quantity loudness has been increasingly used by government and industry sectors for residential ventilation devices because of the operational proximity to human operators of these ventilation devices. For example, ASHRAE 62.2 standards and Energy Star V4.0 mandate loudness requirements for kitchen range hoods, bathroom fans, and utility room fans, and many U.S. state codes and regulations demand loudness controls for whole house ventilations. The Conventional Loudness Model based on the work by Stevens and ANSI S3.4-1980 (2003R) has several limitations in that it encompasses an outdated equal-loudness contour, is incapable of addressing tonal components in acoustic spectrums, and has less accurate relationships between loudness levels in phon and loudness in sone near the hearing threshold. In contrast, an updated and Revised Loudness Model based on the newer ANSI S3.4 and the study by Moore et al. is a promising upgrade to the Conventional Loudness Model because the Revised Model effectively addresses these limitations through sophisticated mathematical modelling of the human loudness perception.

The investigation herein starts with comparing equal-loudness-level contours for the Conventional Model and the Revised Model. The contours for the Conventional Loudness Model are linear in their 1/3 octave band representations, and were found to have several notable discrepancies when compared to the ISO 226:2003 equal-loudness-level contours found in the Revised Model, especially the zero-loudness-level thresholds and the overall contour shapes. Also, different spacing of the contours for each model were found, which may result in inconsistent loudness differences from negative to positive near around 20 phon with a strong possibility of underestimation of the loudness under 20 phon when the conventional loudness is used.

Next, the relationships between loudness levels (phon) and loudness (sone) were studied for these two models. Because the relationship in the Conventional Model is effective over approximately 30 phon, a relationship under the 30 phon needs to be accurately established. The Revised Model by Moore et al. was found to explain more accurately in the lower loudness level range between 0 and 40 phon.

Of special importance, loudness determined by the two models were analyzed by using 394 fan testing data measured during the period 2013-2016. The comparison of these two different loudness calculation approaches is useful because the sound (or noise) emitted from the fan is a broad band spectrum with possible tonal components. Between 0-2 sone, the revised loudness ratings based on the Revised Model were consistently larger than the Conventional Model loudness by 0.1-0.4 sone. Furthermore, the two loudness models resulted in similar loudness values in the 3-6 sone range with several data points having lower loudness based on the Revised Model. However, at

values over 7 sone of the conventional loudness, the Revised Model resulted in lower loudness than the loudness calculated by the Conventional Model, which is opposite of the trend at lower loudness.

Because the fan loudness rating is used nationwide in the U.S. for certification programs, the impact of a potential adoption of the improved loudness was also considered. The statistics made in this study revealed that overall increases in the loudness calculation are observed when the Revised Loudness Model replaces the Conventional Loudness Model with about a 0.5 sone increase being observed for the acoustic rating program requirements. In fact, rating the 394 fans by using the Revised Model with a 2.0 sone requirement results in about 10% of the fans exceeding the old 2.0 sone limit, which would suggest that a new higher limit is appropriate if the revised model is implemented.

Considering that the usage of the psychoacoustic quantity loudness for the residential ventilation codes and programs is for addressing noise exposure to the human occupants in the built environment, the update or improvement of the Conventional Model by replacing it with the Revised Model would seem appropriate. Some forms of adjustment to the loudness requirement is justifiable based on the analysis made herein the study.

CHAPTER VII

CONCLUSIONS

The scope of this dissertation is an investigation of acoustic and energy performances of residential ventilating devices following standard performance testing protocols in order to recommend improvements or updates on future standard testing methods for residential ventilating devices. The following outlines individual topics of the study herein.

1. Study of Bathroom Ventilation Fan Performance Trends for Years 2005 to 2013—Data Analysis of Loudness and Efficacy
2. Methodology for Evaluating Sound Transmission to the External Background
3. Methodology for Evaluating Background Steadiness by Monitoring External Background Signatures
4. Uncertainty and Signal-to-Noise Ratio for Unsteady Background Noise
5. An Impact of an Improved Psychoacoustic Model on Fan Loudness and Acoustic Ratings

Study of Bathroom Ventilation Fan Performance Trends for Years 2005 to 2013—Data Analysis of Loudness and Efficacy

The study presented multi-year statistical analysis of residential bathroom fan performances with particular focus on acoustical, airflow and energy performances. The statistical analysis was conducted on testing data for over 1,500 fans for the test period 2005-2013 with focuses on energy and acoustical performances.

Major findings include that (1) The average loudness of fans with volumetric flow rates under 90 ft^3/min (42.5 L/s) decreased from 2.27 sone in 2005 to 0.78 sone in 2013 and for fans with flow values being equal to or above 90 ft^3/min (42.5 L/s) the decrease was from 2.34 sone in 2005 to 1.06 sone in 2013, (2) Fan efficacy statistics in each year for AC and DC motor fans reveal that most of the fans satisfy IECC 2012 efficiency requirements, which are 1.4 ft^3/W·min (0.66 L/W·s) for fans under 90 ft^3/min (42.5 L/s) and 2.8 ft^3/W·min (1.52 L/W·s) for fans equal to or above 90 ft^3/min (42.5 L/s), and (3) 3. In addition to the ENERGY STAR Most Efficient criteria being implemented, the increased usage of DC-motor fans has led to better efficacy ratings over the year.

Based on the statistical analysis, relationships were analyzed including linear regression lines with negative coefficients between fan efficacies and loudness ratings for AC and DC motor fans. AC and DC motor fans showed different linearly decaying trends with DC-motor fans having less slope of -0.04 W·sone·min/ft^3 (-0.08 W·sone·s/L) and -0.14 W·sone·min/ft^3 (-0.29 W·sone·s/L) for under and over 90 ft^3/min (42.5 L/s) respectively compared to AC-motor fan regression slopes of -0.75 W·sone·min/ft^3 (-1.59 W·sone·s/L) and -0.69 W·sone·min/ft^3 (1.45 W·sone·s/L) for under and over 90 ft^3/min (42.5 L/s), respectively. These negatively sloped correlations between efficacy and loudness is that vibrations and turbulences leads to both a loss of efficiency and an increase in loudness.

Methodology for Evaluating Sound Transmission to the External Background

The intrusion of the acoustic background noise results in background noise characterizations and treatment processes in different areas of the acoustic performance evaluations of sound sources (or unit under test) as demanded by various international standards. The treatment of the background noise has been extensively studied by a number of researchers, and most of the efforts have focused on eliminating its effect on the signal emitted from the unit under test, such as background corrections that follows measurements of the unit under test. However, the assessment of the background steadiness has been less studied, and its implementations have been limited to the use of the measurement uncertainty and comparisons of the two different background noises.

As the first part of the background steadiness study, the two methods are introduced, namely the spatial background difference method and the insertion loss method, for evaluating the sound transmission through the semi-reverberant chamber.

As a real world-example, the study herein analyzed 200 individual tests, and it was found that the average external background noise was 47.1 dB, which was quieter than the moderate residential background noise levels of 55-65 dB. Because of this relatively quiet background, multiple frequency bands are expected to experience the overestimated transmission when the spatial background difference method was used. As an alternative, the insertion loss method, which uses the acoustic signature of the RSS to evaluate the sound transmission characteristics, was necessary for the multiple bands that suffered from the overestimated transmission. Because the insertion loss method needs to determine the sound transmission of the RSS, the method may intrinsically

involve either the statistical inference to predict the RSS sound transmission or the assumption that the background randomness can be substituted with the transmitted RSS signal. Despite these statistical inferences or assumptions, the insertion loss method does not result in the overestimation of the sound transmission.

The fundamental motivation of these two methods is the assessment of the transmission of the unit under test or the RSS when monitoring the external background. The signal-to-noise ratio (SNR) analytics were also presented as an example for these methods. Depending on the value of the SNRs, the sound transmission can be considered negligible, or if the external SPLs are being significantly influenced by the transmission of the unit under test or the RSS, then the external background is conditionally acceptable for a further background steadiness assessment. As an example, the SNR criteria were set to over 20 dB the for the transmission effect being negligible, between 6 and 20 dB for the transmission correction being necessary, and less than 6 dB for the external SPLs being conditionally acceptable for the usage of the external background. A majority of the sound transmission of the unit under test did not readily affect the external background SPLs in terms of the SNRs, being larger than 20 dB. However, for 6 tests out of 200 tests showed the SNRs less than 20 dB, and even lower than 6 dB at the high frequency band (over 1,600 Hz band). It is a reasonable and intuitive fact that the lower SNR is expected as the louder the unit is; however, another interesting finding was that the background unsteadiness as well as the level of the background noise affected the variations in SNRs.

Methodology for Evaluating Background Steadiness by Monitoring External Background Signatures

The study herein implemented the measurement of the external background noise, while conducting acoustic testing. The fundamental motivation of the need of the background steadiness assessment is that a number of the test subject (unit-under-test) have sound emissions that are not easily separated in terms of signal-to-noise ratios (SNRs) from the background noise. Despite the same lower SNRs, the poor SNRs of the two frequency groups were caused by a different nature of the sound emission. The low frequency group (up to 80 Hz band frequency) showed large variations in the background noise along with more sound transmission as characterized in the Chapter III of this study. Also, relatively larger background noise levels are also coupled with a similar amount of the unit noise. In contrast, the high frequency group (over 2,500 Hz band frequency) showed relatively less variations in the background noise inside the measurement space, namely the semi-reverberant chamber, along with lower background noise levels compared to the lower frequency background noise.

Comparisons of the average external (or outside-the-chamber) background SPLs in the UNIT, BGD, and RSS phases revealed that the interquartile range (IQR) of the external background SPLs remain similar with IQR being 4 to 5 dB throughout the entire 1/3 octave frequency bands. Meanwhile, each frequency band showed different mean and median SPLs. Next, similar patterns of the external background distributions were found among the measurement phases. In this light, the proposed external background

monitoring is potentially a better background comparison methodology in that the wider coverage of the measurement phases including the UNIT and the RSS phases.

Comparisons of the standard deviations of the measurement phases led to the findings that the distributions were similar to the measurement phases irrespective of the transmission characteristics, which enables a more convenient comparison. Also, this finding led to a methodology of another background steadiness assessment with similar standards deviations being a clue to the background steadiness in that the background can be considered to be steady once the same background fluctuation as well as the similar average background were identified.

Based on the findings in the external background study herein, several points can be made. First, it is necessary to identify how much the sound transmission of the unit under test or the RSS affects the external background before assessing the background steadiness. Second, despite the wide applicability of the external background monitoring method, the background steadiness assessment can be done effectively in the range of frequencies where the poor SNR can be an issue. Third, the average external background signals can provide a clue to the validity of the usage of the internal background signal for the background correction purposes. Lastly, fluctuation of the external backgrounds such as in terms of the standard deviations, can provide an insight that how much background fluctuation or s occurred, and how similar are their fluctuations and variations between measurement phases periods, such as the UNIT, the BGD, or the RSS phases.

Uncertainty and Signal-to-Noise Ratio for Unsteady Background Noise

This study investigated the impact of background noise variations on acoustical ratings by using a combination of standard guidelines and test data from 200 fan units. A majority of standard acoustical testing is susceptible to the intrusion of background noise, and the measured signal has to be corrected so as to eliminate background noise contribution. When a testing environment experiences variations or fluctuations of background noises, the precision of the acoustic rating can be compromised. Two methodologies are presented herein for evaluating the impact of the background variations, namely uncertainties and zero loudness SNRs. The uncertainty is determined from the sensitivity coefficients of the background corrections and standard deviations of the measured background noise.

Using data from 200 fan units, it was found that the uncertainty becomes exceedingly larger when an SNR of a test subject and a background noise, $SNR^{UT,B}$, is low. When loudness is used for the acoustic rating, another SNR metric, namely zero-loudness SNR, SNR_{zl}, can be used to evaluate the background impact on the acoustic rating, which is the second methodology.

The zero-loudness SNR, SNR_{zl}, is defined as an SNR of imaginary sound source whose sound emissions is at the zero loudness threshold. Using data from 200 fan units, the SNR_{zl} at the low to mid frequency bands up to 3,150 Hz showed large SNR_{zl} over 20 dB, which means less contribution of background noise to the resulting loudness. Lastly, the SNR_{zl} at high bands (exceeding a 4,000 Hz frequency band) were in most cases between 10 and 20 dB, which is significantly lower than the low frequency SNR_{zl}.

Based on these findings, the combined usage of both the uncertainty and the zero loudness SNR can provide more useful estimations of background variations and its impact on acoustic ratings, especially for low-to-medium sound emissions of test subjects.

An Impact of an Improved Psychoacoustic Model on Fan Loudness and Acoustic Ratings

The psychoacoustic quantity loudness has been increasingly used by government and industry sectors for residential ventilation devices because of the operational proximity to human operators of these ventilation devices. The Conventional Loudness Model based on the work by Stevens and ANSI S3.4-1980 (2003R) has several limitations in that it encompasses an outdated equal-loudness contour, is incapable of addressing tonal components in acoustic spectrums, and has less accurate relationships between loudness levels in phon and loudness in sone near the hearing threshold.

First, equal-loudness-level contours for the Conventional Model and the Revised Model were compared. The contours for the Conventional Loudness Model are linear in their 1/3 octave band representations, and were found to have several notable discrepancies when compared to the ISO 226:2003 equal-loudness-level contours found in the Revised Model, especially the zero-loudness-level thresholds and the overall contour shapes with most noticeable differences being different spacing between each contour.

Next, the comparisons of relationships between loudness levels (phon) and loudness (sone) in the Conventional and Revised Models revealed that the Revised Model by

Moore et al. was found to have a more accurate explanation in the lower loudness level range between 0 and 40 phon.

The comparison of two different loudness calculation approaches by Conventional and Revised Models, respectively, was performed for 396 fan testing data. Between 0-2 sone, the revised loudness ratings based on the Revised Model were consistently larger than the Conventional Model loudness by 0.1-0.4 sone. Furthermore, the two loudness models resulted in similar loudness values in the 3-6 sone range with several data points having lower loudness based on the Revised Model. However, at values over 7 sone of the conventional loudness, the Revised Model resulted in lower loudness than the loudness calculated by the Conventional Model, which is opposite of the trend at lower loudness.

Because the fan loudness rating is used nationwide in the U.S. for certification programs, the impact of a potential adoption of the improved loudness was also considered. Rating the 394 fans by using the Revised Model with a 2.0 sone requirement results in about 10% of the fans exceeding the old 2.0 sone limit, which would suggest that a new higher limit is appropriate if the revised model is implemented.

CHAPTER VIII

RECOMMENDATIONS FOR FUTURE STUDY: STOCHASTIC ANALYSIS OF BACKGROUND NOISE FOR REVISED BACKGROUND CORRECTION

Motivation

Ideal background conditions for acoustical testing are devoid of change, variation, or interruption, which qualitatively defines a background steadiness. However, a mathematical or quantitative definition of the background steadiness has not been determined in engineering societies and industries. For example, a majority of international or national acoustic testing standards do not provide definitions of the background steadiness. The reason could primarily be because background noise itself has not been significantly and adequately investigated as it relates to acoustical testing of large sound sources or controlled acoustic measurement spaces. Evidence can be found in many acoustical testing standards, such as ISO, ANSI, AHRI, AMCA, etc [9-11, 32, 42, 68, 79], where common criteria can be outlined below.

1. Background noise shall be suppressed to the extent to achieving sufficient separation from the signal of interest, e.g., sound or noise from unit-under-test in terms of Signal-to-Noise Ratio (SNR).
2. Otherwise, the impact of the background noise variation is quantified by using uncertainties.

More detailed discussions on these two criteria can be found in Chapter V.

Recently, a few researchers started focusing on the background steadiness for standard acoustical testing based on their field testing results along with statistical analysis. Oppenheimer and Bard [120] investigated statistical distributions of the background noise when the noise is broadband and uncorrelated without tonal components. This background noise characteristic leads to the random combinations of each phased background noise component. In their study, they defined the mathematical definition of the background steadiness as the ratio of mean and variance of the squared sound pressure, p^2 in Pa^2, based on their statistical formulation of the broadband and uncorrelated background noises. This chapter introduces their mathematical framework along with statistics of measured background noise by using their definition of the background steadiness.

Statistical Distribution of Background Noises

Based on the statistical study of ocean acoustics by Dyer [121], Oppenheimer and Bard [120] formulated the background noise as combinations of sinusoids in different phases. The following equations outline the mathematical framework used to model background noise and to define background steadiness.

$$p_m = \sum_{n=1}^{N_m} A_{mn} \cos\left(\omega_m t + \phi_{mn}\right) \tag{8-1}$$

, where each symbol denotes

p_m: sound pressure (in Pa) of a frequency component m

A_{mn}: amplitude of a sinusoid

ω_m: angular velocity of a frequency component m

ϕ_{mn}: phase of a sinusoid

N_m: the number of phase contributors.

m, n: frequency components and phased sinusoidal contributions, respectively.

In order to obtain energy term in spectral density, Eq. (8-1) is squared. It should be noted that trigonometric expansion is available for cosine terms, and cross-term $\sin(\omega_m t)\cos(\omega_m t)$ becomes zero after time-averaging process over the given measurement time t=T. A simple manipulation of Eq. (8-1) may result in the following forms.

$$\frac{2p_m^2}{N_m\sigma_\xi^2} = \left(\frac{\sum_n \xi_{1n}}{\sqrt{N_m}\sigma_\xi}\right)^2 + \left(\frac{\sum_n \xi_{2n}}{\sqrt{N_m}\sigma_\xi}\right)^2 \tag{8-2}$$

, where random variables, ξ_{1n}, ξ_{2n}, are defined as

$$\begin{cases} \xi_{1n} \equiv A_{mn}\cos\phi_{mn} \\ \xi_{2n} \equiv A_{mn}\sin\phi_{mn} \end{cases} \tag{8-3}$$

, and σ_ξ^2 is the variance of the random variables, ξ_{1n}, ξ_{2n}.

When the noise is broadband and uncorrelated without tonal components, the summation of random variables, $\Sigma\xi_{1n}, \Sigma\xi_{2n}$, follow normal distribution as dictated by the Central Limit Theorem [65]. Furthermore, the square sum of each parenthesis in Eq. (8-2) results in a Chi-Square distribution with 2 degree of freedom. As such, summation throughout the phase contributions results in a Chi-Square distribution with 2M degree of freedom. Unlike the typical assumption of the normal distribution in leading acoustical testing standards such as ISO and ANSI [10, 11, 122], the statistical distribution of the background noise is essentially a Chi-Square distribution [65, 120].

A simple representation of this Chi-Square distribution, χ^2, is expressed as follows.

$$w \equiv \frac{4\langle p^2 \rangle}{N\langle A^2 \rangle} \approx \sum_{m=1}^{M} y_m \sim \chi^2_{2M} \tag{8-4}$$

, where

w: square of the sound pressure over entire phased-background-noise components

$\langle p^2 \rangle$: average of squared sound pressure in Pa^2 over entire phase-background-noise components

$N\langle A^2 \rangle$: average of mean square amplitudes of phase-background-noise components

y_m: sinusoid of phased background noise

m: each phase component

M: total number of frequency component.

Of special importance, mean and variance of a Chi-Square are 2*M* and 4*M*, (i.e., degree of freedom and twice of degree of freedom, respectively) [65]. By using these two relationships, the following formulation is available.

$$M = \frac{E\left(\chi^2_{2M}\right)^2}{Var\left(\chi^2_{2M}\right)} = \frac{\mu^2_{p^2}}{\sigma^2_{p^2}} \approx \frac{\hat{\mu}^2_{p^2}}{\hat{\sigma}^2_{p^2}} \tag{8-5}$$

, where

$E(\chi^2_{2M})$: mean value of the Chi-Square distribution

$\mathrm{Var}(\chi^2_{2M})$: variance of the Chi-Square distribution

$\mu^2_{p^2}$, $\hat{\mu}^2_{p^2}$: population mean and sample mean (i.e., estimated mean) of squared sound pressure, respectively

$\sigma_{p^2}^2$, $\widehat{\sigma}_{p^2}^2$: population variance and sample variance (i.e., estimated mean) of squared sound pressure

Several insights are available from the formulation process in Eq. (8-81) through Eq. (8-5) as follows.

1. Summation of phase sinusoid in Eq. (8-3) follows a normal distribution because each sound pressure component is randomly developed in a control volume, and thus results in a normal distribution according to the Central Limit Theorem.

2. The degree of freedom, 2*M*, also represents twice of the number of frequency components. It is intuitive that more frequency components result in increased degree of freedom. When this observation is combined with Eq. (8-5), a degree of freedom is proportional to mean square of the sound pressures, $\mu_{p^2}^2$, and inversely proportional to variance of the mean square of the sound pressures, $\sigma_{p^2}^2$.

Based on these observations, *M* is defined as the quantitative background steadiness. Then, by using this definition, the external acoustic signature is analyzed and discussed by using extensive laboratory measurement data.

REFERENCES

[1] Delp, W. W., and Singer, B. C., 2012, "Performance Assessment of U.S. Residential Cooking Exhaust Hoods," Environmental Science & Technology, 46(11), pp. 6167-6173.

[2] EPA, 1999, "ENERGY STAR for Residential Ventilation Fans," http://www.energystar.gov/index.cfm? c=partners.most_efficient_development_2011.

[3] Singer, B. C., Delp, W. W., Price, P. N., and Apte, M. G., 2012, "Performance of installed cooking exhaust devices," Indoor Air, 22(3), pp. 224-234.

[4] Tung, Y.-C., Shih, Y.-C., Hu, S.-C., and Chang, Y.-L., 2010, "Experimental performance investigation of ventilation schemes in a private bathroom," Building and Environment, 45(1), pp. 243-251.

[5] Kuo, I.-S., and Lai, C.-M., 2005, "Assessment of the potential of roof turbine ventilators for bathroom ventilation," Building Services Engineering Research and Technology, 26(2), pp. 173-179.

[6] Lai, C.-M., 2006, "Prototype development of the rooftop turbine ventilator powered by hybrid wind and photovoltaic energy," Energy and Buildings, 38(3), pp. 174-180.

[7] Yang, C., Yang, X., Xu, T., Sun, L., and Gong, W., 2009, "Optimization of bathroom ventilation design for an ISO Class 5 clean ward," Build. Simul., 2(2), pp. 133-142.

[8] AMCA, 2014, "AMCA Standard 301-14, Methods for Calculating Fan Sound Ratings from Laboratory Test Data," Air Movement and Control Association, Arlington Heights, IL.

[9] HVI, 2015, "HVI Publication 915, HVI Loudness Testing and Rating Procedure," Home Ventilating Institute, Morehead City, NC.

[10] ISO, 2010, "ISO 3744:2010 Acoustics -- Determination of sound power levels and sound energy levels of noise sources using sound pressure -- Engineering methods for an essentially free field over a reflecting plane," International Organization for Standardization, Geneva, Switzerland.

[11] ISO, 2010, "ISO 3741:2010 Acoustics -- Determination of sound power levels and sound energy levels of noise sources using sound pressure -- Precision methods for

reverberation test rooms," International Organization for Standardization, Geneva, Switzerland.

[12] ANSI, 2012, "ANSI S12.51: Acoustics - Determination of sound power levels of noise sources using sound pressure - Precision methods for reverberation rooms," American National Standards Institute, Melville, NY.

[13] Barron, R. F., 2002, Industrial noise control and acoustics, CRC Press, New York, NY.

[14] da Costa-Félix, R. P. B., 2006, "Type B uncertainty in sound power measurements using comparison method," Measurement, 39(2), pp. 169-175.

[15] Kubica, J., and Moore, A. W., "Probabilistic noise identification and data cleaning," Proc. ICDM, pp. 131-138.

[16] Lu, Y., and Loizou, P. C., 2008, "A geometric approach to spectral subtraction," Speech communication, 50(6), pp. 453-466.

[17] ISO, 2009, "ISO/IEC Guide 98-1:2009 Uncertainty of measurement -- Part 1: Introduction to the expression of uncertainty in measurement," International Organization for Standardization, Geneva, Switzerland.

[18] Davis, G. M., 2002, Noise Reduction in Speech Applications, CRC Press, Boca Raton, FL.

[19] ANSI, R2003, "ANSI S3.4 American National Standard-Procedure for the computation of loudness of noise," American National Standards Institute, Melville, NY.

[20] Stevens, S. S., 1972, "Perceived Level of Noise by Mark VII and Decibels (E)," The Journal of the Acoustical Society of America, 51(2B), pp. 575-601.

[21] Scharf, B., and Hellman, R., "How to best predict human response to noise on the basis of acoustic variables," Proc. Proceedings of the Third International Congress on Noise as a Public Health Problem, ASHA report.

[22] Hellman, R. P., 2007, "Standards News: A New ANSI Loudness Standard," Acoustics Today, 3(1), pp. 41-44.

[23] ICC, 2012, "International Energy Conservation Code 2012," R-33, International Code Council, Country Club Hills, IL.

[24] Capps, L., 2012, "Whole-house mechanical ventilation in a mixed-humid climate," Masters, Georgia Institute of Technology Atlanta, GA.

[25] Wray, C. P., Matson, N. E., and Sherman, M. H., 2000, "Selecting whole-house ventilation strategies to meet proposed ASHRAE standard 62.2: energy cost considerations," ASHRAE Transactions, 106(Part II).

[26] US DOE, 2012, "2012 IECC Residential Fan Efficiency," U. S. D. o. Energy, ed., U.S. Department of Energy, Washington, DC.

[27] EIA, U., 2012, "Annual Energy Review 2011," U. S. D. o. Energy, ed., U.S. Energy Information Administration, Washington, DC, pp. 37-39.

[28] EIA, U., 2013, "Annual Energy Outlook 2013," U. S. D. o. Energy, ed., U.S. Energy Information Administration, Washington, DC, pp. 60-62.

[29] Moran, M. J., Shapiro, H. N., Boettner, D. D., and Bailey, M. B., 2010, Fundamentals of engineering thermodynamics, John Wiley & Sons, Hoboken, NJ.

[30] Waye, K. P., Rylander, R., Benton, S., and Leventhall, H., 1997, "Effects on performance and work quality due to low frequency ventilation noise," Journal of Sound and Vibration, 205(4), pp. 467-474.

[31] HVI, 2009, "HVI Publication 915, HVI Loudness Testing and Rating Procedure," Home Ventilating Institute, Wauconda, IL.

[32] AHRI, 2012, "ANSI/AHRI Standard 260 (I-P) Sound Rating of Ducted Air Moving and Conditioning Equipment," Air-Conditioning, Heating, and Refrigeration Institute, Arlington, VA.

[33] ASHRAE, 2013, "ANSI/ASHRAE Standard 62.2-2013, Ventilation and Acceptable Indoor Air Quality in Low-Rise Residential Buildings," American Society of Heating, Refrigerating, and Air-Conditioning Engineers, Atlanta, GA.

[34] HVI, 2014, "HVI-Certified Products Directory," Complete Home Ventilating Institute Certified Products Directory-Section 1, Home Ventilating Institute, Morehead City, NC.

[35] Pavlovas, V., 2004, "Demand controlled ventilation: A case study for existing Swedish multifamily buildings," Energy and buildings, 36(10), pp. 1029-1034.

[36] McWhinney, M., Fanara, A., Clark, R., Hershberg, C., Schmeltz, R., and Roberson, J., 2005, "ENERGY STAR product specification development framework: using data and analysis to make program decisions," Energy Policy, 33(12), pp. 1613-1625.

[37] ANSI, 2012, "American National Standard Acoustics – Determination of sound power levels and sound energy levels of noise sources using sound pressure – Precision methods for reverberation test rooms," Acoustical Society of America, Melville, NY.

[38] ANSI, 2007, "ANSI S3.4: American National Standard Procedure for the Computation of Loudness of Steady Sound," American National Standards Institute, Melvilly, NY.

[39] AMCA, 2013, "AMCA Standard 260-13: Laboratory Methods of Testing Induced Flow Fans for Rating," Air Movement and Control Association, Arlington Heights, IL.

[40] Bailey, A., 2011, "Letter to Stakeholders, Energy Star Most Efficient Final Criteria," U. S. E. P. Agency, ed.Washington, DC.

[41] Bailey, A., 2013, "Final Criteria, November 20, 2012," U. S. E. P. Agency, ed.Washington, DC.

[42] AMCA, 2014, "ANSI/AMCA Standard 300-14: Reverberant Room Method for Sound Testing of Fans," Air Movement and Control Association International, Inc., Arlington Heights, IL.

[43] ASHRAE, 2011, ASHRAE Handbook-HVAC Applications, American Society of Heating, Refrigerating, and Air-Conditioning Engineers, Atlanta, GA.

[44] Moreland, J., 1974, "Housing effects on centrifugal blower noise," Journal of Sound and Vibration, 36(2), pp. 191-IN192.

[45] Beranek, L. L., and Ver, I. L., 1992, "Noise and vibration control engineering-principles and applications," Noise and vibration control engineering-Principles and applications John Wiley & Sons, Inc., 814 p., 1.

[46] Jeon, W.-H., 2003, "A numerical study on the effects of design parameters on the performance and noise of a centrifugal fan," Journal of Sound and Vibration, 265(1), pp. 221-230.

[47] Velarde-Suárez, S., Ballesteros-Tajadura, R., Hurtado-Cruz, J. P., and Santolaria-Morros, C., 2006, "Experimental determination of the tonal noise sources in a centrifugal fan," Journal of sound and vibration, 295(3), pp. 781-796.

[48] Fastl, H., and Zwicker, E., 2007, Psychoacoustics: Facts and models, Springer Science & Business Media, New York, NY.

[49] Stevens, S., 1972, "Perceived level of noise by Mark VII and decibels (E)," The Journal of the Acoustical Society of America, 51(2B), pp. 575-601.

[50] McKay, M., Fitzgerald, M. A., and Beckman, R. J., 1999, "Sample size effects when using R2 to measure model input importance," Technical Report LA-UR-99-1357. Los Alamos National Laboratory, Los Alamos, NM.

[51] Gustafsson, S., Jax, P., and Vary, P., "A novel psychoacoustically motivated audio enhancement algorithm preserving background noise characteristics," Proc. Acoustics, Speech and Signal Processing, 1998. Proceedings of the 1998 IEEE International Conference on, IEEE, pp. 397-400.

[52] Tang, Z., and Miao, Z., "Fast background subtraction and shadow elimination using improved gaussian mixture model," Proc. Haptic, Audio and Visual Environments and Games, 2007. HAVE 2007. IEEE International Workshop on, IEEE, pp. 38-41.

[53] Boll, S. F., 1979, "Suppression of acoustic noise in speech using spectral subtraction," Acoustics, Speech and Signal Processing, IEEE Transactions on, 27(2), pp. 113-120.

[54] Vaseghi, S. V., 2008, Advanced digital signal processing and noise reduction, John Wiley & Sons, Hoboken, NJ.

[55] Mann, M., and Lees, J., 1996, "Robust estimation of background noise and signal detection in climatic time series," Climatic Change, 33(3), pp. 409-445.

[56] Brandstein, M., and Ward, D., 2001, Microphone arrays: signal processing techniques and applications, Springer Science & Business Media, New York, NY.

[57] Vasseur, D. A., and Yodzis, P., 2004, "The color of environmental noise," Ecology, 85(4), pp. 1146-1152.

[58] Everest, F. A., Pohlmann, K. C., and Books, T., 2001, The master handbook of acoustics, McGraw-Hill New York, New York, NY.

[59] Lee, Y. S., 2010, "Office layout affecting privacy, interaction, and acoustic quality in LEED-certified buildings," Building and Environment, 45(7), pp. 1594-1600.

[60] Lilly, J. G., and Wowk, R., 2010, "Acoustical performance standards for schools," Consulting-specifying engineer,< http://www. csemag. com/home/singlearticle/ acoustical-performance-standards-for-schools/974cf1571a. html>(Feb. 11, 2014).

[61] Moiseev, N., 2011, "Acoustic performance measurement protocols," ASHRAE journal, 53(1), p. 28.

[62] Beranek, L. L., 1989, "Balanced noise-criterion (NCB) curves," The Journal of the Acoustical Society of America, 86(2), pp. 650-664.

[63] Delp, W. W., and Singer, B. C., 2012, "Performance assessment of US residential cooking exhaust hoods," Environmental science & technology, 46(11), pp. 6167-6173.

[64] Environmental Protection Agency, 2015, "ENERGY STAR® Program Requirements for Residential Ventilating Fans V4.0," E. P. Agency, ed.Washington, DC.

[65] Montgomery, D. C., and Runger, G. C., 2010, Applied statistics and probability for engineers, John Wiley & Sons, New York, NY.

[66] Kang, J., 2006, Urban sound environment, CRC Press, New York, NY.

[67] Lebiedowska, B., 2005, "Acoustic background and transport noise in urbanised areas: A note on the relative classification of the city soundscape," Transportation Research Part D: Transport and Environment, 10(4), pp. 341-345.

[68] Fahy, F. J., 2000, Foundations of Engineering Acoustics, Academic Press.

[69] Xu, S., Qiu, C., and Liu, Z., 2012, "Acoustic transmission through asymmetric grating structures made of cylinders," Journal of Applied Physics, 111(9), p. 094505.

[70] Wang, Q., Yang, Y., Ni, X., Xu, Y.-L., Sun, X.-C., Chen, Z.-G., Feng, L., Liu, X.-p., Lu, M.-H., and Chen, Y.-F., 2015, "Acoustic asymmetric transmission based on time-dependent dynamical scattering," Scientific reports, 5.

[71] ISO, 1999, "Acoustics -- Requirements for the performance and calibration of reference sound sources used for the determination of sound power levels."

[72] ISO, 1999, "ISO 6926:1999 Acoustics -- Requirements for the performance and calibration of reference sound sources used for the determination of sound power level," International Organization for Standardization, Geneva, Switzerland.

[73] Choi, W., Pate, M. B., and Sweeney, J. F., 2016, "Study of Bathroom Ventilation Fan Performance Trends for Years 2005 to 2013—Data Analysis of Loudness and Efficacy," Energy and Buildings, 116, pp. 468-477.

[74] Cowan, J. P., 1993, Handbook of environmental acoustics, John Wiley & Sons, New York, NY.

[75] Ravi, S., 2010, "Performance Evaluation of Reverberant Chamber Background Noise Levels," Texas A&M University.

[76] Killion, M. C., 1976, "Noise of ears and microphones," The Journal of the Acoustical Society of America, 59(2), pp. 424-433.

[77] Zuckerwar, A. J., Kuhn, T. R., and Serbyn, R. M., 2003, "Background noise in piezoresistive, electret condenser, and ceramic microphones," The Journal of the Acoustical Society of America, 113(6), pp. 3179-3187.

[78] Gabrielson, T. B., 1993, "Mechanical–thermal noise in acoustic and vibration sensors," IEEE Trans Electron Devices, 40, pp. 903-909.

[79] AHRI, 2014, "ANSI/AHRI Standard 220 Reverberation Room Qualification and Testing Procedures for Determining Sound Power of HVAC Equipment," Air-Conditioning, Heating, and Refrigeration Institute, Arlington, VA.

[80] Payne, R., and Simmons, D., 2000, Assessment of reproducibility uncertainties for use in international standards on the determination of sound power, National Physical Laboratory. Great Britain, Centre for Mechanical and Acoustical Metrology, Middlesex, UK.

[81] Loyau, T., 2007, "Determination of sound power levels using sound pressure: The uncertainties related with the measurement surface and the number of microphones," Noise control engineering journal, 55(1), pp. 89-97.

[82] Hansen, C. H., and Sehrndt, C., 2001, "Fundamentals of acoustics," Occupational Exposure to Noise: Evaluation, Prevention and Control. World Health Organization.

[83] ISO, 2012, "ISO 26101:2012 Acoustics -- Test methods for the qualification of free-field environments," International Organization for Standardization, Geneva, Switzerland.

[84] Martin, R., 1994, "Spectral subtraction based on minimum statistics," power, 6, p. 8.

[85] Gustafsson, H., Nordholm, S. E., and Claesson, I., 2001, "Spectral subtraction using reduced delay convolution and adaptive averaging," Speech and Audio Processing, IEEE Transactions on, 9(8), pp. 799-807.

[86] Monnet, A., Mittal, A., Paragios, N., and Ramesh, V., "Background modeling and subtraction of dynamic scenes," Proc. Computer Vision, 2003. Proceedings. Ninth IEEE International Conference on, IEEE, pp. 1305-1312.

[87] Doretto, G., Chiuso, A., Wu, Y. N., and Soatto, S., 2003, "Dynamic textures," International Journal of Computer Vision, 51(2), pp. 91-109.

[88] Choi, W., Pate, M. B., and Sweeney, J. F., 2016, "Study of Bathroom Ventilation Fan Performance Trends for Years 2005 to 2013—Data Analysis of Loudness and Efficacy," Energy and Buildings.

[89] Fastl, H., and Zwicker, E., 2007, Psychoacoustics: Facts and models, Springer Science & Business Media.

[90] Stevens, S. S., 1961, "Procedure for Calculating Loudness: Mark VI," The Journal of the Acoustical Society of America, 33(11), pp. 1577-1585.

[91] ANSI, 2015, "ANSI S3.20 Bioacoustical Terminology," American National Standards Institute, Melville, NY.

[92] AHRI, 2012, "ANSI/AHRI Standard 1140-2012, Sound Quality Evaluation Procedures for Air-Conditioning and Regrigration Equipment," Air-Conditioning, Heating, and Refrigeration Institute, Arlington, VA.

[93] ANSI, 2007, ANSI S3.4: American National Standard Procedure for the Computation of Loudness of Steady Sound, American National Standards Institute.

[94] HVI, 2009, HVI Publication 920 Product Performance Certification Procedure Including Verification and Challenge, Home Ventilating Institute, Wauconda, IL.

[95] ICC, 2014, 2015 Vermont Residential Building Energy Standards, International Code Council, Country Club Hills, IL.

[96] ICC, 2015, Washington State Residential Building Code International Code Council, Country Club Hills, IL.

[97] ICC, 2015, International Residential Code, International Code Council, Country Club Hills, IL.

[98] Stevens, S., 1961, "Procedure for calculating loudness: Mark VI," The Journal of the Acoustical Society of America, 33(11), pp. 1577-1585.

[99] Stevens, S. S., 1936, "A scale for the measurement of a psychological magnitude: loudness," Psychological Review, 43(5), p. 405.

[100] ISO, 2003, "ISO 226:2003 Acoustics -- Normal equal-loudness-level contours," International Organization for Standardization, Geneva, Switzerland.

[101] Glasberg, B. R., and Moore, B. C., 2006, "Prediction of absolute thresholds and equal-loudness contours using a modified loudness model," The Journal of the Acoustical Society of America, 120(2), pp. 585-588.

[102] Moore, B. C., Glasberg, B. R., and Baer, T., 1997, "A model for the prediction of thresholds, loudness, and partial loudness," Journal of the Audio Engineering Society, 45(4), pp. 224-240.

[103] Charbonneau, J., Novak, C., and Ule, H., 2009, "Loudness prediction model comparison using the equal loudness contours," Canadian Acoustics, 37(3), pp. 64-65.

[104] Bray, W. R., 2011, "Help wanted now," Sound & Vibration, 45(9), pp. 4-5.

[105] HVI, 2009, HVI Publication 915, HVI® Loudness Testing and Rating Procedure, Home Ventilting Institute.

[106] Moore, B. C., 2014, "Development and current status of the “Cambridge” loudness models," Trends in hearing, 18, p. 2331216514550620.

[107] Fletcher, H., and Munson, W. A., 1933, "Loudness, Its Definition, Measurement and Calculation*," Bell System Technical Journal, 12(4), pp. 377-430.

[108] Yost, W. A., 1994, Fundamentals of hearing: An introduction, Academic Press, San Diego, CA.

[109] Stevens, S., 1957, "Calculating loudness," Noise control, 3(5), pp. 11-22.

[110] Stevens, S. S., 1956, "The Direct Estimation of Sensory Magnitudes: Loudness," The American Journal of Psychology, 69(1), pp. 1-25.

[111] Suzuki, Y., and Takeshima, H., 2004, "Equal-loudness-level contours for pure tones," The Journal of the Acoustical Society of America, 116(2), pp. 918-933.

[112] Zwislocki, J., and Hellman, R., 1960, "On the “Psychophysical law.”," The Journal of the Acoustical Society of America, 32(7), pp. 924-924.

[113] Takeshima, H., Suzuki, Y., Ozawa, K., Kumagai, M., and Sone, T., 2003, "Comparison of loudness functions suitable for drawing equal-loudness-level contours," Acoustical Science and Technology, 24(2), pp. 61-68.

[114] Hellman, R. P., "Predicting the loudness of tone-noise complexes from Steven's and Zwicker's procedures," Proc. INTER-NOISE and NOISE-CON Congress and Conference Proceedings, Institute of Noise Control Engineering, pp. 491-498.

[115] Natrella, M., 2010, "NIST/SEMATECH e-handbook of statistical methods," Engineering Statistics, National Institute of Standards and Technology, ed., U.S. Department of Commerce,, Washington, DC.

[116] Schomer, P. D., Suzuki, Y., and Saito, F., 2001, "Evaluation of loudness-level weightings for assessing the annoyance of environmental noise," The Journal of the Acoustical Society of America, 110(5), pp. 2390-2397.

[117] Hellman, R., and Zwicker, E., 1987, "Why can a decrease in dB (A) produce an increase in loudness?," The Journal of the Acoustical Society of America, 82(5), pp. 1700-1705.

[118] Nilsson, M. E., 2007, "A-weighted sound pressure level as an indicator of short-term loudness or annoyance of road-traffic sound," Journal of Sound and Vibration, 302(1), pp. 197-207.

[119] Charbonneau, J., 2010, "Comparison of loudness calculation procedure results to equal loudness contours," Masters, University of Windsor, Windsor, Ontario, Canada.

[120] Oppenheimer, C., and Bard, S., "An ambient noise model for background noise corrections," Proc. INTER-NOISE and NOISE-CON Congress and Conference Proceedings, Institute of Noise Control Engineering, pp. 679-687.

[121] Dyer, I., 1970, "Statistics of sound propagation in the ocean," The Journal of the Acoustical Society of America, 48(1B), pp. 337-345.

[122] ANSI, 2012, ANSI S12.51: Acoustics - Determination of sound power levels of noise sources using sound pressure - Precision methods for reverberation rooms, Acoustical Society of America.